DESIGN OF A SUPERCONDUCTING BEAM TRANSPORT CHANNEL AND BEAM DYNAMICS FOR A STRONG-FOCUSING CYCLOTRON

A Dissertation

by

KARIE ELIZABETH BADGLEY

Submitted to the Office of Graduate and Professional Studies of
Texas A&M University
in partial fulfillment of the requirements for the degree of

DOCTOR OF PHILOSOPHY

Chair of Committee,	Peter McIntyre
Committee Members,	Alfred McInturff
	Bhaskar Dutta
	Pavel Tsvetkov
	Robert Webb
Head of Department,	George R. Welch

May 2016

Major Subject: Physics

ABSTRACT

There is an increasing interest in high power proton accelerators for use as neutron and muon sources, accelerator driven systems (ADS) for nuclear waste transmutation, high energy physics, medical physics, nuclear physics, and medical isotope production. Accelerating high current beams has a number of challenges; including avoiding harmful resonance crossing, space charge effects and, specific to cyclotrons, sufficient turn separation at injection and extraction. The Accelerator Research Laboratory at Texas A&M University is developing a high-power strong-focusing cyclotron with two main technologies to overcome these challenges. The first is a superconducting RF cavity to provide the energy gain required for fully separated turns. The second is the use of superconducting beam transport channels within the sectors of the cyclotron to provide strong-focusing with alternating focusing and defocusing quadrupoles. A method has been developed to find the equilibrium spiral orbit through the cyclotron which maintains isochronicity. The isochronous spiral orbit was then used to perform full linear optics calculations. The strengths of the quadrupoles were adjusted to hold the horizontal and vertical betatron tunes constant per turn to avoid resonance crossing. Particle tracking was performed with a modified MAD-X-PTC code and Synergia to provide a framework for future space charge studies. Magnetic modeling was performed on a 2D cross section of the beam transport channel. The wire locations were adjusted to reduce the higher order multipoles and a good field region was obtained at 70% of the beam pipe aperture with multipoles less than 10^{-4}. The 2D model was also used to determine the required current density needed to produce the quadrupole gradients. MgB_2 superconducting wire was chosen as it meets all the field and current requirements and can operate

at a reduced cryogenic cost. A winding mandrel was also designed and fabricated which minimized the bend radius for the superconducting MgB_2 wire.

To my mother.

ACKNOWLEDGMENTS

This work would not have been possible without the guidance and support of many people. I would like to thank Peter McIntyre who originally encouraged me to go into Physics ("It's the king of all sports and the sport of all kings") and who, many years after our first encounter, became my advisor. I may never fully know or appreciate all that I learned from him. I would also like to acknowledge the members of my committee, Alfred "Mac" McInturff, Bhaskar Dutta, Pavel Tsvetkov, and Robert Webb. For their tremendous assistance in the lab, I would like to thank Tim Elliot and Andrew Jaisle; without their help, nothing could be found or finished. I am especially grateful for the support of my numerous friends, co-workers, and mentors (in no particular order): Elizabeth Sooby, Kelley Reaves, Abid Mujtaba, Matt Sears, Jonathan Button, Tyler Morrison, Michael Cone, Tristan Leggett, Indara Suarez, Abram Krislock, Trey Holik, Johnathan Asaadi, Lucas Naviera, Bert Ortega, Glenn Agnolet, Tatiana Erukhimova, Akhdiyor Sattarov, Saeed Assadi, Charles Crawford, Eric Stern, Leo Michelotti, Jeremiah Holzbauer, and Mauricio Lopes. Finally and most importantly, I would like to thank my family for years of emotional, and sometimes financial, support through this process.

This dissertation work would not have been possible without funding from the DOE Accelerator Stewardship Program (grant number 01-GR-SN50095-15-00) and from The Cynthia and George Mitchell Foundation.

TABLE OF CONTENTS

Page

LIST OF FIGURES

FIGURE Page

LIST OF TABLES

TABLE Page

1. INTRODUCTION

One of the goals of the Accelerator Research Lab at Texas A&M University is to develop an accelerator-driven sub-critical molten salt system (ADSMS) to destroy long lived nuclear waste. The accelerator portion of the system needs to produce a 10 mA 800 MeV proton beam to obtain the required spallation neutron flux and spectrum. No cyclotron to date is capable of producing such a high-power proton beam. There are a number of challenges in accelerating high current beams in cyclotrons; intense space charge forces, neighboring beam interactions, sitting on or crossing harmful resonances, and sufficient separation at extraction. Currently, the high power record is held by the Paul Scherrer Institute (PSI) with a 2 mA 590 MeV ring cyclotron (Figure 1.1). The right hand side of Figure 1.2 shows the last few turns of the PSI cyclotron. In the plot, the three turns previous to extraction are overlapping with one another [2]. The tune plot of PSI displaying coupling and Walkinshaw resonance line crossing as the tune of the machine drifts from initial to final energy is shown on the left in Figure 1.2. Both the beam overlap and resonance crossing can lead to beam blow up.

The Accelerator Research Lab is developing a strong-focusing cyclotron with two key innovations to overcome the challenges in accelerating high currents; a superconducting RF cavity capable of providing sufficient turn separation and a beam transport channel which will provide strong focusing. One of the main advantages in our strong-focusing cyclotron design, is the ability to set and maintain the tune to avoid any major resonance crossing. This is accomplished with the addition of beam transport channels within the sectors which contain alternating focusing and defocusing quadrupoles. The beam dynamics of the strong focusing cyclotron and the develop-

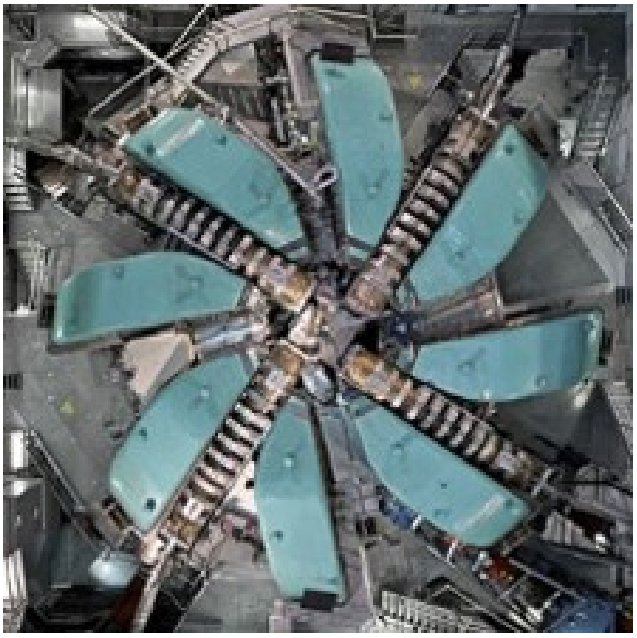

Figure 1.1: Top view of the PSI ring cyclotron [1].

ment of the transport channel will be the focus of this dissertation. Section 2 gives a brief history of cyclotron development with a concentration on focusing methods. The separated orbit cyclotron and previous designs are discussed. The section wraps up with a description of the proposed Texas A&M strong-focusing cyclotron system. Section 3 presents the method developed to find the equilibrium isochronous orbit. The orbit is then used to perform linear beam optics and the quadrupole strengths are adjusted to control the beam size and phase advance through the machine. The results of the beam dynamics studies and simulations in the TAMU100 cyclotron are presented. The section also describes the two particle tracking methods used and the differences in their results. Section 4 discusses the detailed design of the beam transport channel. The 2D magnetic model of the quadrupole is presented and a comparison is made with previous strong focusing designs. Results of magnetic

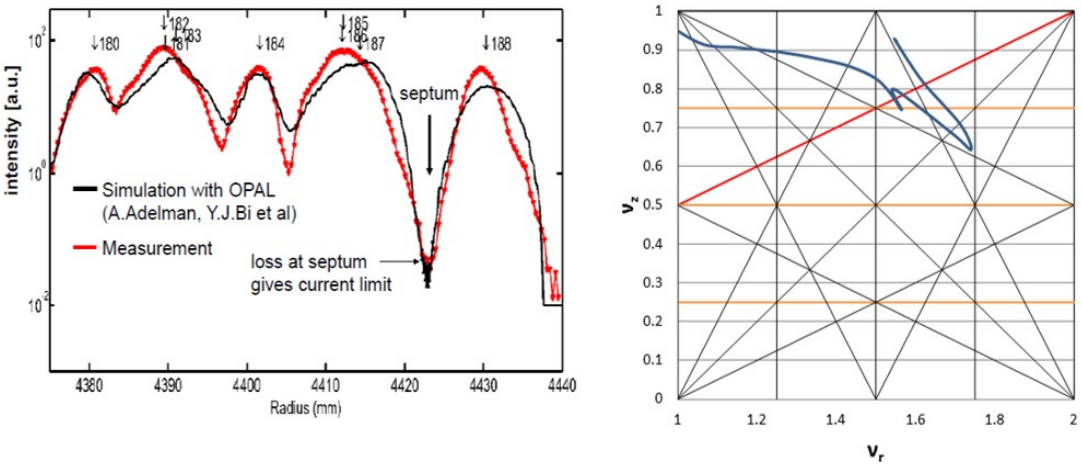

Figure 1.2: (Left) Position of the last eight turns of the PSI Ring Cyclotron. (Right) PSI Tune plot

modeling in 3D as well as the mechanical winding mandrel design are presented. Section 5 briefly covers the properties of the superconductor MgB_2, including the pros and cons of this superconductor for the beam transport channel. Section 6 contains a conclusion of the work and goals for future work.

2. STRONG-FOCUSING CYCLOTRON

2.1 Cyclotron History and Basics

The cyclotron was first proposed by E. O. Lawrence in 1930 [3] with the goal of accelerating protons to 1 MeV for use in nuclear studies. The idea was to accelerate protons in a circular path in an external magnetic field produced by two D-shaped pole pieces with alternating voltage. Within a year of the proposal, Lawrence and Livingston were able to experimentally verify the concept and accelerate protons up to 1 MeV. The Lorentz force causes particles with mass M, velocity v, and charge q, in an external magnetic field B_z, to move in a circle of radius r in a plane perpendicular to the field according to:

$$qvB_z = \frac{Mv^2}{r} \tag{2.1}$$

The revolution frequency, or cyclotron frequency, of the ion is then given by:

$$\omega = \frac{qB}{M} \tag{2.2}$$

It was also found that the curvature in the magnetic field lines from a radially decreasing magnetic field would create a restoring force for particles which deviate vertically from the central plane (Figure 2.1). A field index, n, can be defined according to:

$$n = -\frac{r}{B}\frac{dB}{dr}, \tag{2.3}$$

such that the equations of motion take the form:

$$r'' + (1-n)r = 0,\ y'' + ny = 0. \tag{2.4}$$

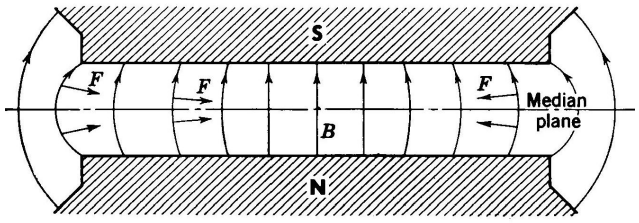

Figure 2.1: Restoring force on particles in a radially decreasing magnetic field [4]

For the vertical direction, $\frac{dB}{dr} < 0$ which makes $n > 0$. Similarly, (1-n)>0 must be true for oscillations about the radial position. This condition is known as weak focusing. The sinusoidal motion in both the radial and vertical directions are referred to as betatron oscillations. The number of betatron oscillations made in one full turn is the betatron tune (Q or sometimes ν), which is defined below for the vertical and radial directions. For weak focusing, the tunes are less than one.

$$Q_r = \sqrt{1-n},\ Q_y = \sqrt{n} \tag{2.5}$$

Only seven years after its invention, H. Bethe and M. Rose[5] reported what they considered to be a serious issue in obtaining higher energies in cyclotrons. The increasing relativistic mass, equation 2.6, would require a corresponding increase in the bending magnetic field to maintain isochronicity, or constant revolution frequency.

$$M = \frac{M_0}{\sqrt{1-\beta^2}} = \gamma M_0 \tag{2.6}$$

Where β and γ are defined as:

$$\beta = v/c,\ \gamma = \frac{1}{\sqrt{1-\beta^2}}. \tag{2.7}$$

The increase in radial field would in turn destroy focusing and limit the obtainable energy to 5 MeV for protons, a number they later increased to 12 MeV.

2.2 Focusing

2.2.1 Transverse Focusing

In response to Bethe and Rose, L.H. Thomas[6] proposed that an azimuthally varying magnetic field would provide sufficient axial focusing to overcome the defocusing from an increasing radial field. The Thomas field would vary azimuthally as $\cos(n\theta)$ and increase radially with nearly the relativistic mass increase to produce stable orbits. Although there was focusing due to the varying magnetic field in the Thomas cyclotron, the main source of focusing was from the distortion the field created in the orbits. Instead of circular orbits, the orbits become scalloped and the particles experience an edge focusing (Figure 2.2 and Figure 2.3).

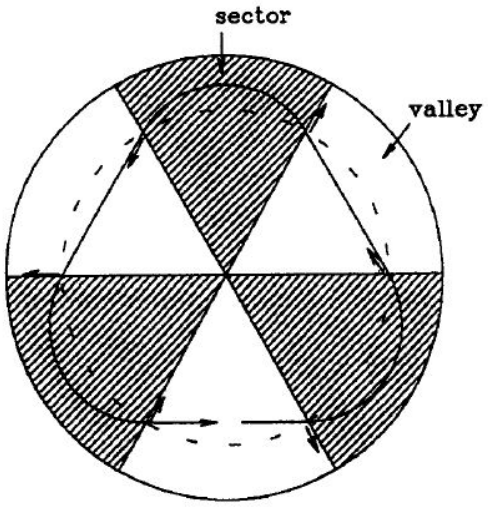

Figure 2.2: Scalloped orbits in a cyclotron with an azimuthally varying magnetic field [6]

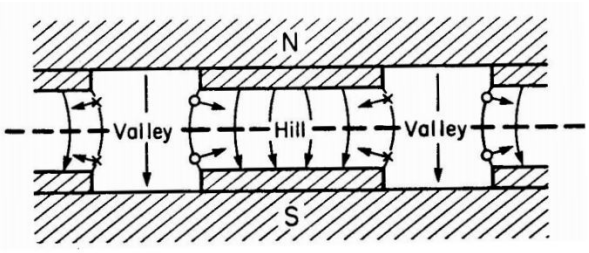

Figure 2.3: Edge focusing of particles above a below the midplane in a sector cyclotron [7].

D.W. Kerst[8] suggested increasing the edge focusing by increasing the angle the particles make with the sector by spiraling the sectors. There are a number of facilities with this style of cyclotron, including, the 500 MeV cyclotron at TRIUMF, the K500 at Texas A&M University and Michigan State University, and the ring cyclotron at the Paul Scherrer Institute. The downside of this geometry is the spiral sectors either greatly reduce the space for the RF cavity or the RF cavity is forced to have a complicated geometry [9, 10].

The idea of strong focusing, defined here as focusing in both planes and tunes larger than one, was proposed by Courant, Livingston and Snyder in 1952 [12]; although it was later discovered that Christofilos [13] had patented the idea two years before. To achieve strong focusing, alternating converging and diverging magnetic lenses are placed in series, focusing (F) and defocusing (D), to create an overall net focusing (Figure 2.5).

2.2.2 Longitudinal Focusing

The previous sections dealt only with focusing in the transverse direction due to magnetic fields but there is also a mechanism for longitudinal, or phase, focusing due to the RF cavities. In an ideal isochronous cyclotron, all particles arrive at the same

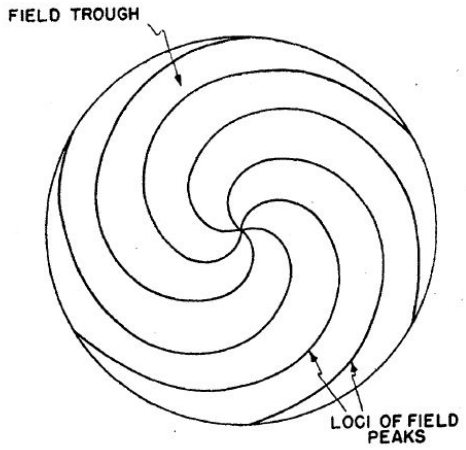

Figure 2.4: Six sector cyclotron design with spiral edge geometry[11].

time regardless of energy. This is because particles with a higher energy travel at a larger radius and similarly for lower energies, particles are on a smaller radius. In an actual cyclotron though this will not be the case, so longitudinal focusing becomes important. The cyclotron is designed so the reference particle hits the RF wave at a desired phase (ϕ_s), as shown in Figure 2.6. All other particles in the bunch will be slightly ahead (early) or slightly behind (late) the reference particle. This is due to slight differences in energy and leads to particles with higher energy hitting the RF wave earlier in its ramp up cycle and receiving a smaller energy gain. The slower particles hit the RF wave after the reference particle where the RF wave has risen higher and thus receive a larger energy gain. By the next RF cavity, or on the next RF cycle, the particles have been adjusted toward the timing of the reference particle, and oscillate about its timing.

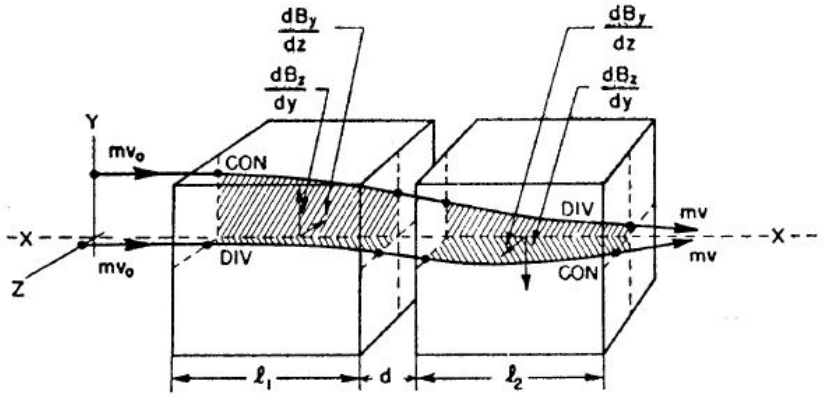

Figure 2.5: Strong focusing in a doublet of alternating divergent and convergent magnetic forces [12]

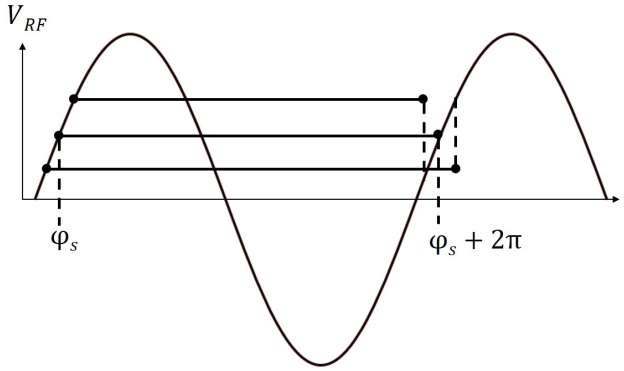

Figure 2.6: RF cavity acceleration cycle

2.3 Separated Orbit Cyclotron

There have been a few proposals to fully separate and focus beams along their orbits in accelerators. The first separated orbit cyclotron (SOC) was put forth by Russell in 1963[10] and had a helical orbit (Figure 2.7). He was unable to arrange the orbits in a flat plane since the higher energy orbits would overlap. The main reason for this overlap was the 150 kV accelerating voltage did not provide enough energy gain for sufficient turn separation. A machine of this type was never built.

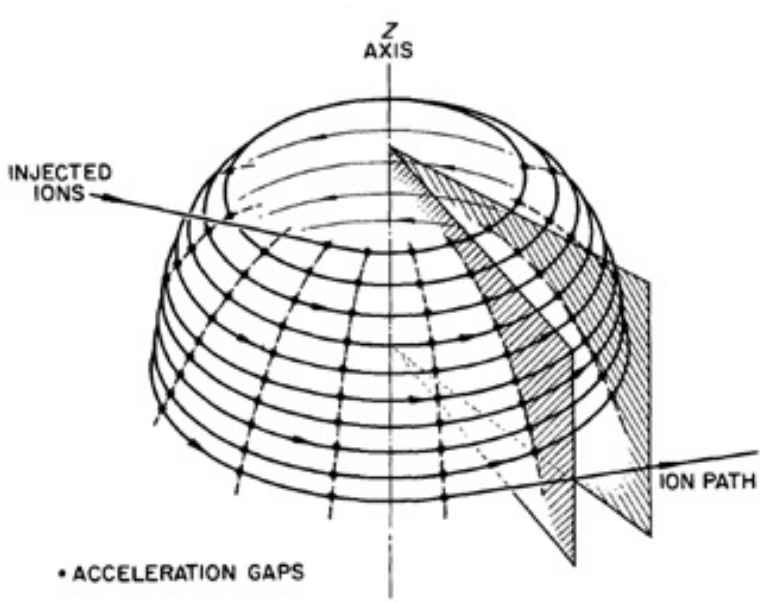

Figure 2.7: Beehive structure from Russell's separated orbit cyclotron.

Lord and Hudson [14], in 1965, proposed a magnet for an 800 MeV planar separated orbit cyclotron. The contoured pole tips, shown in Figure 2.8, provide bending

and focusing with alternating gradient fields. The design was able to get 15 T/m in the 1.5 in beam tube, but the spacing between beam tubes needed to be 4.5-5 in, which would produce a large machine. A $\frac{1}{8}$ scale model of the sector magnet was fabricated, but a full machine was never created.

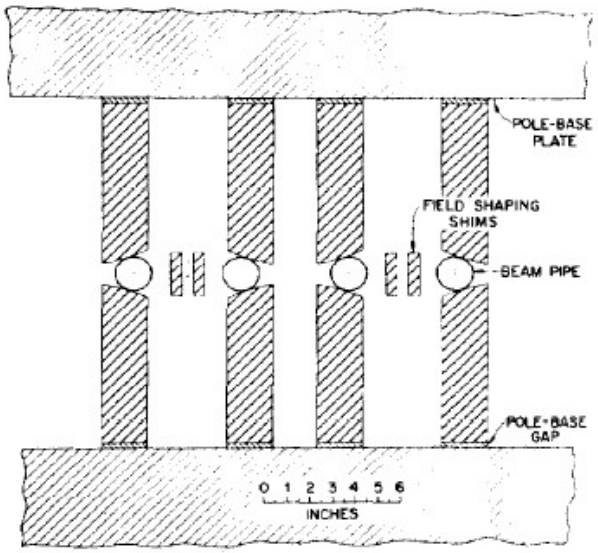

Figure 2.8: Cross section of four of the Lord and Hudson poles [14].

Another SOC, put forth by Martin [15], used the shape of the pole tip to produce about a 3 T/m gradient along the turns, which is not sufficient for our machine. Both the Martin and Lord and Husdon SOCs rely on the main dipole field and iron shape to produce the focusing and so cannot be adjusted individually. The TRITRON [16], the only SOC that was actually built, had dipole windings for each beam tube in a coil-dominated setup. The axial focusing was produced by two methods, edge focusing with a tilt of 9 degrees at the entrance to the sectors, and

gradient windings along the length of the sector arc. When the TRITRON was built, it was unknown if the designed superconducting cavities would work and as a result the turn separation, and beam aperture, were kept as small as possible, limiting the TRITRON to low beam currents. The TRITRON group came to the conclusion that "future separated orbit cyclotrons can be planned with enlarged turn separation, say 10 cm, which would leave a geometrical aperture for the beam of about 5cm. This would reduce the requirements on the stability of the injector considerably and make the acceleration of high intensity beams with low losses much easier [17]."

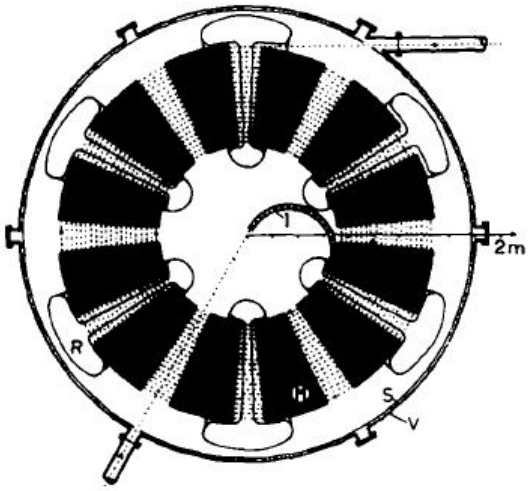

Figure 2.9: Top view cross section of the TRITRON cyclotron [16].

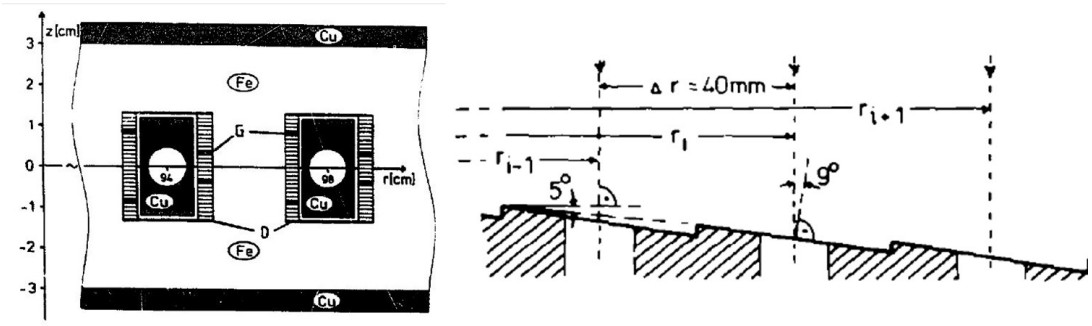

Figure 2.10: Cross section of two channels from the TRITRON [18] (Left). Top view of sector edge showing 9 degree tilt [16] (Right).

2.4 TAMU Strong-Focusing Cyclotron

The accelerator portion of the ADS system, shown in Figure 2.11, consists of the front end, an injector or booster cyclotron (TAMU100), and a main cyclotron (TAMU800). The front end [19] contains a dual ECR ion source, a low energy beam transport (LEBT) line, a radio-frequency quadrupole (RFQ), an interdigital H-type structure (IH) [20], and a medium energy beam transport (MEBT) line to bring the protons to an energy of 6.5 MeV. The TAMU100 has six sectors with a sector angle of just under 60 degrees and four RF cavities. Each sector is a straight edge wedge that has been offset from the center to create a gap for the RF cavities. The RF cavities will be made of superconducting niobium and have a tapered shape (Figure 2.12). TAMU800 consists of 12 sectors, with a sector angle of 30 degrees, and ten RF cavities. Like the TAMU100, the sectors are straight edge and offset from the center of the cyclotron to provide spacing for the RF cavities. Both cyclotrons are isochronous continuous wave (CW) separated sector cyclotrons. The parameters of the TAMU100 and TAMU800 cyclotrons are given in Table 2.1. Each sector will house a focusing and defocusing superconducting beam transport channel to

provide the required strong focusing. The layout of the beam transport channels on one of the sectors is shown in Figure 2.13. The details of the beam transport channel (Figure 2.14) will be given in chapter 4. Unless otherwise stated, the booster cyclotron, TAMU100, will be the cyclotron referred to for the remainder of this thesis.

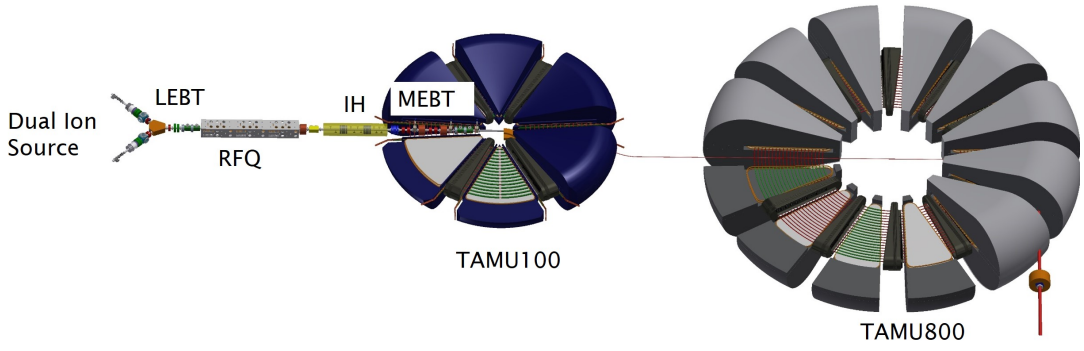

Figure 2.11: TAMU ADS accelerator system. The TAMU100 accelerates protons from 6.5 MeV to 100 MeV and feeds into the TAMU800 which accelerates the protons to a final energy of 800 MeV.

Figure 2.12: Tapered RF cavity to be used in both the TAMU100 and TAMU800 [21].

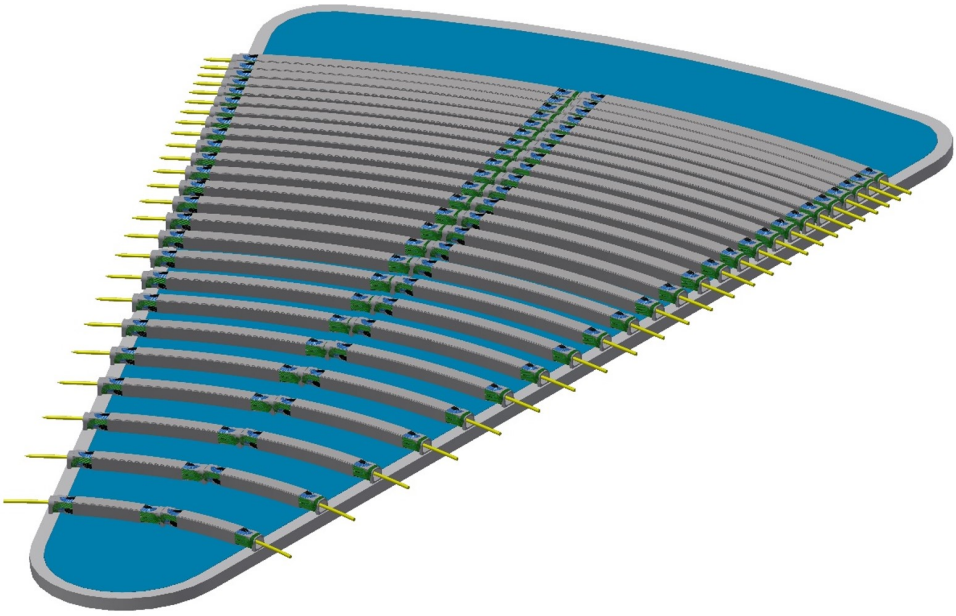

Figure 2.13: View of the bottom cold face of a sector magnet. The top plate and warm iron return have been removed to show the placement of two beam transport channels per turn.

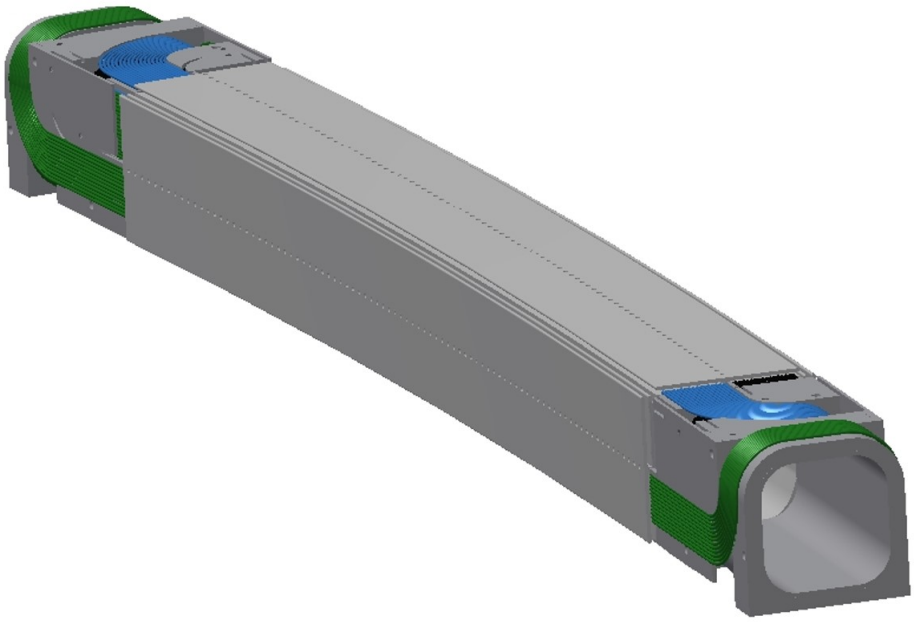

Figure 2.14: Isometric view of beam transport channel.

Table 2.1: Parameters of the TAMU100 and TAMU800 cyclotrons

Parameter	**TAMU100**	**TAMU800**
Injection Energy	6.5 MeV	100 MeV
Extraction Energy	100 MeV	800 MeV
Injection Radius	1.12 m	3.28 m
Extraction Radius	4.26 m	6.47 m
B (Inj./Ext.)	1.1/0.5 T	0.92/1.16 T
Dipole Aperture	7 cm	7 cm
Number of Sectors	6	12
Number of RF Cavities	4	10
Frequency	117 MHz	117 MHz
Harmonic	25	19
Number of Orbits	14	20

3. BEAM DYNAMICS

3.1 Reference Orbit

The equilibrium orbit in an accelerator is the path which a particle with the designed momentum would travel and is used as a reference system to discuss particle motion and for calculations in most optics codes. For cyclotrons, the equilibrium orbit and corresponding magnet parameters are often calculated based on a series of closed orbits, assuming no energy gain through one turn of the machine. Although the actual orbit is a spiral, this approximation works because the actual path of the beam is allowed to drift within the cyclotron. In the TAMU cyclotron, the path of the beam will not be allowed to drift and will need to be clearly defined to live inside the beam transport channels in each sector. As described in the previous chapter, the TAMU100 consists of six separated sector magnets, a series of beam transport channels, and four superconducting RF cavities. The general layout of the TAMU100 cyclotron can be seen in Figure 3.1. A geometric approach was used to determine the isochronous spirals which maintain a minimum 6 cm spacing between successive turns and a path which passes straight through the RF cavities. A set of parametric equations were developed to describe a spiral path through the sectors and RF cavities, based on initial inputs and parameters to be optimized. An optimization was then performed using these equations combined with the energy in each section of the cyclotron to bring the total time to the isochronous time.

3.1.1 Geometric Layout and Constraints

In order to determine parametric equations, the geometry of the system must first be defined. The six sectors are offset from the machine center on a circle of radius a. The minimum of the circle radius is set by the width of the required RF

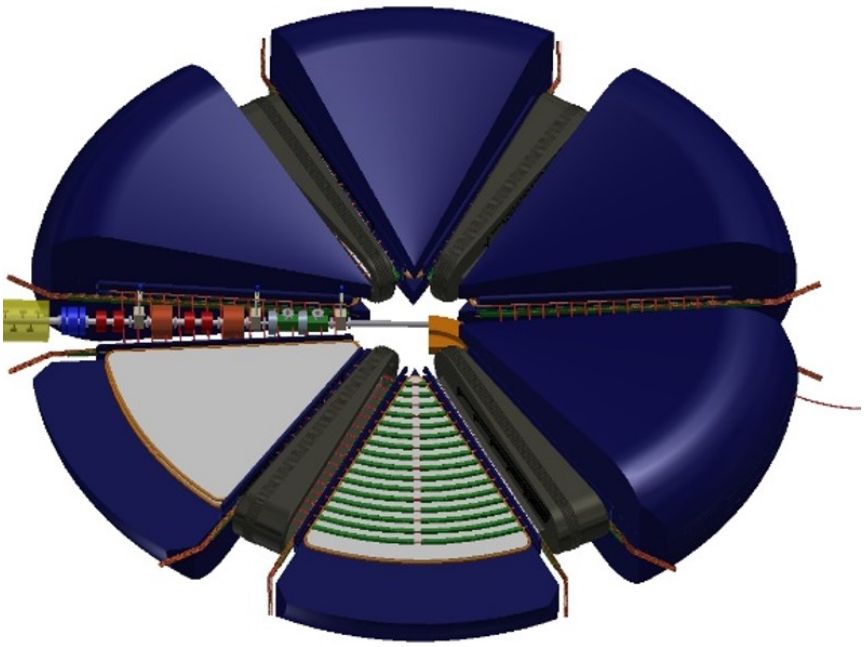

Figure 3.1: Layout of the TAMU100. The six wedge shaped sectors are separated to allow room for the 4 tapered RF cavities. The remaining two gaps allow room for injection and extraction. The upper half of two of the sectors have been removed to show the cold iron pole piece and the layout of the beam transport channels on the cold iron pole piece (bottom middle sector). A portion of the front end MEBT is shown in the left gap.

cavity gap. This is a result of each sector being centered on a multiple of 60 degrees around the circle, forming an equilateral triangle with the space required for the RF cavity as one side of the triangle. Since each sector is less than 60 degrees, the gap between the sectors increases toward the outside of the machine, creating room for the tapered cavities (Figure 3.2). By setting the initial injection radius (ri) and angle (θ_i) of approach to the first sector, requiring the straight path of the particle to be tangent to the circular path within the sector, and requiring the path out of the sector to be perpendicular to the centerline of the following cavity, the center

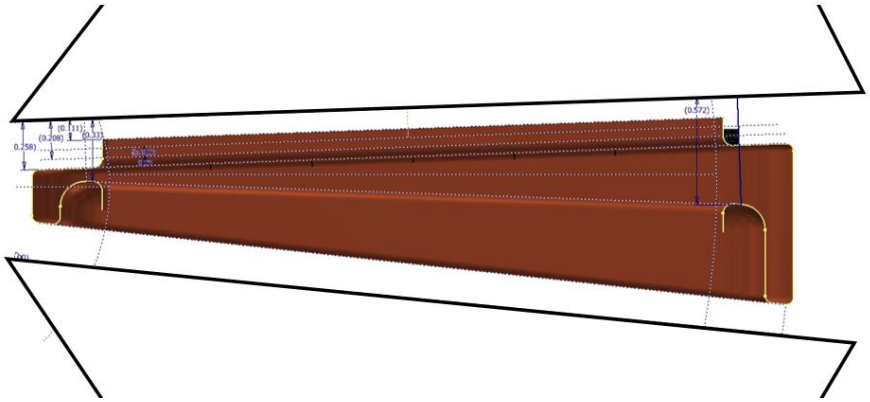

Figure 3.2: Cross section of the tapered RF cavity between the sectors.

location (s1 in Figure 3.3 and 3.4) and radius of the path within the first sector is fully determined. A similar set of requirements determines all but two of the remaining centers, those in sector three and sector six (s3 and s6). Sector three and sector six are followed by a gap for injection or extraction, which does not contain a cavity, so the constraint on the path through the gap being perpendicular to the cavity is removed. Adjusting the position of s3 or s6 is equivalent to shortening or lengthening the total path through the sector, which in turn affects the total path length through the entire machine. The full set of parametric equations can be found in reference 22.

3.1.2 Optimization

A Mathematica [23] script was written to perform the calculation and optimization of the isochronous orbit. The optimization takes two forms, one for the first orbit and another for the subsequent orbits. In the first orbit, the inputs are the initial injection radius, initial angle of injection, and the injection energy. The initial injection radius is found by calculating the circumference as $(harmonicnumber/RFfrequency)*$

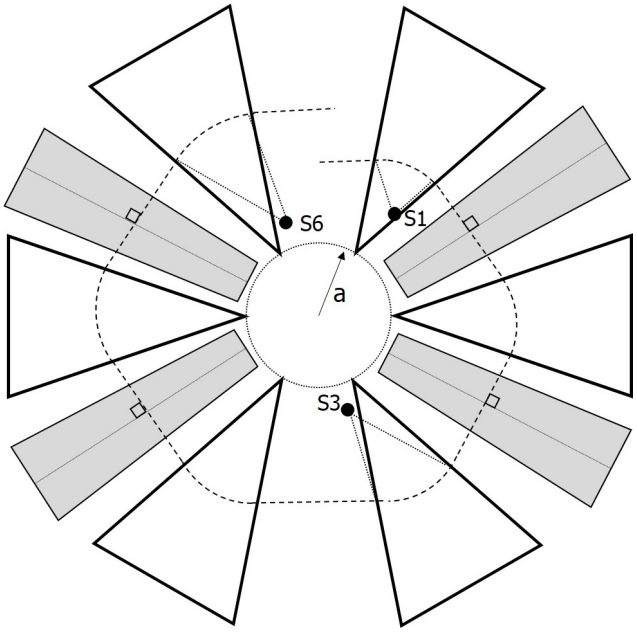

Figure 3.3: Geometric layout and optimization variables for the isochronous orbit

initialvelocity and dividing by 2π as though the particle travels in a closed circle. The variables which are used in the first optimization are the tilt of each cavity, the distance each cavity is offset, a gain factor for each cavity, and the location of s3 and s6. These variables are each given an optimization range to avoid unrealistic solutions, such as cavities overlapping sectors. The path lengths in each sector, gap between sectors, and cavity are calculated based on the initial values of the variables. The energy gained [24] in each cavity is calculated based on

$$\Delta E \approx qV(r)[2\beta c\frac{sin(\frac{\omega_{RF}L}{2\beta c})}{\omega_{RF}L}]cos(\omega_{RF}T - \phi_s), \tag{3.1}$$

where V is the radial dependent voltage from the cavity shown in Figure 3.5, ω_{RF} is the frequency of the cavity, ϕ_s is the phase the particle hits the cavity, and the bracketed value is the transit time factor across the cavity gap L. In this equation,

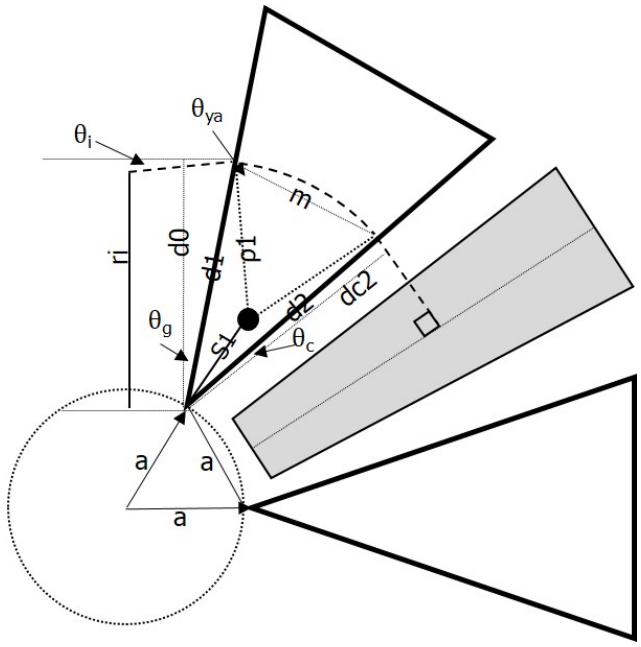

Figure 3.4: Geometry and variables used to describe the equations through the first sector.

the assumption has been made that the change in the particle velocity going through the cavity is small. Once the total path length is found, the time is then obtained by dividing each path segment by its corresponding velocity. A change in the cavity offset, which is the distance the cavity is placed from the center of the machine, would cause the particle to have a higher or lower energy gain in the subsequent sections. A change in the cavity tilt, which is allowed to run from zero to an angle projecting the particles away from the center of the machine, would cause a larger path length through the subsequent sections. The goal is for all path times between cavities, calculated as path length divided by velocity, to be the corresponding isochronous time. A minimization is performed to bring the total time to the isochronous time by varying the tilt angle of each cavity,the cavity offset, the total gain of the cavity, and

the location of s3 and s6. There is also a set of constraints imposed by the minimum spacing of successive orbits.

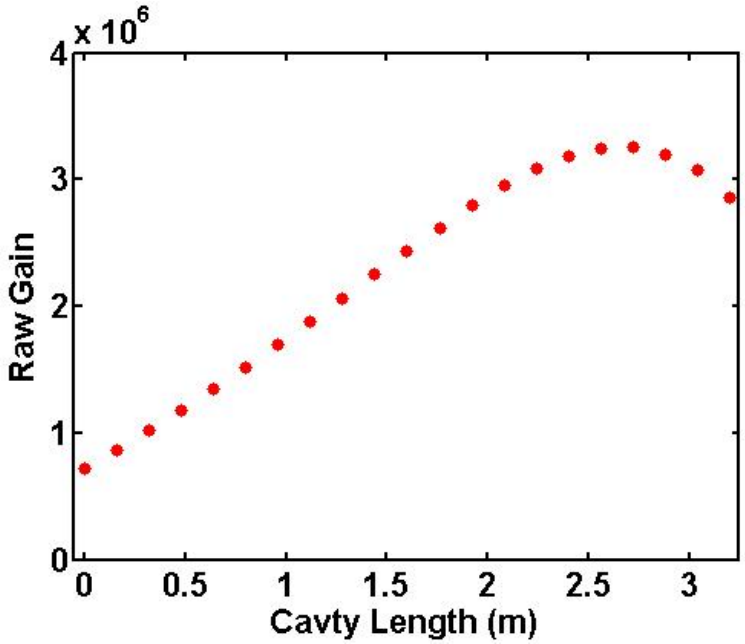

Figure 3.5: Raw gain for the TAMU100 cavity

In the first orbit optimization, the distance from the center of the first cavity to the center of the second cavity (T2 in Figure 3.6) is minimized to equal one sixth the isochronous time, the time from the second cavity to the third (T3) minimized to one third the isochronous time, the time from the third to the fourth (T4) is minimized to one sixth the isochronous time, and the time from injection to the first cavity plus the time from the fourth cavity to injection (T1) is minimized to one third the isochronous time. The isochronous time is defined as $harmonic/f_{RF}$.

After the first orbit optimization is performed, the tilt angle, the cavity offset,

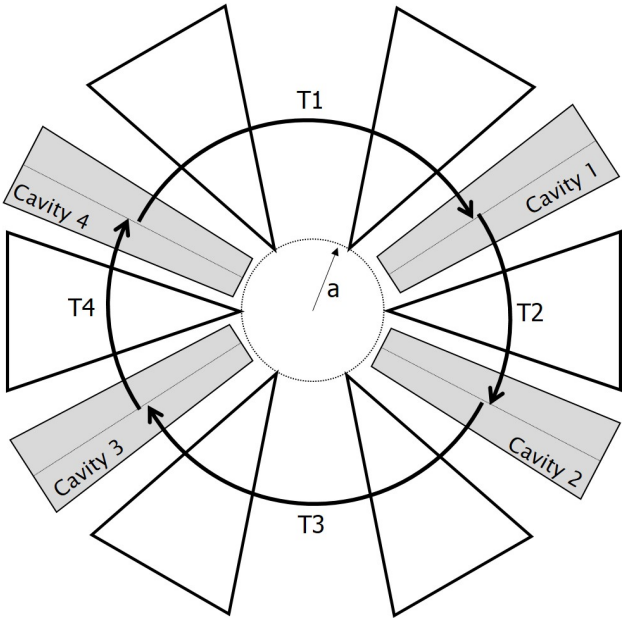

Figure 3.6: Cavity time definitions for isochronous orbit

and the cavity gain factor for each cavity is set. The phase, ϕ_s from equation 3.1, of each cavity with respect to the global time is also set so the reference particle hits the cavity at 15 degrees behind the RF maximum for the first orbit. The optimization for the remaining orbits only use two times, T1 and T3, since the only parameters left to optimize are the location of s3 and s6. These two parameters are equivalent to changing the center location of the arc through two of the sector magnets. During these optimizations, the energy gain depends not only on the radial position in the cavity, but also the time, or phase, the particle hits the cavity. An example of the isochronous spiral and phase at each cavity are shown in figures 3.7 and 3.8.

In the reference orbit method described above, the energy of the particle was determined during the optimization. Assuming a hard edge model, the magnetic field profile for each sector can be calculated from the energy, path length, and

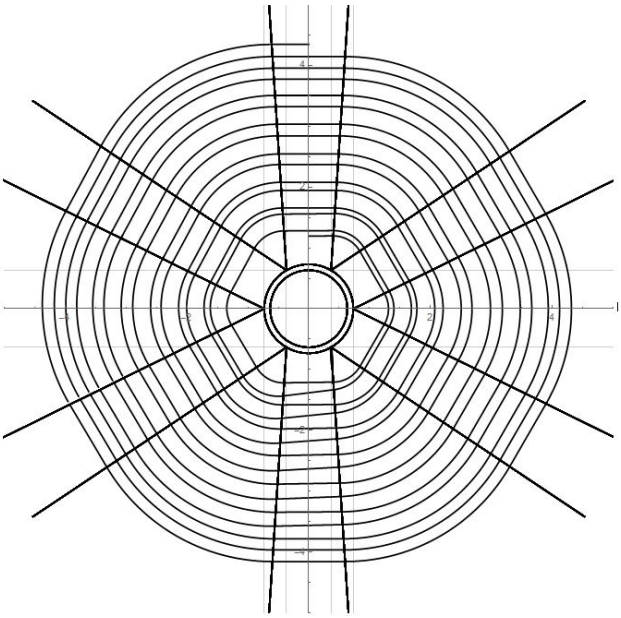

Figure 3.7: Isochronous spiral orbit

bending angle. An example profile of the magnetic field calculated for one sector is shown in Figure 3.9.

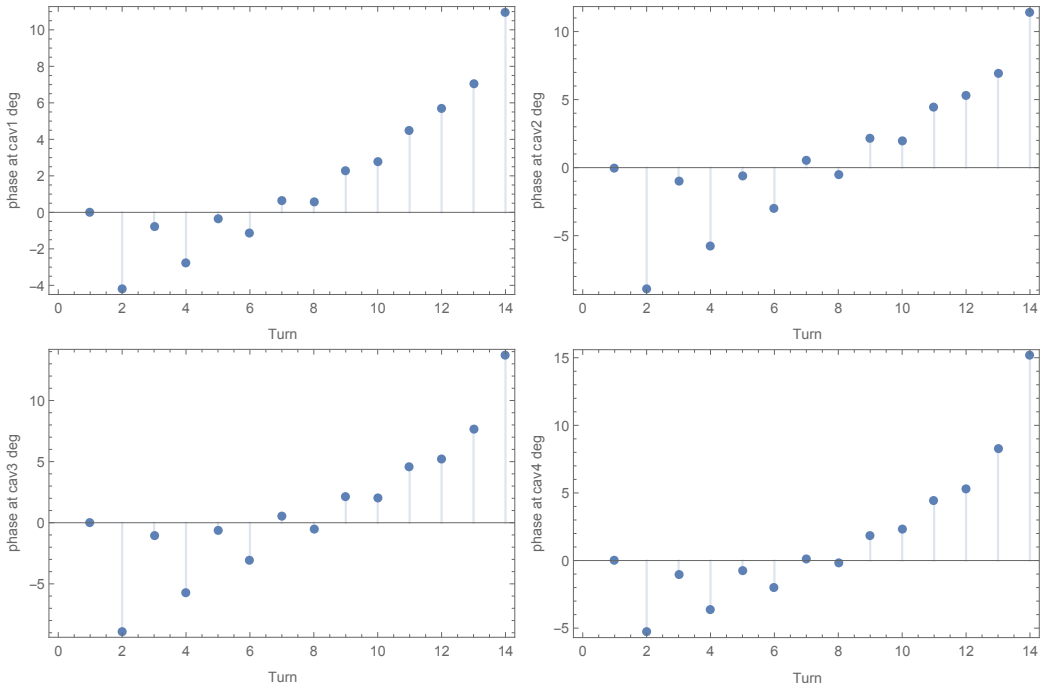

Figure 3.8: Phase the particle hits the RF cavities. The zero point corresponds to -15 degrees from the RF wave crest.

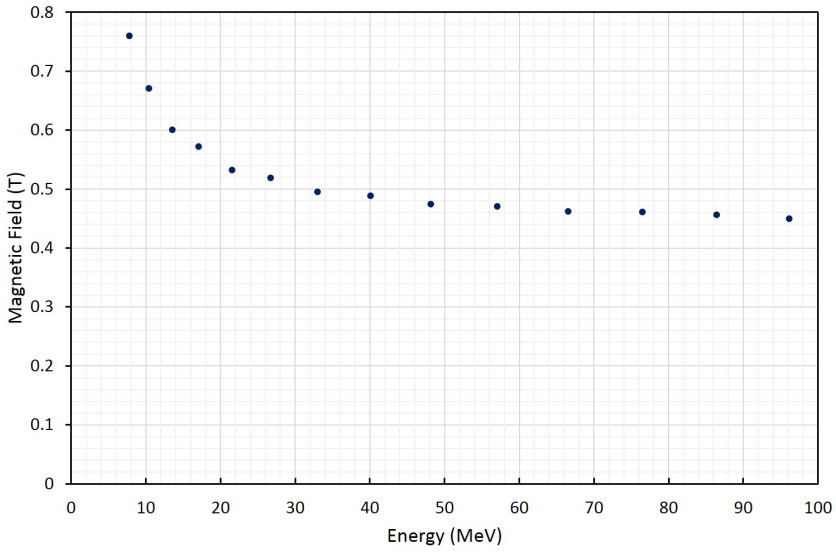

Figure 3.9: Profile of mid-plane dipole calculated for one of the sectors

3.2 Beam Optics

3.2.1 Linear Beam Optics

For the case of our strong focusing cyclotron, the bending of the beam is assumed to occur only in the x direction with focusing in both x and y. The magnetic fields produced by the dipole and quadrupole are

$$B_x = -gy,\ B_y = B_d + gx, \tag{3.2}$$

where B_d is the dipole field and g is the gradient of the quadrupole. The transverse equations of motion can be written as [25]

$$x'' - (k + k_d^2)x = 0,\ y'' - ky = 0. \tag{3.3}$$

For simplicity, the dipole and quadrupole parameter can be combined as $\kappa = k + k_d^2$, where $k = \frac{eG}{p}$ and $k_d = \frac{1}{\rho}$, and the equations of motion, for either x or y, take the form of Hill's equation:

$$u'' + \kappa u = 0, \tag{3.4}$$

with known solutions of the form:

$$u(s) = C(s)u_i + S(s)u_i', \tag{3.5}$$

For κ >0:

$$C(s) = cos(\sqrt{\kappa}s), S(s) = \frac{1}{\sqrt{\kappa}}sin(\sqrt{\kappa}s), \tag{3.6}$$

and for κ <0:

$$C(s) = cosh(\sqrt{\kappa}s), S(s) = \frac{1}{\sqrt{\kappa}}sinh(\sqrt{\kappa}s), \tag{3.7}$$

Any general solution to the equations can be expressed as a linear combination of the pair of equations,

$$u(s) = C(s)u_i + S(s)u_i' \tag{3.8}$$

$$u'(s) = C'(s)u_i + S'(s)u_i, \tag{3.9}$$

or in matrix form

$$\begin{pmatrix} u(s) \\ u'(s) \end{pmatrix} = \begin{pmatrix} C(s) & S(s) \\ C'(s) & S'(s) \end{pmatrix} \begin{pmatrix} u_i \\ u_i' \end{pmatrix} \tag{3.10}$$

Each matrix transporting a particle from the initial conditions u_i, u'_i to a location s, is only valid over a region of constant κ, so a transport matrix must be defined for each element in the strong-focusing cyclotron. Information on the particle after the n^{th} element can be found by combining the transport matrices according to:

$$M = M_n M_{n-1} ... M_2 M_1 \tag{3.11}$$

The initial hard edge model consists of drifts, combined function magnets, and sector dipoles whose transport matrices are:

$$Drift = \begin{pmatrix} 1 & L \\ 0 & 1 \end{pmatrix}, \tag{3.12}$$

$$Combined\ Function = \begin{pmatrix} cos(\sqrt{\kappa}L) & \frac{sin(\sqrt{\kappa}L)}{\sqrt{\kappa}}) \\ -\sqrt{\kappa}sin(\sqrt{\kappa}L) & cos(\sqrt{\kappa}L) \end{pmatrix}, \tag{3.13}$$

$$Sector\ Dipole = \begin{pmatrix} cos(k_d L) & \frac{sin(k_d L)}{k_d}) \\ -k_d sin(k_d L) & cos(k_d L) \end{pmatrix}. \tag{3.14}$$

The sector dipole uses the same matrix as the combined function with the quadrupole

strength set to 0.

Instead of transporting a particle from a single point in phase space to the next, it is often more useful to work with the overall beam ellipse. The solution to Hill's equations can also be written in phase amplitude form as:

$$u(s) = \sqrt{\epsilon}\sqrt{\beta(s)}cos[\psi(s) - \psi_0], \tag{3.15}$$

where ϵ and ψ_0 are integration constants, and $\beta(s)$ is the betatron function mentioned in section 2.1.

Liouville's Theorem states the area of phase space remains constant under linear transformations, which allows, in a similar manner as the single particle case, the parameters of the ellipse to be propagated with a transport matrix. The beam ellipse and orientation can be written in terms of the Courant-Snyder [26] parameters (equation. 3.16) and describe the shape of the ellipse according to Figure 3.10.

$$\epsilon = \gamma(s)u^2 + 2\alpha(s)uu' + \beta(s)u'^2,\ \gamma = \frac{1+\alpha^2}{\beta} \tag{3.16}$$

The transport matrix in equation 3.10 can also be written in terms of the Courant-Snyder parameters:

$$\begin{pmatrix} u_f \\ u'_f \end{pmatrix} = \begin{pmatrix} \sqrt{\frac{\beta_f}{\beta_i}}(cos(\Delta\psi) + \alpha_i sin(\Delta\psi)) & \sqrt{\beta_i\beta_f}sin(\Delta\psi) \\ -\frac{1+\alpha_i\alpha_f}{\sqrt{\beta_i\beta_f}}sin(\Delta\psi) + \frac{\alpha_i-\alpha_f}{\sqrt{\beta_i\beta_f}}cos(\Delta\psi) & \sqrt{\frac{\beta_i}{\beta_f}}(cos(\Delta\psi) - \alpha_f sin(\Delta\psi)) \end{pmatrix} \begin{pmatrix} u_i \\ u'_i \end{pmatrix} \tag{3.17}$$

The functions, beta, alpha, and gamma can also be transformed using the ele-

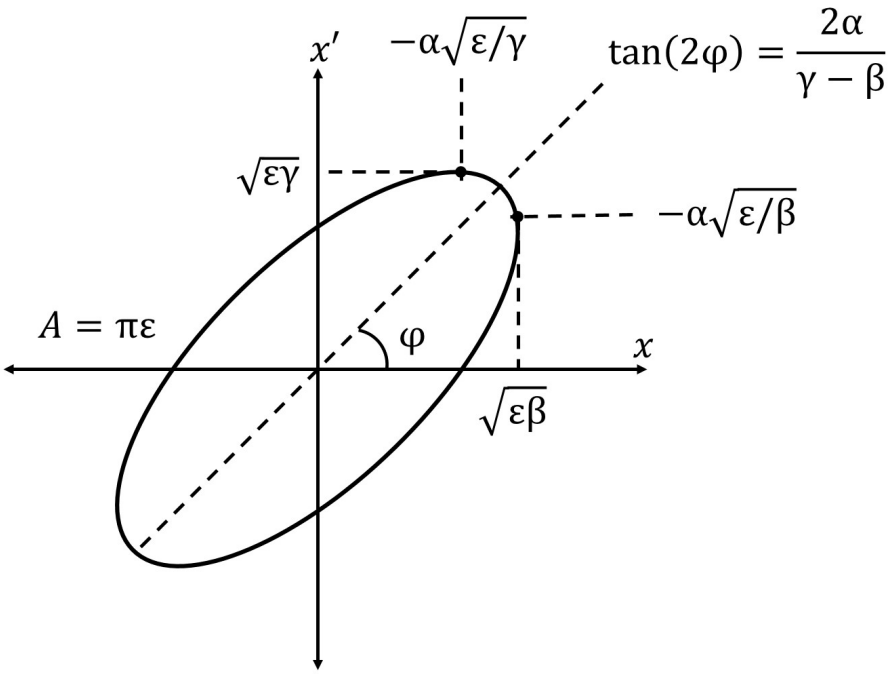

Figure 3.10: Phase ellipse parameters

ments of the transport matrix M:

$$\begin{pmatrix} \beta(s) \\ \alpha(s) \\ \gamma(s) \end{pmatrix}_f = \begin{pmatrix} M_{11}^2 & -2M_{11}M_{12} & M_{12}^2 \\ -M_{11}M_{21} & 1 + 2M_{12}M_{21} & -M_{12}M_{22} \\ M_{21}^2 & -2M_{21}M_{22} & M_{22}^2 \end{pmatrix} \begin{pmatrix} \beta(s) \\ \alpha(s) \\ \gamma(s) \end{pmatrix}_i \tag{3.18}$$

The phase advance is given by:

$$\psi(s) = \int_0^s \frac{ds}{\beta(s)}, \tag{3.19}$$

and the number of oscillations for one turn can be obtained by integrating equation 3.19 around a complete turn and dividing by 2π. The total number of oscillations in known as the tune, and is found for both transverse planes. If the values for

the tunes are not carefully chosen, it can lead to harmful resonances which in turn can lead to beam blow-up. Integer values for the tune in both x and y should be avoided. If, for example, one of the sectors was misaligned, then at every turn an integer tune would get an error kick in the same location.

Although the transverse directions have been treated as being separate, coupling between the two planes can arise from a number of sources, such as alignment errors and magnetic field errors. A few of the coupling tunes to avoid are: an integer sum of the two tunes, Q_x+Q_y=m; the half-integers tunes, $2Q_x$=$\pm$m and $2Q_y$=$\pm$m; the Walkinshaw [27] resonance, Q_x-$2Q_y$=m; $\pm 3Q_x$=m and many higher order resonances. A plot of the tunes in x and y with the resonances to avoid up to third order are shown in Figure 3.11. The marked spot on the plot shows an example working location of the tunes for the TAMU100.

3.2.2 MAD-X

A variety of computational tools are available to study the beam properties in an accelerator with a large number of matrix elements. One standard code used in particle accelerator design is the Methodical Accelerator Design (MAD) [28] code developed at CERN. MAD-X is the successor of MAD8 which was originally designed for the LHC, so the code is well suited for high energy, large radius circular machines. As a result, the code does not have the acceleration capabilities to properly model the TAMU100. MAD-X reads in a sequence file, which is a list of beamline elements, and a corresponding energy. The momentum is then internally computed and used to determine the beamline element strengths. Each time the energy in a sequence changes (a cavity is encountered), a new sequence file must be read and reference momentum changed. In order to model the TAMU100, 84 (6 sectors and 14 turns) sequence files had to be generated. As an example, the breakup of the first orbit,

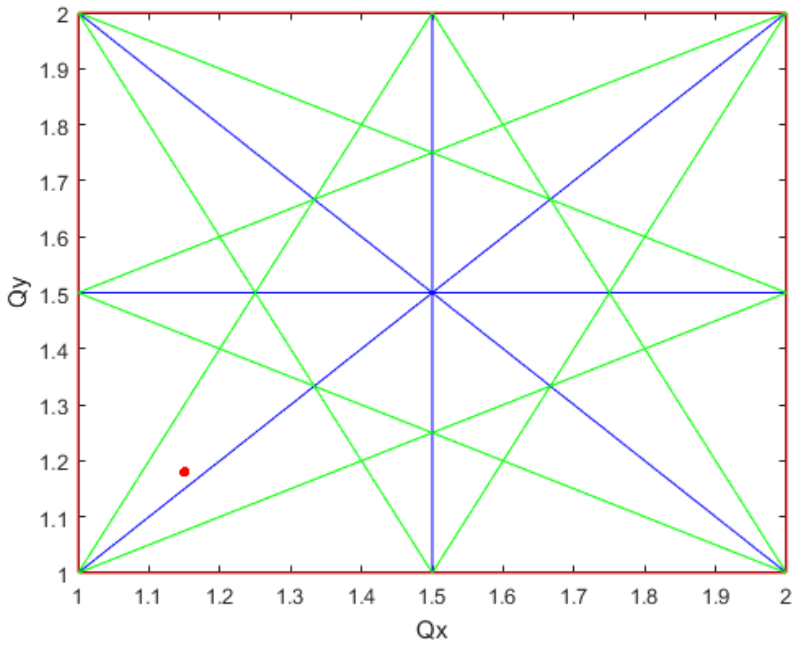

Figure 3.11: Tune diagram showing the first(red), second(blue), and third(green) order resonances. The point indicates one example working location for the TAMU100

Figure 3.12, is shown in Figure 3.13. The section is set up as a drift, combined function focusing magnet, bending magnet, combined function defocusing magnet and drift. At this stage, since MAD-X is not able to handle the RF cavity, the cavity is treated as two drifts, the first half with the initial energy and the second half with the energy gained after going through the cavity. The MAD-X representation of one of these sections is shown in Figure 3.14.

In order to create the MAD-X sequence file, a MATLAB [29] script was created to read in the output of the Mathematica isochronous spiral code. As an initial step, the entire cyclotron was entered as one sequence with the initial energy used throughout. Constraints were placed on the phase advance per turn and the maximum allowable beta functions in x and y. The focusing quadrupole strengths (k_F) and defocusing

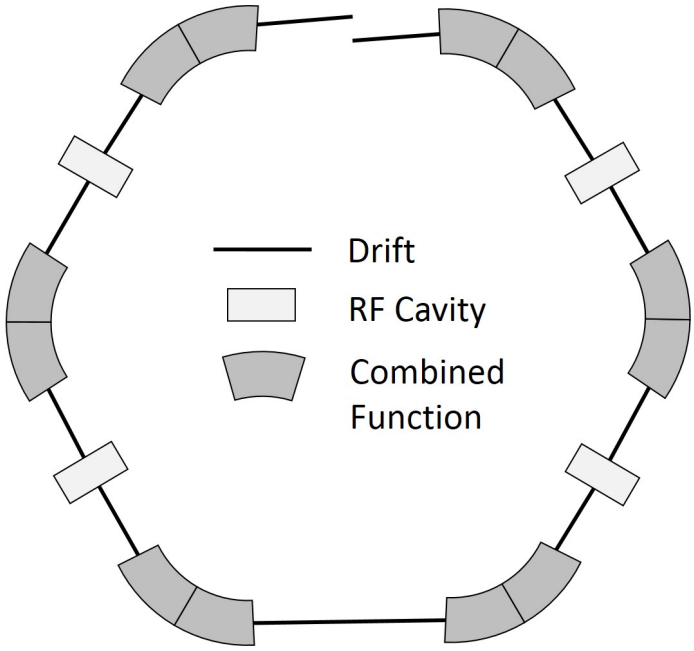

Figure 3.12: Layout of elements in the first orbit

quadrupole strengths (k_D) were kept constant for all quadrupoles in a single turn. The beta functions for one of the initial runs is shown in Figure 3.15. Although this method is incorrect for every section after the first cavity, it gives an initial idea of the required quadrupole strengths (Figure 3.16).

The next step was to divide the sequence files into single turns. This time the strength of each quadrupole were allowed to change for a total of 6 k_Fs and 6 k_Ds per turn. Again, this is only correct for the portion of the turn before the first cavity, but is more accurate than the total cyclotron case. A set of plots, Figure 3.17, show the beta functions through each of the 14 turns in which the tune per turn is kept constant. Figure 3.18 shows the required quadrupole strengths for this setup. The quadrupole strengths are then entered into 84 sequence files, for all 84 individual cells, and the total tune of the machine, with the correct energy being taken into account,

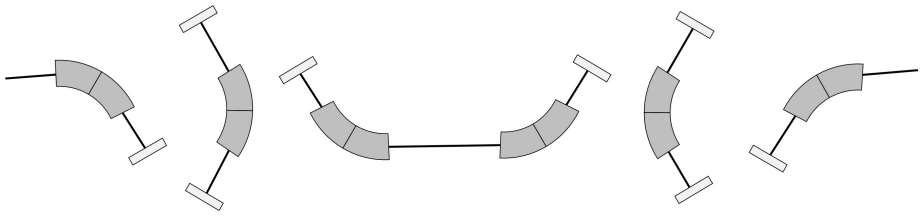

Figure 3.13: Sections of the first orbit broken into regions of constant energy

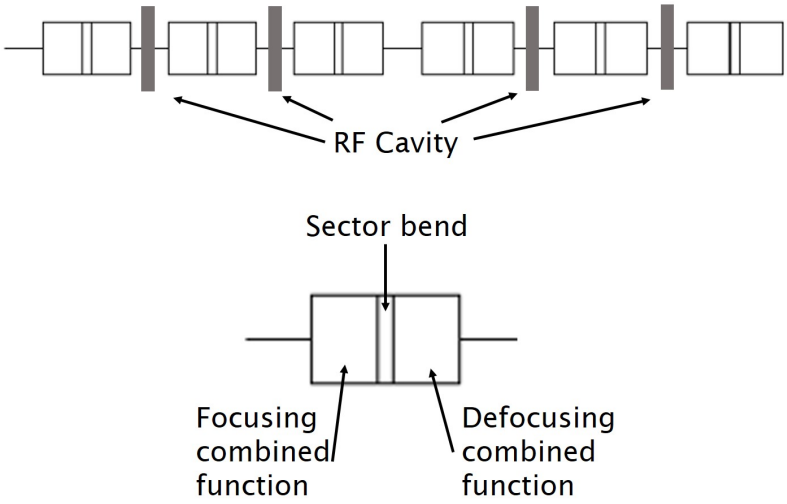

Figure 3.14: MAD-X representation of a combined function sector bend and drifts for one orbit. Each sector is divided into three parts, the focusing combined function sector bend, a plain sector bend, and a defocusing combined function sector bend.

is calculated. The resulting tune plot, for all 14 turns, is shown in Figure 3.19 where many of the points overlap one another as desired.

The final step, for proper quadrupole strengths, is to run the individual sections. Unfortunately, the total tune per turn cannot be held with this method as the code only has information about one section, not the global tune. The individual section tunes can be added up, and individual quadrupole strengths adjusted to ensure the

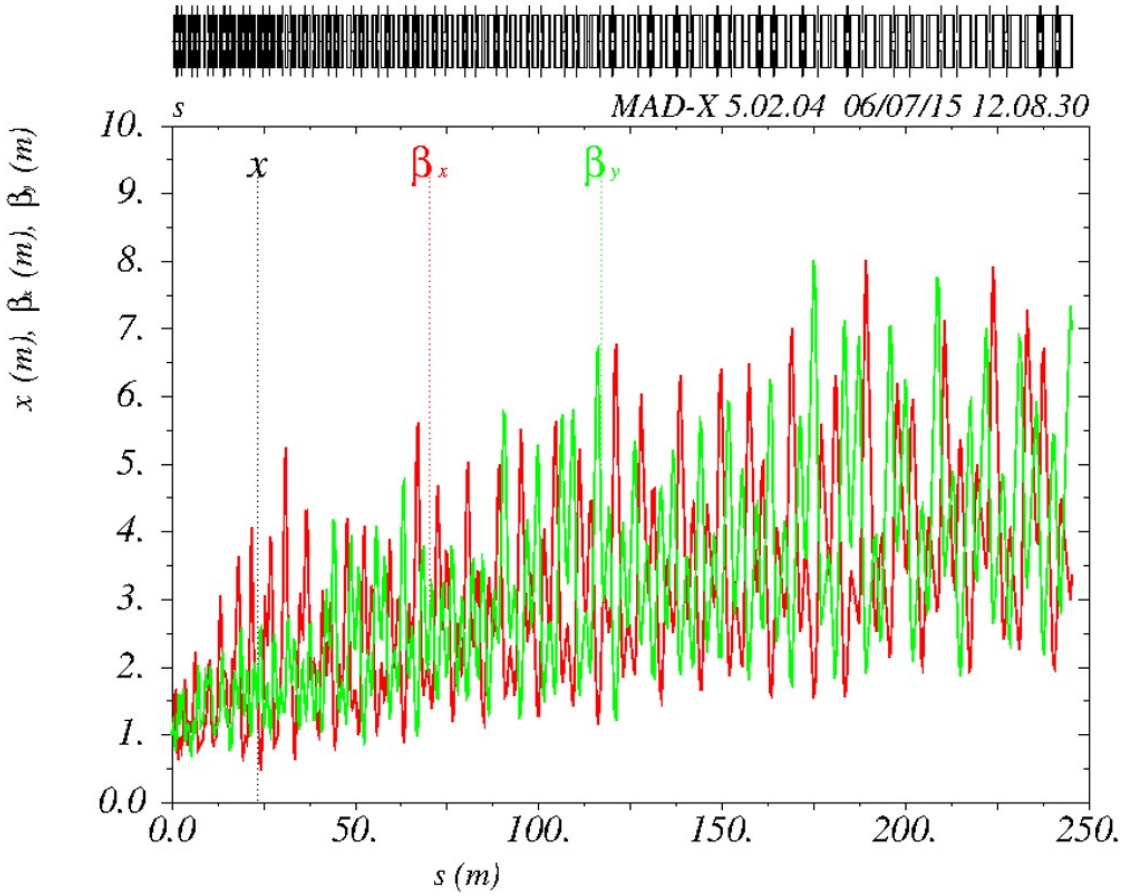

Figure 3.15: Beta functions through TAMU100.

tune per turn remains constant.

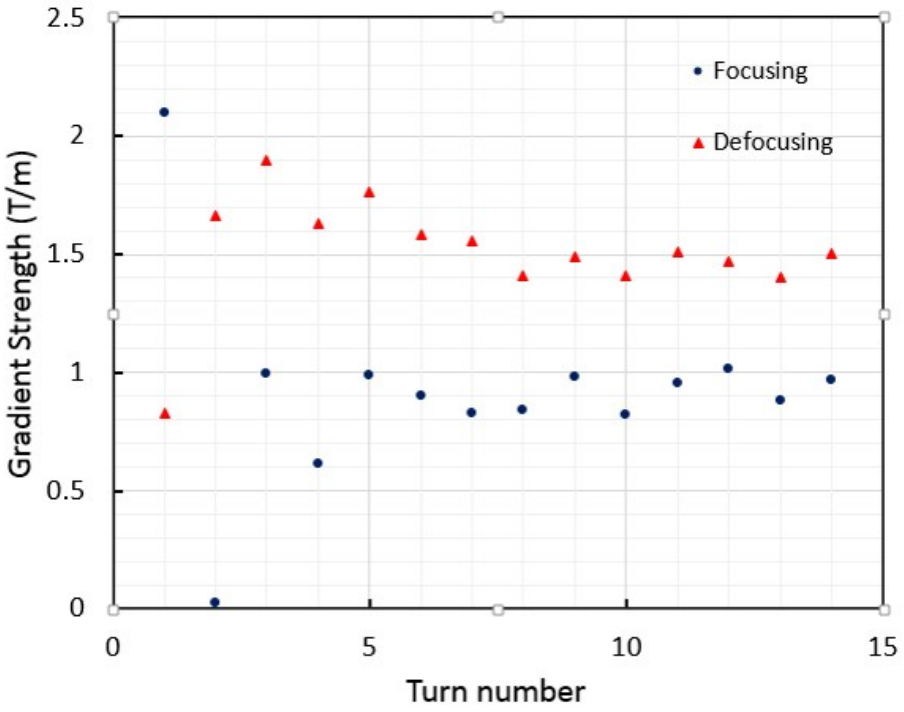

Figure 3.16: Initial quadrupole strengths which hold the tune constant while treating the whole machine at the constant injection energy.

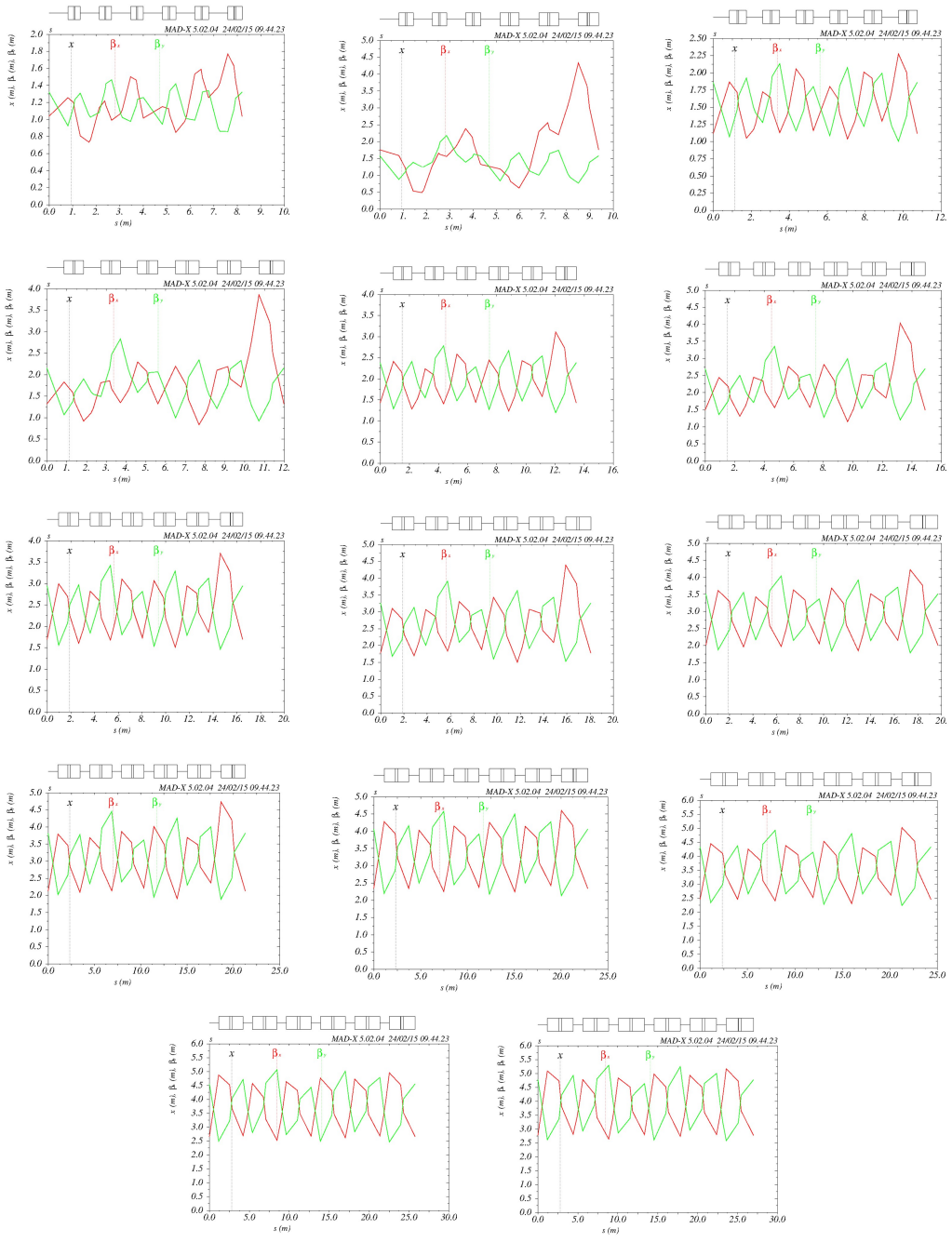

Figure 3.17: Beta functions for the 14 turns with phase advance held constant per turn. The first turn starts at the top left and the last turn on the bottom right.

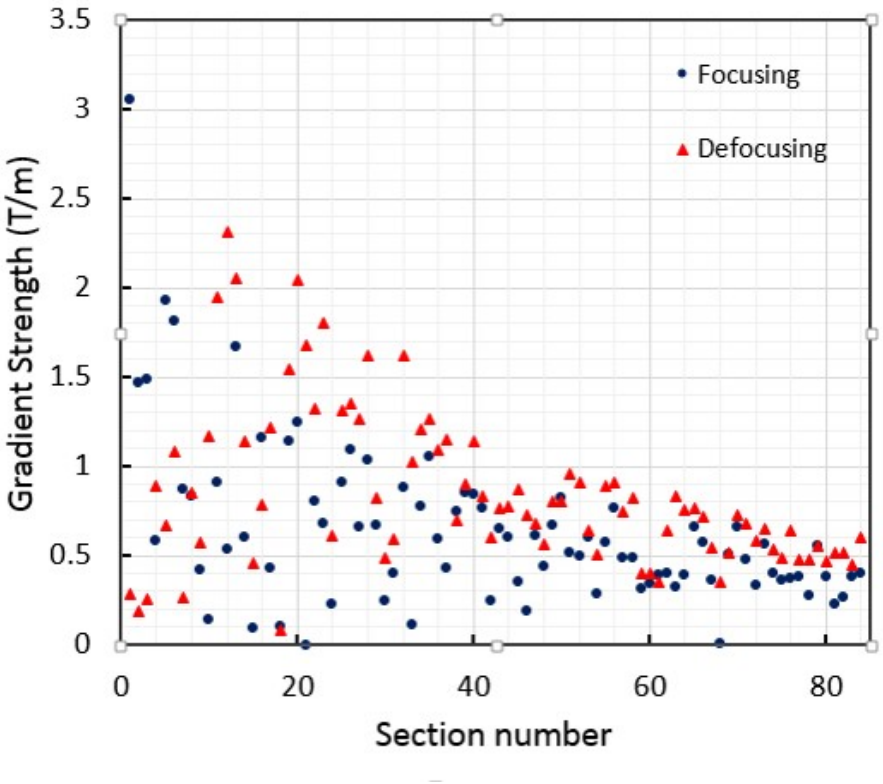

Figure 3.18: Quadrupole strengths which hold the tune constant when treating each turn at a constant energy.

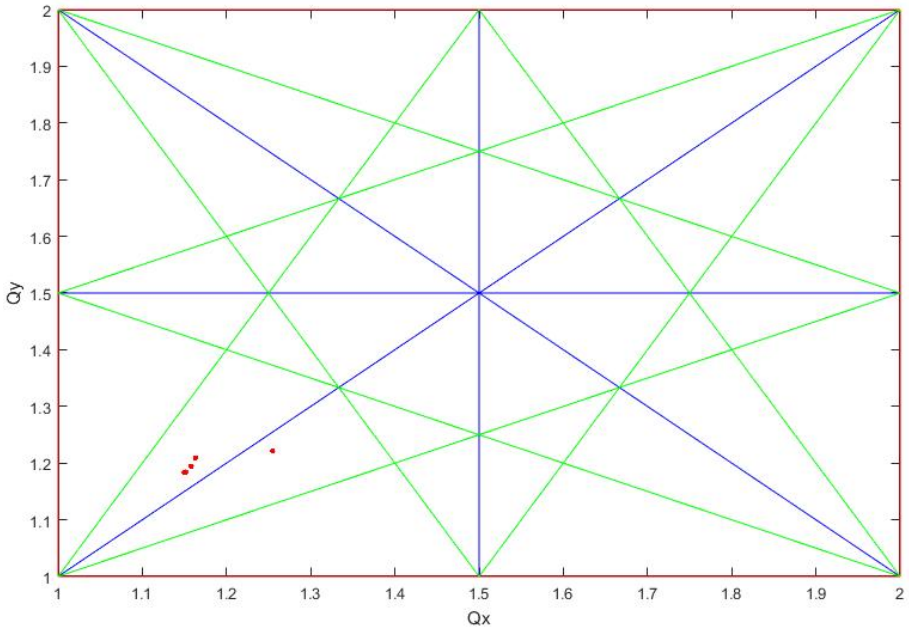

Figure 3.19: Tune plot for the 14 turns after optimization. As is desired for a constant tune, many of the points overlap.

3.3 Particle Tracking Simulations

A more complete picture of the behavior of particles in an accelerator can be obtained through particle tracking. A large number of particles can be tracked simultaneously and the individual particles can be allowed to interact with each other, as in space charge effects, or interact with the machine itself, impedance effects. The quality of the results, like many codes, depends largely on the input, which for particle tracking is the initial distribution. A realistic particle bunch has the shape of a 6D ellipsoid. Within this ellipsoid, the particles have a Gaussian distribution according to

$$\rho(x,y,z) = \frac{Nq}{(2\pi)^{3/2}\sigma_x\sigma_y\sigma_z} exp^{-\frac{x^2}{2\sigma_x^2}-\frac{y^2}{2\sigma_y^2}-\frac{z^2}{2\sigma_z^2}} \tag{3.20}$$

where N is the number of particles per bunch and q is the charge per particle. The "waterbag" distribution is often used, which is a simplified model where the 6D ellipsoid is uniformly populated. Figure 3.20 shows a comparison between the two distributions.

Another important requirement, to ensure accurate results, is that the particle tracking code be symplectic. The symplectic condition guarantees that the area of the phase space is conserved through the mapping or integration of the beamline elements [25]. Mathematically, a transport matrix is said to be symplectic if it satisfies:

$$S = M^T S M, \tag{3.21}$$

where

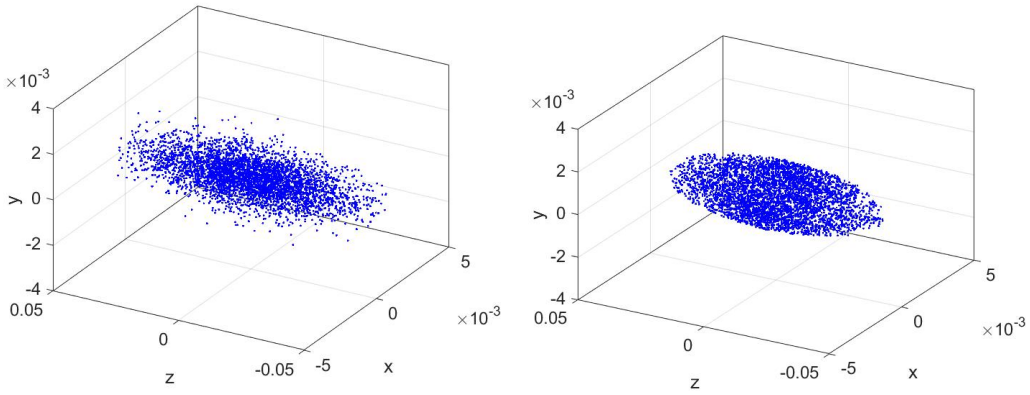

Figure 3.20: 6D ellipsoid with Gaussian(Left) and Waterbag (Right) particle distributions.

$$S = \begin{pmatrix} 0 & 1 & 0 & 0 & 0 & 0 \\ -1 & 0 & 0 & 0 & 0 & 0 \\ 0 & 0 & 0 & 1 & 0 & 0 \\ 0 & 0 & -1 & 0 & 0 & 0 \\ 0 & 0 & 0 & 0 & 0 & 1 \\ 0 & 0 & 0 & 0 & -1 & 0 \end{pmatrix}. \tag{3.22}$$

Another condition for symplecticity is

$$detM = 1. \tag{3.23}$$

The determinant of the map gives the amount of magnification of the phase space area, so if $det = 1$, the phase space area is conserved.

There are two types of symplectic tracking codes: the matrix or polynomial codes, which use a Taylor series expansion to generate a map; and the symplectic integration

codes. The matrix codes (such as TRANSPORT [30], MARYLIE [31], COSY [32]) use an expansion about the design trajectory to map through each type of magnet or beamline element. The final state may be written as an expansion about an initial phase space point, $u^i = (x, p_x, y, p_y, z, p_z)$, as a power series [33]:

$$\begin{aligned} u_1^f &= T_1(u_1^i, ..., u_m^i), \\ &. \\ &. \\ u_m^f &= T_m(u_1^i, ..., u_m^i), \end{aligned} \tag{3.24}$$

where the T_j are a set of Taylor series expanded about the initial point.

$$u_a^f = K_a + \sum_b R_{ab} u_b^i + \sum_{bc} T_{abc} u_b^i u_c^i + \sum_{bcd} U_{abcd} u_b^i u_c^i u_d^i + \ldots . \tag{3.25}$$

Here the indices $a, b, c..$ run from 1 to 6 for the dimension of the phase space. The K_a terms are constants, the R_{ab} term is the first order transfer matrix, and the T_{abc} and U_{abcd} are higher-order transfer matrices. Since the expansion is about the design trajectory, the map can only be trusted up to some radius in phase space. The main drawback of the Taylor map method is the series must be truncated at some order. This truncation, if not handled properly, will violate the symplectic condition and may add artificial components to the magnet. The Taylor method also requires a large number of expansion coefficients to be calculated and stored in the code for each element.

A solution to the truncation issue can be found using Lie algebraic methods. The mapping from an initial phase space point to a final phase space point can also be written as:

$$u^f = \mathcal{M}u^i,\ \mathcal{M} = e^{:f:}. \tag{3.26}$$

The Lie transformation, $e^{:f:}$, is defined by:

$$e^{:f:} = \sum_{n=0}^{\infty} \frac{:f:^n}{n!}, \tag{3.27}$$

and the Lie operator has the form:

$$:f: = \sum_i (\frac{\partial f}{\partial q_i}\frac{\partial}{\partial p_i} - \frac{\partial f}{\partial p_i}\frac{\partial}{\partial q_i}). \tag{3.28}$$

If $\mathcal{M}$ is a symplectic map with a Taylor expansion of the form in equation 3.25, then $\mathcal{M}$ can be written in the Lie factored product form [33]:

$$\mathcal{M} = e^{:f_1:}e^{:f_2^c:}e^{:f_2^a:}e^{:f_3:}e^{:f_4:}\ldots. \tag{3.29}$$

Each of the functions f_m is a polynomial of degree m with independent coefficients. The number of coefficients for a Lie factored map is less than a Taylor series map through the same order, and so take less computer memory. Also, since the coefficients for each order are independent, truncation at any order will still produce a symplectic map. The total map though will only be symplectic to that order and will only represent a symplectic approximation to the original map $\mathcal{M}$.

The method which has become increasingly viewed as the more reliable method for particle tracking [34, 35, 36], is that of symplectic integration. This method uses a split of the Hamiltonian into two (or more) parts,

$$H = H_1 + H_2. \tag{3.30}$$

If a map $\mathcal{M}_1$ can be found corresponding to H_1 and a map $\mathcal{M}_2$ corresponding to H_2, a map which is accurate through second order can be written:

$$\mathcal{M}(\tau) = \mathcal{M}_1(\frac{\tau}{2})\mathcal{M}_2(\tau)\mathcal{M}_1(\frac{\tau}{2}). \tag{3.31}$$

This map can be extended up to fourth order [37] with the following algorithm:

$$\mathcal{M}(\tau) = \mathcal{M}_1(\frac{s}{2})\mathcal{M}_2(s)\mathcal{M}_1(\frac{\alpha s}{2})\mathcal{M}_2((\alpha-1)s)\mathcal{M}_1(\frac{\alpha s}{2})\mathcal{M}_2(s)\mathcal{M}_1(\frac{s}{2}), \tag{3.32}$$

with

$$\alpha = 1 - 2^(1/3),\ s = \frac{\tau}{1+\alpha}. \tag{3.33}$$

Finally, this map can be extended up to any order $2n+2$ if the map of order $2n$ is known. This method, developed by Yoshida [38], is given by:

$$\mathcal{M}_{2n+2}(\tau) = \mathcal{M}_{2n}(z_0\tau)\mathcal{M}_{2n}(z_1\tau)\mathcal{M}_{2n}(z_0\tau), \tag{3.34}$$

where

$$z_0 = \frac{1}{2 - 2^{1/(2n+1)}},\ and\ z_1 = \frac{-2^{1/(2n+1)}}{2 - 2^{1/(2n+1)}}. \tag{3.35}$$

There are a number of particle tracking codes, but like the optics codes, no code, in its present state, was capable of accurately tracking in our strong-focusing cyclotron. Two codes, MAD-X-PTC and Synergia, have been modified toward this purpose. The modifications and results from these codes are presented in the next sections.

3.3.1 MAD-X-PTC

The Polymorphic Tracking Code [39] (PTC) exists as a module within MAD-X and allows tracking through thick elements. Similar to MAD-X, it was designed for

circular machines and requires the sequences be divided into sections with constant energy.

In order to add acceleration, a MATLAB code was written which externally adds the acceleration and feeds it back into the PTC tracking in MAD-X. The code works as follows (and is shown graphically in Figure 3.21):

1. The output of the isochronous spiral code is used to create a series of sequence files. This is the same as was done for the MAD-X runs.

2. An initial particle distribution is created and input into a MAD-X PTC file.

3. The PTC module in MAD-X is used to track particles through a constant energy sequence.

4. The particle data, {X,PX,Y,PY,T,PT} is read from the output file.

5. Acceleration is applied, described in detail below, and the new particle distribution is created within a MAD-X PTC file.

6. The next sequence is called. Steps 3 through 6 are repeated until the end of the cyclotron has been reached.

3.3.1.1 Acceleration Module

The particle data output by MAD-X-PTC must be properly handled to perform acceleration. The horizontal and vertical position (x and y) are measured as an offset of the ideal orbit, and do not need to be unnormalized. The horizontal and vertical momentum have both been normalized with respect to the reference momentum, $PX = p_x/p_0$ and $PY = p_y/p_0$. The value output for time has been multiplied by the speed of light and is the difference between the particle and the time of the reference particle, $T = -ct$. The sign is set so that a particle arriving before the reference

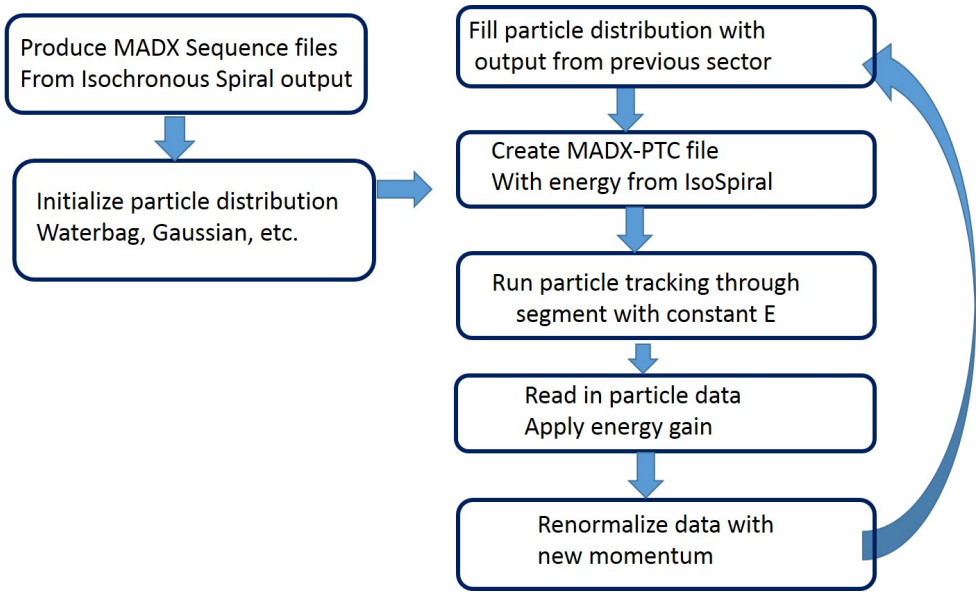

Figure 3.21: Sequence of steps for MAD-X-PTC with the MATLAB acceleration module

particle will have a positive value, and the reference particle arrives at the end of the sequence with a time of zero. The transverse momentum is the change in energy between the particle and reference particle energy, normalized to the longitudinal portion of the reference momentum and the speed of light $PT = \Delta E/p_s c$. For each call to the acceleration module, the reference momentum for the previous sequence ($prevmom$) and the reference momentum($refmom$) for the sequence following are calculated from the known energies from the sequence file. The horizontal and vertical momentum for each particle are unnormalized then renormalized according to:

$$PX = prevmom * \frac{PX}{refmom}, \; PY = prevmom * \frac{PY}{refmom}. \tag{3.36}$$

The time difference T is divided by the speed of light to get the relative time for each particle to the reference particle and saved in the variable $relativetime$. The

energy for each particle is pulled from the PT variable in a similar unnormalization process as with momentum,

$$EbeforeCavity = PT * prevmom * c + prevenergy, \tag{3.37}$$

where the *prevenergy* is from the previous sequence file. The energy gain is calculated with the same form as equation 3.1, and the resulting energy, $EafterCavity = EbeforeCavity + \Delta$E, is renormalized and saved as the new PT value.

$$PT = \frac{(EafterCavity - refenergy)}{(refmom * c)}. \tag{3.38}$$

3.3.1.2 Combined Function Magnet

As the TAMU100 is mainly composed of combined function magnets, separated only by drifts and RF cavities, it is important to look at how these are treated within MAD-X-PTC. PTC is a symplectic integration code using a second order integration method. For a combined function sector bend there are two main options for how the Hamiltonian can be split. The TEAPOT split [40]:

$$H = \underbrace{-(1+\frac{x}{\rho})\sqrt{(1+p_t)^2 - p_x^2 - p_y^2}}_{T_1} + \underbrace{V(x, y : \rho^{-1})}_{T_2}, \tag{3.39}$$

which is a drift-kick split, where T_1 represents a drift in polar coordinates and T_2 is the kick described by equation 3.41, and the second Hamiltonian split is written as:

$$H = \underbrace{-(1+\frac{x}{\rho})\sqrt{(1+p_t)^2 - p_x^2 - p_y^2} + b_1(x + \frac{x^2}{2\rho})}_{H_1} + \underbrace{V(x, y : \rho^{-1}) - b_1(x + \frac{x^2}{2\rho})}_{H_2}, \tag{3.40}$$

where H_1 is the Hamiltonian of a sector bend with a vertical field and H_2 is the kick portion. According to Etienne Forest [39], PTC must compute a template from which it extracts the B field from the multipole components. The potential is given by:

$$\{(p_d + x)(\frac{\partial^2}{\partial x^2} + \frac{\partial^2}{\partial y^2} - \frac{\partial}{\partial x}) - \frac{\partial}{\partial x}\}V = 0, \tag{3.41}$$

and solved by an iterative process to order $SECTOR\_NMUL$, which is a variable set by the user. When $SECTOR\_NMUL$=2 the results are consistent with the Ripken [41] formalism, and when $SECTOR\_NMUL$=3 the results line up with those of MAD-X based on the work by Karl Brown [42]. The user is also able to set the number of integration steps per element.

3.3.1.3 Results

A sequence file was created from the isochronous spiral code output which contains 84 sequences (6 cells per turn for 14 turns). A marker was placed after each cavity, or in the middle of the drift space for sequences without cavities, to record the six phase space coordinates for each particle. The sequence file used for the MAD-X-PTC particle tracking can be found in appendix A. The MAD-X convention is a phase lag of 1 corresponds to 360 degrees. In order to operate at 15 degrees behind the crest, which is located at 90 degrees, the desired phase lag is set in the sequence file to 5/24. Since space charge is not being considered in this model, the distribution of the particles is not as critical and instead of a Gaussian bunch, a waterbag distribution is sufficient. Injection into the TAMU100 is expected to have an initial transverse emittance of 1 mm-mrad and a longitudinal spread of 6°. The size of the beam pipe is also specified in the sequence file as an aperture in the combined function magnets and sector bends(labeled sbends in MAD). The aperture sets the radial dimension, and all particles going beyond this radius are removed or "lost".

The code does not allow a beam pipe aperture to be set for the drift regions. The initial particle distribution and phase space distribution in x and y are plotted in Figure 3.22. The energy gain through the machine (Figure 3.23) is consistent with the expected energy gain obtained with the isochronous spiral code. As an initial run,

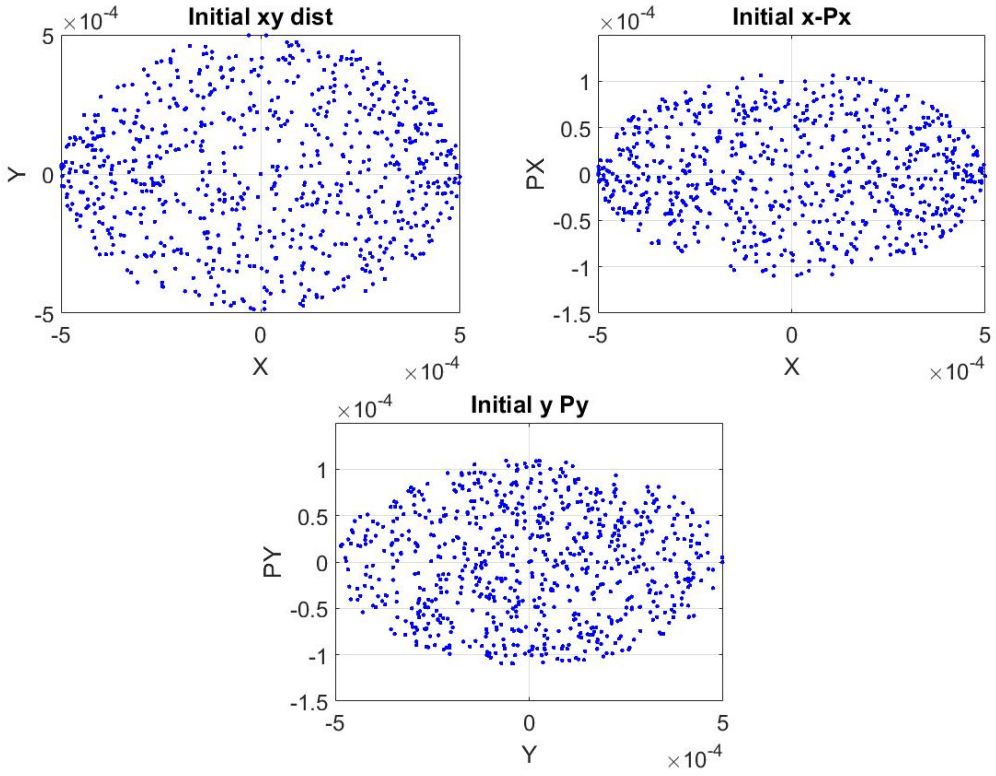

Figure 3.22: The initial waterbag particle distribution used for tracking in x-y(Top), x-py(Middle), and y-py(Bottom)

the particles were tracked through the machine with the quadrupoles set to nearly zero. The initial x-y distribution and phase space plots are shown in Figure 3.22. In this arrangement the beam grows significantly in the y direction (Figure 3.24).

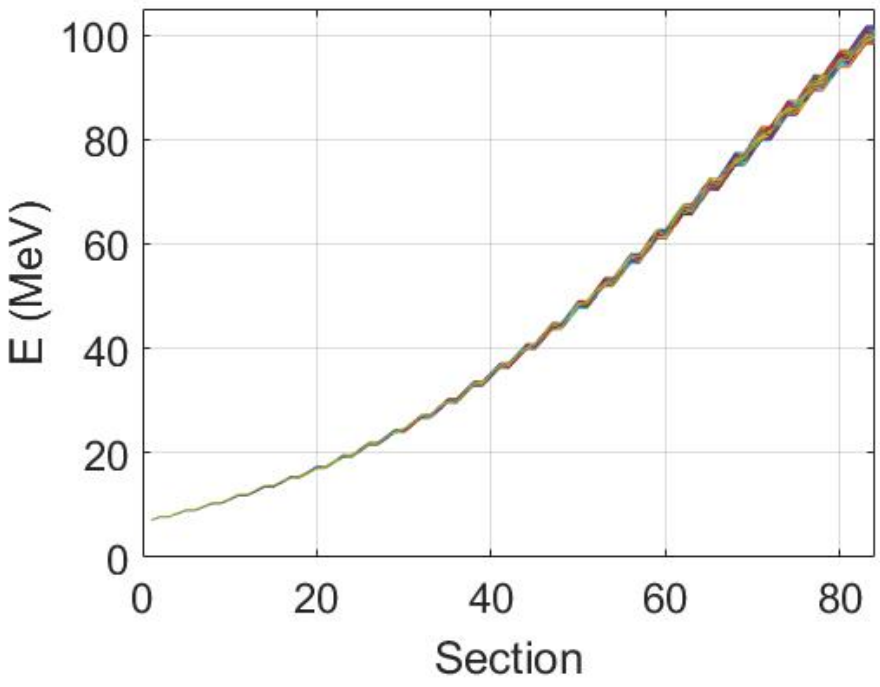

Figure 3.23: Energy gain through the TAMU100

Two methods of particle tracking were then performed using the strengths for the quadrupoles which maintain constant tunes per turn, as found from the MAD-X runs. For each of these two methods, an emittance of 1, 5, and 10 mm-mrad were used for the initial particle distributions, with the 1 mm-mrad shown in Figure 3.22. One method is characterized by setting the flag in PTC to use the "exact" Hamiltonian, which is of the form found in equation 3.39 or 3.40. The final phase space plots in x and y and the final particle x-y distribution for the "exact" Hamiltonian cases are shown in Figure 3.25. In the figure, the emittance increases from top to bottom. The other method had the PTC flag set to "extended" Hamiltonian, which expands the square root portion of the exact Hamiltonian. The results of the final phase space plots and distribution for the expanded Hamiltonian cases are shown in Figure 3.26.

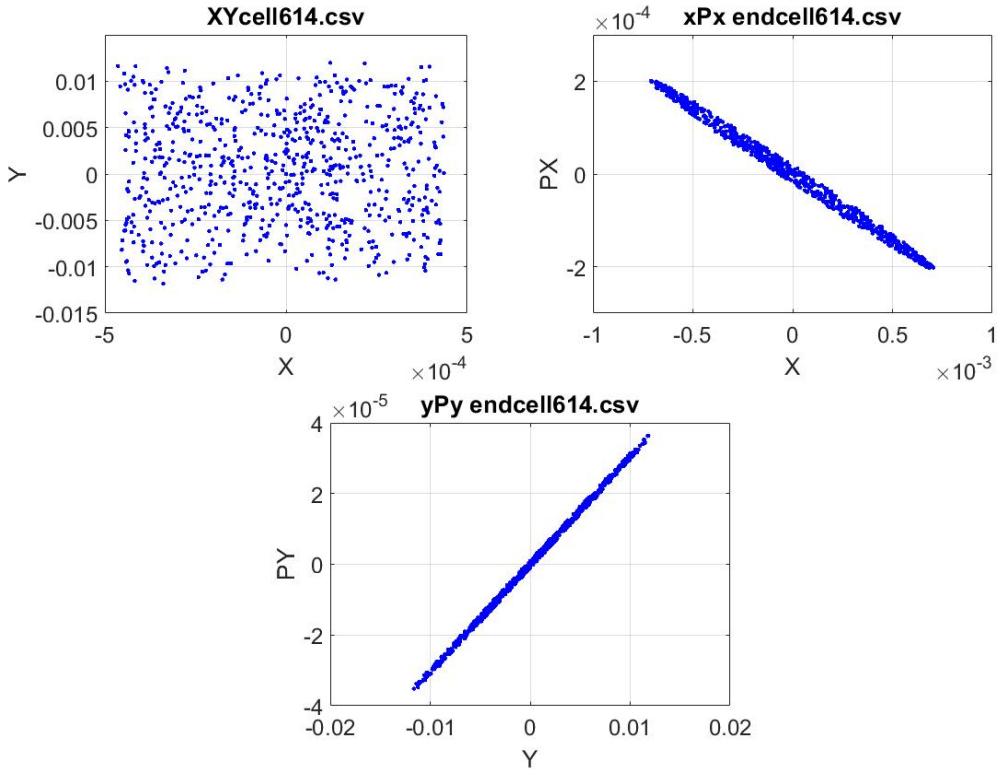

Figure 3.24: The final particle distribution for the case with the quadrupole strengths set to nearly zero in x-y(Top), x-py (Middle), and y-py (Bottom)

3.3.2 Synergia

Synergia [43] is a particle tracking code out of Fermilab with the capability for single or multiple bunch tracking. The code can include collective effects, such as space charge, which is important for high intensity beams, and one of the main reasons it is of interest for simulating the TAMU100. Similar to MAD-X and PTC, the code was designed for high energy, large circumference rings and had the same issues with acceleration as was dealt with in MAD-X. A new element has been built within the CHEF portion of Synergia to handle an RF cavity of a given length. This element takes into account the transit time factor and phase according to equation 3.1.

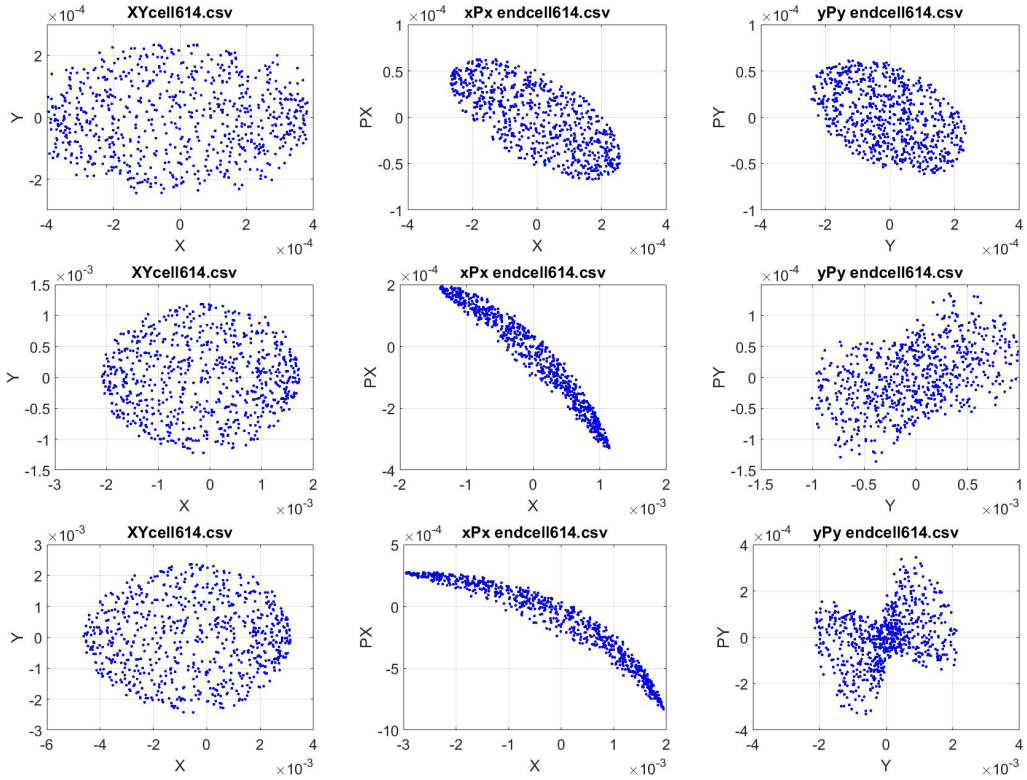

Figure 3.25: The final particle distribution for the constant tune case using the "exact" Hamiltonian form of PTC. Emittances shown are 1 mm-mrad(Top), 5 mm=mrad(Middle), and 10 mm-mrad(Bottom) Plots are x-y(Left), x-py(Middle), and y-py(Right)

Although this modification is not available in the main Synergia distribution, there are future plans to implement it.

3.3.2.1 Combined Function Magnet

Synergia, or more accurately CHEF which is called within Synergia, treats the combined function as a pure dipole with thin quadrupole kicks. The element is divided into two ends and a body. The body section is based on a unit of four thin quadrupoles and three dipole sections, and can be made of any number of units (with 40 units the current default). The position of the thin quadrupoles within the unit

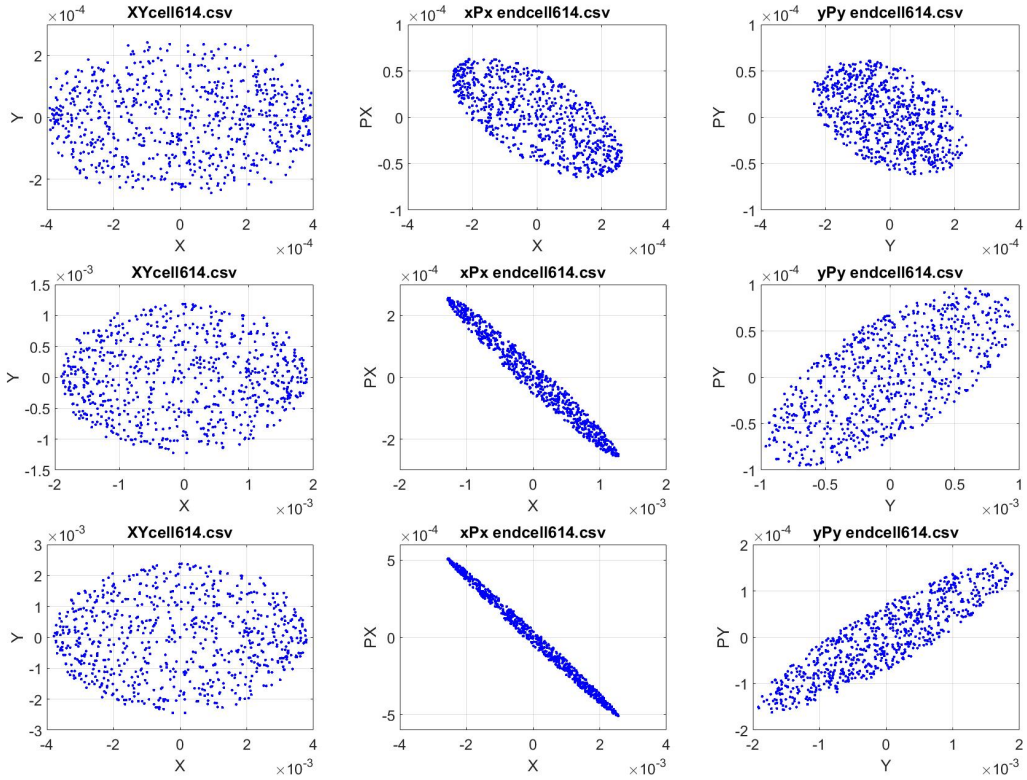

Figure 3.26: The final particle distribution for the constant tune case using the "expanded" Hamiltonian form of PTC. Emittances shown are 1 mm-mrad(Top), 5 mm-mrad (Middle), and 10 mm-mrad(Bottom) Plots are x-y(Left), x-py (Middle), and y-py (Right)

is based on the work of R. Talman [40]. A visual representation of the optimum quadrupole placement and strength for four quadrupoles can be seen in the bottom of Figure 3.27. The length of the total quadrupole is L and the quadrupole strength is $4q$. In the four thin quadrupole setup, the end sections have length $\frac{6}{15}\frac{L}{4}$ and the equal strength quadrupoles are separated by a distance $\frac{16}{15}\frac{L}{4}$. Two ends and three separations make $\frac{2*6}{15}\frac{L}{4} + \frac{3*16}{15}\frac{L}{4} = L$. When there are n of these units, the $\frac{L}{4}$ term becomes $\frac{L}{n4}$ and the strength of each quadrupole becomes $\frac{q}{n}$. Tracking of the particles through the dipole section is done as an exact map of a charged particle traveling on

a helical path through a magnetic field. The details can be found in reference 44.

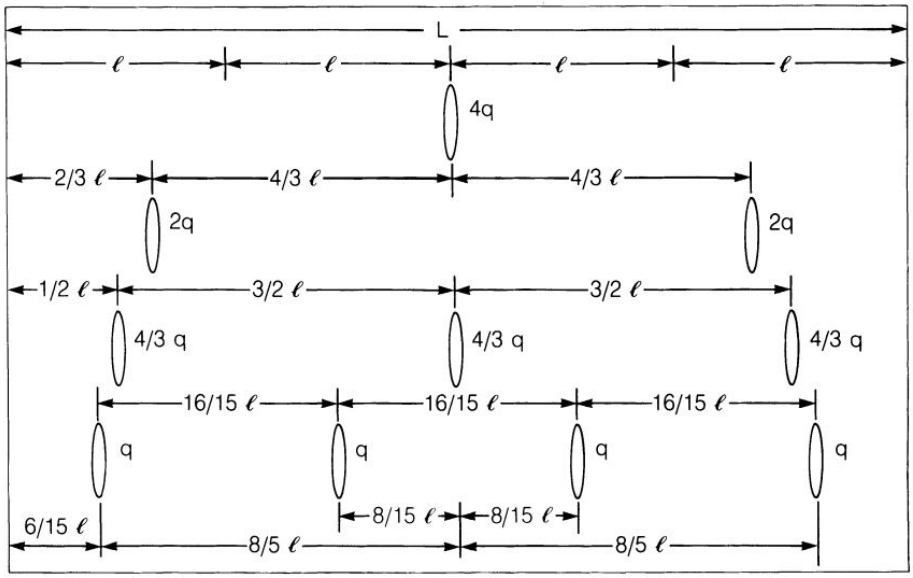

Figure 3.27: Representation of thick quadrupole by n thin quadrupoles, for n=1 (top) through n=4 (bottom) [40].

3.3.2.2 Results

The same initial waterbag particle distribution used in the MAD-X-PTC tracking was used for the Synergia simulations. The sequence file used for Synergia particle tracking can be found in appendix A. The sequence file differs from the MAD version since the RF cavities could be directly added. The sequence still has to be split into 84 cells since Synergia scales the strength of the elements (dipoles,quadrupoles, etc.) following a cavity to the energy of the reference particle after the cavity. In order to avoid this rescaling, the energy is explicitly set at the beginning of the 84 sequence files, and the RF cavity is placed at the end of the cell. The results of the simulation

with the quadrupole strength set nearly to zero (Figure 3.28) agrees with the MAD-X-PTC results fairly well. The final particle distribution is the same size and the phase space plots have a similar shape and size. A second simulation was also run with the strengths of the quadrupoles set to maintain a constant tune, these were the same strengths used for the MAD-X-PTC run. Compared to the MAD run, the y dimension is the same, but the x dimension is a factor of 100 larger. This is due to the x dimension of the beam blowing up toward extraction. This blowup can be seen in the top plot of Figure 3.31. The results of this run are plotted in Figure 3.30. This is also reflected in the phase space plots. The x and y position of a few of the particles is shown in Figure 3.31. Toward the end of the cyclotron, what appears to be a resonance buildup can be seen. In fact, if they tunes are not properly adjusted, nearly all particles are lost. In order to calculate the tunes in Synergia, the transfer matrix for each section was output. Using the matrix elements and the transfer matrix form of equation 3.17, the phase advance($\Delta\psi$), beta at the end of the section(β_f), and alpha($alpha_f$) at the end of the section can be found according to:

$$\Delta \quad = arctan[\frac{m_{12}\beta_i}{\beta_i(m_{11}\beta_i - \alpha_i m_{12})}], \tag{3.42}$$

$$\beta_f = \frac{1}{\beta_i}(\frac{m_{12}}{sin(\Delta\psi)})^2, \tag{3.43}$$

and

$$\alpha_f = -\frac{\sqrt{\frac{\beta_f}{\beta_i}}m_{22} - cos(\Delta\psi)}{sin(\Delta\psi)}. \tag{3.44}$$

The Synergia tune plot, which uses the same quadrupoles as the MAD tune plot in Figure 3.19, is shown in Figure 3.32. The tunes have clearly shifted compared to the

desired working point and MAD tunes. The differences in the two codes is discussed further in the following section.

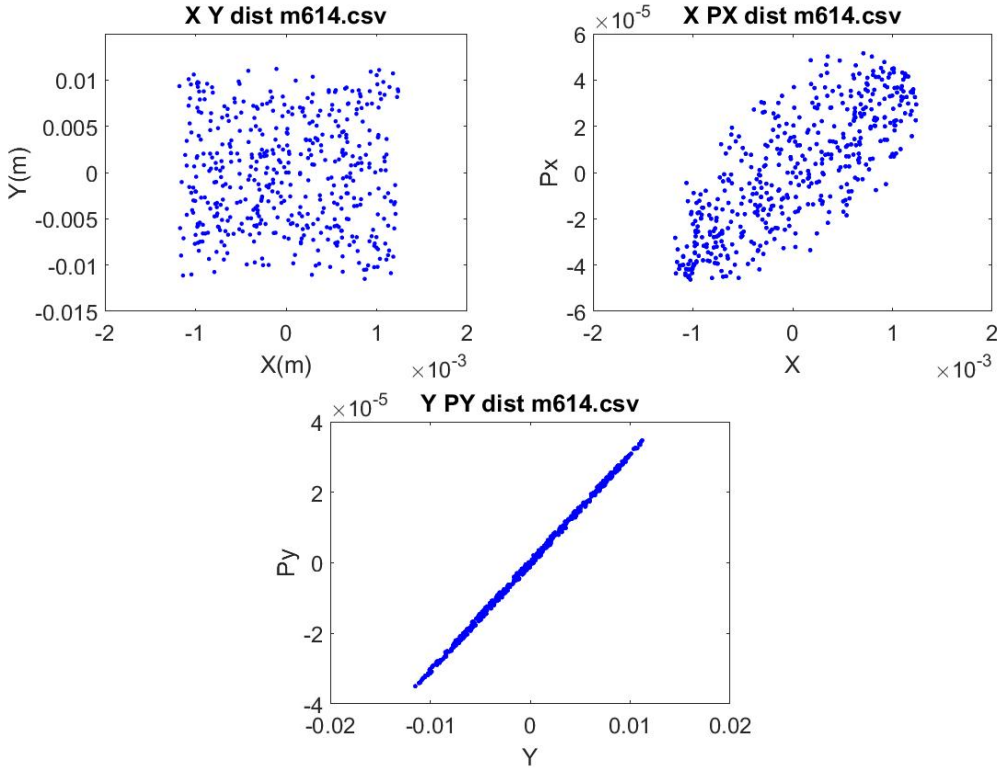

Figure 3.28: The final Synergia particle distribution for the case with the quadrupole strengths set to zero in x-y(Top), x-py (Middle), and y-py (Bottom).

3.3.3 Comparison of MAD-X-PTC and Synergia

As a form of benchmarking, the results of the modified MAD-X-PTC tracking and Synergia tracking were compared. Initially the energy gain plots did not agree, which led to the previously mentioned modification of the RF cavity module in Synergia. Since Synergia had been designed for high energy machines, the length of the RF

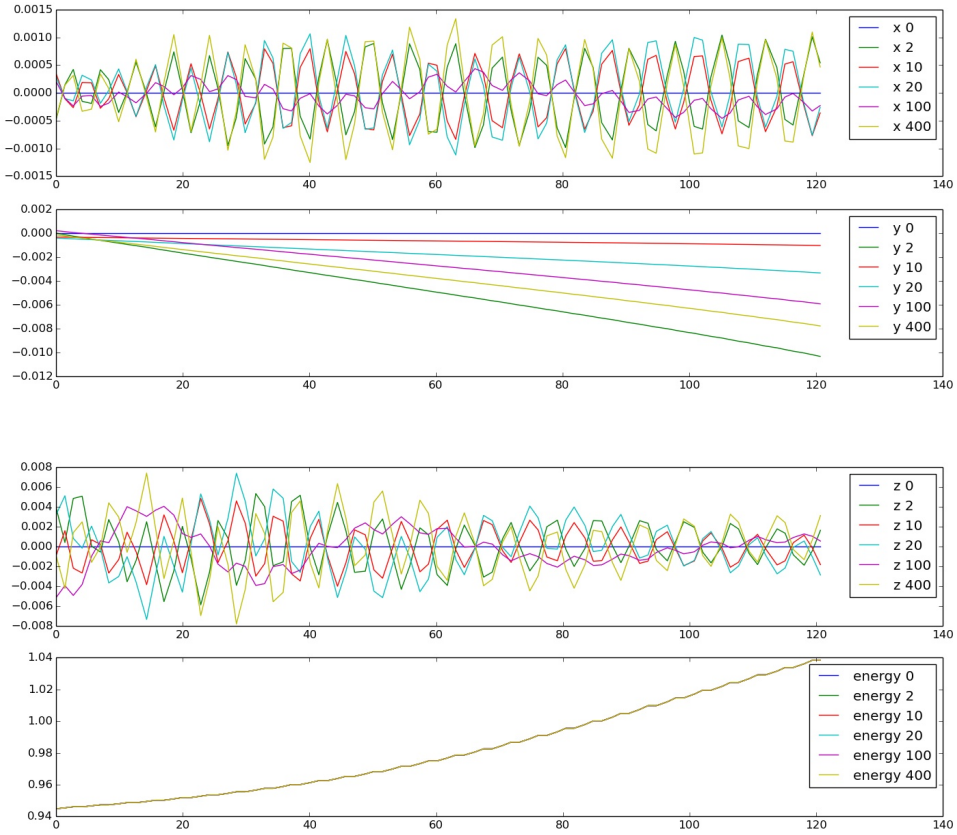

Figure 3.29: A few of the Synergia particle trajectories showing the x, y, z, and energy gain through the length of the cyclotron for the case with the quadrupole strengths set to zero.

cavity had been ignored, and the transit time factor had not been included. Once this fix was in place, both energy gains agreed. The next disagreement showed up in the particle positions after going through a single sector. This disagreement is due to the different treatments of the combined function magnet as outlined in the previous sections. As this was a known issue, a version of Synergia had already been created to make the results agree between MAD-X-PTC and Synergia. In this version of Synergia (which will be referred to as Synergia-PTC), a few modifications needed

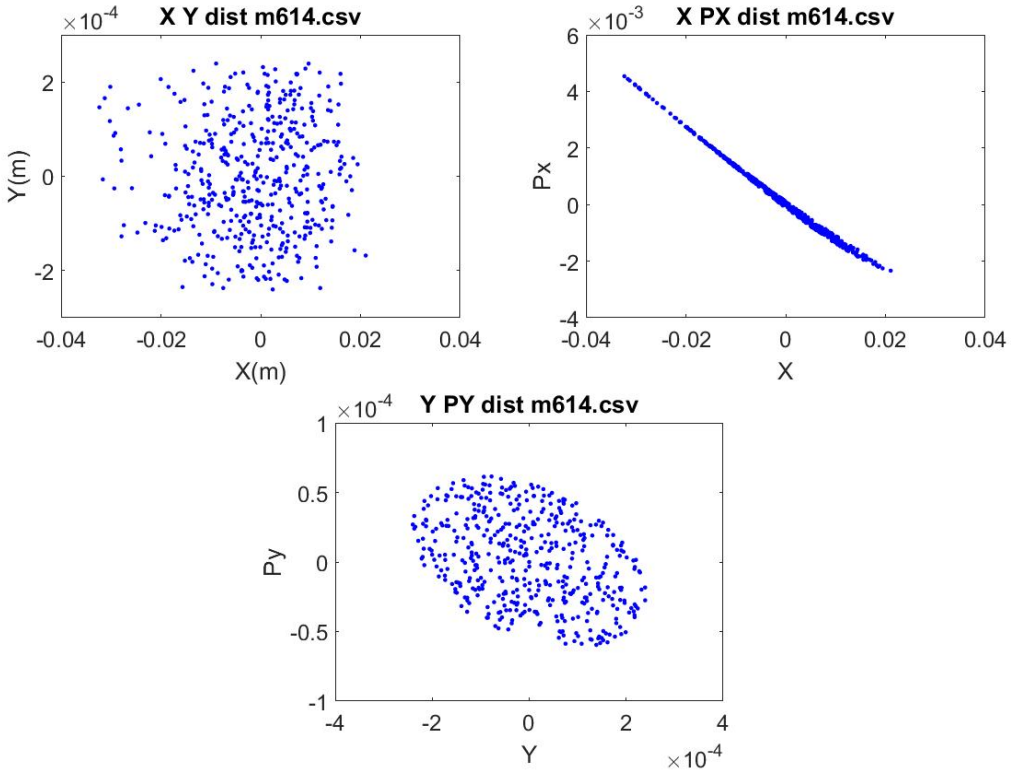

Figure 3.30: The final Synergia particle distribution for the case with the quadrupole strengths set to hold the tunes constant in x-y(Top), x-py (Middle), and y-py (Bottom).

to be made, one of which is the combined function magnet has a term subtracted in order to make the two codes agree [45]. The term is the second term in the H_2 portion of equation 3.40,

$$b_1 = (x + \frac{x^2}{2\rho_d}). \tag{3.45}$$

Using this modified Synergia-PTC to compare to the MAD-X-PTC with acceleration runs, the difference in particle position, after the first sector, agrees to less than 10^{-9}. This comparison does not show that either code is correct, only that the treatment of the TAMU100 in the modified MAD-X-PTC code agrees with what would be

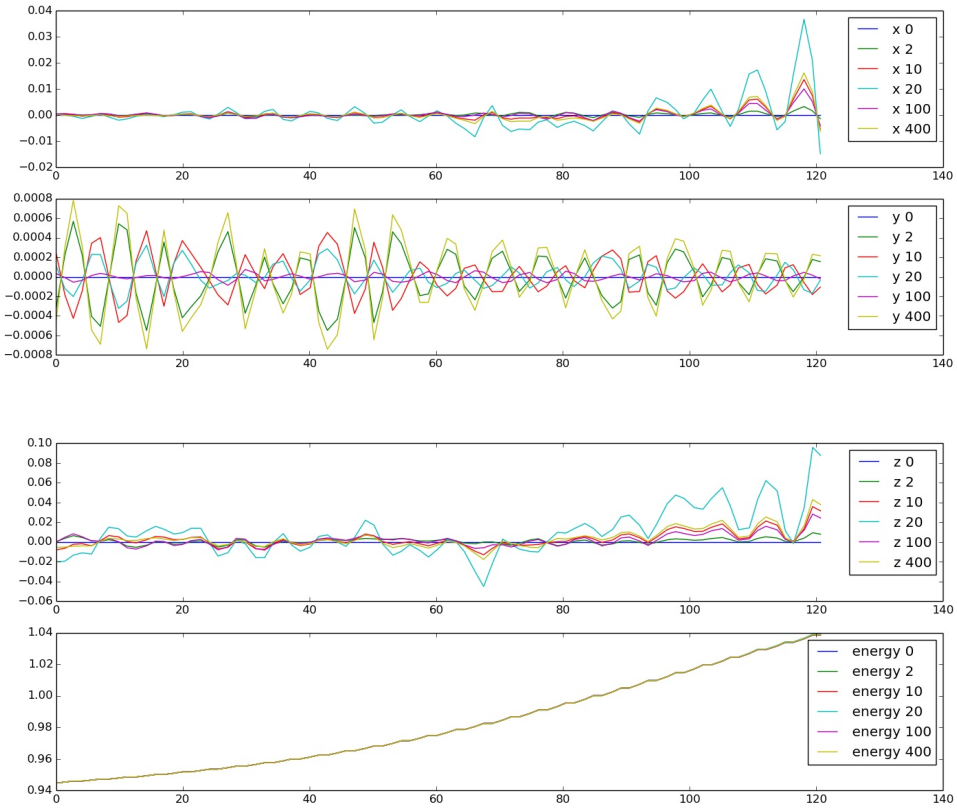

Figure 3.31: A few of the Synergia particle trajectories showing the x, y, z, and energy gain through the length of the cyclotron for the case with the quadrupole strengths set to maintain tune.

expected out of MAD-X-PTC and verified with Synergia-PTC. These comparisons assumed an initial x-y particle distribution as in Figure 3.22, but the transverse momentums, Px and Py, were set to zero. The momentums, Px and Py, are assigned using randomly generated numbers and would add an un-necessary difficulty in trying to compare the two codes. The quadrupole strengths for this run were also set to nearly zero. The difference in the x and y position are plotted in Figure 3.33.

The correct treatment of the combined function magnet is an active research area

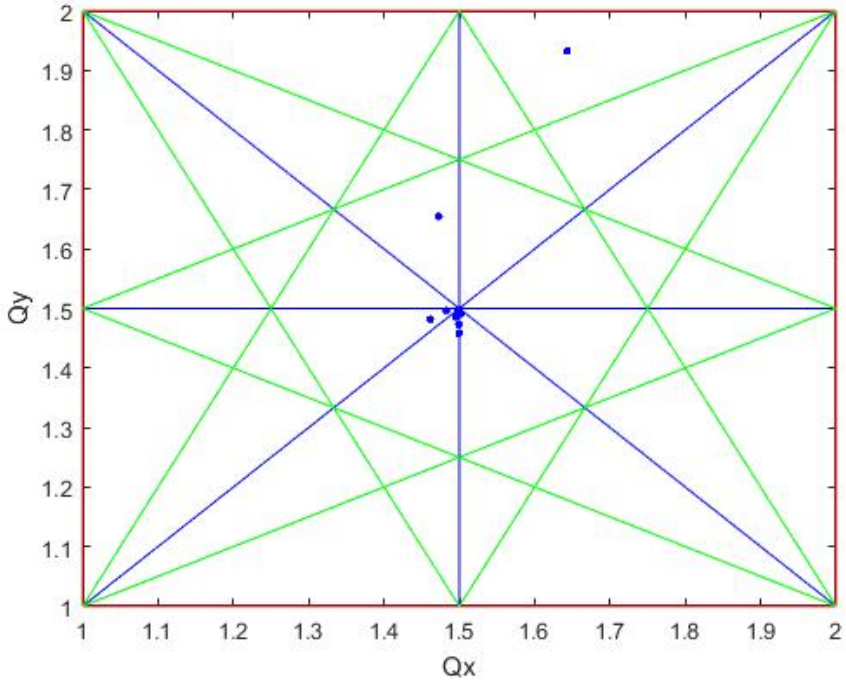

Figure 3.32: Tune plot from Synergia with the quadrupole values set to those in MAD-X-PTC.

for both MAD-X-PTC and Synergia.

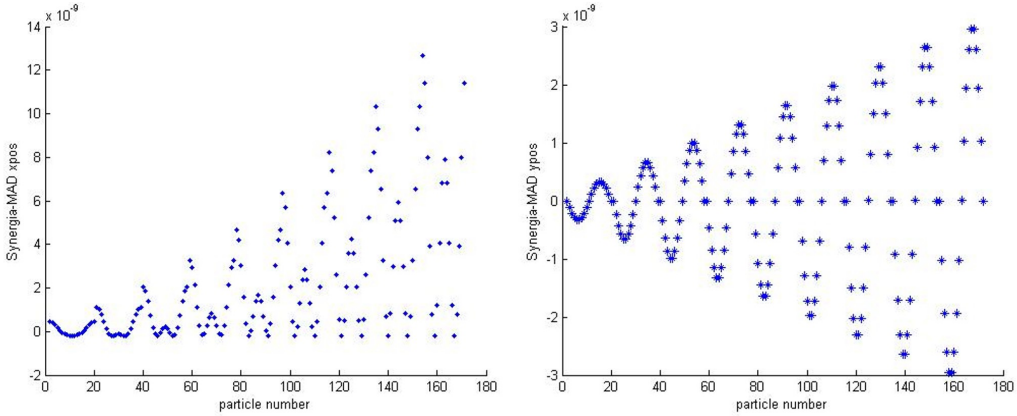

Figure 3.33: Difference between MAD-X-PTC and Synergia-PTC in the x position (left) and y position (right) of the particles after the first section.

4. BEAM TRANSPORT CHANNEL

The beam transport channel (BTC) is the heart of the strong-focusing cyclotron. It is composed of a curved beam pipe which lies along the arc of the particle trajectories in the mid-plane of the sector magnets. Surrounding the beam pipe is a quadrupole magnet, to supply the required strong-focusing, and a trim dipole magnet to help correct sector field errors. A first step in the design of the beam transport channel is an understanding of how magnetic fields are calculated and how these calculations are implemented in finite element modeling codes (FEM).

4.1 Magnetic Field Calculations

The magnetic field, in free space, must obey Maxwell's Equations:

$$\nabla \cdot \vec{B} = 0 \tag{4.1}$$

$$\nabla \times \vec{H} = 0, \tag{4.2}$$

with $\vec{B} = \mu\vec{H}$. For the transverse field, these equations become:

$$\frac{\partial B_x}{\partial x} + \frac{\partial B_y}{\partial y} = 0 \tag{4.3}$$

$$\frac{\partial B_y}{\partial x} = \frac{\partial B_x}{\partial y}. \tag{4.4}$$

The magnetic field can be expanded in a series of multipoles according to [46]:

$$B_x = B_0 \sum_{n=0}^{\infty} (\frac{r}{R_{ref}})^n (a_n cos(n\theta) + b_n sin(n\theta)), \tag{4.5}$$

$$B_y = B_0 \sum_{n=0}^{\infty} (\frac{r}{R_{ref}})^n (b_n cos(n\theta) - a_n sin(n\theta)). \tag{4.6}$$

Here the B_0 is the amplitude of the main field and R_{ref} is the reference radius taken to be at 70% of the beam aperture. The b_n coefficients are called the normal multipoles and the a_n are the skew multipoles, which are the same as the normal multipoles, but rotated about the z axis. The b_n or a_n coefficients give the relative strength of the $2(n+1)$ pole. The strength of the multipoles are commonly described in "units", and are often reported by multiplying by 10^4, which are defined as:

$$b_n = \frac{B_n}{B_0}(R_{ref})^n, \; a_n = \frac{A_n}{B_0}(R_{ref})^n. \tag{4.7}$$

Where n=0 corresponds to a dipole, n=1 to a quadrupole, and so on. Upon current reversal, the dipole has π rotational symmetry, the quadrupole has $\pi/2$ rotational symmetry, and an n pole has $2\pi/n$ symmetry. These forced symmetries only allow certain higher order multipoles. The dipole can have a sextupole (n=2), decapole (n=4), and other higher orders according to (n+1)(2i+1)-1, where i is an integer which starts at zero. The first allowed multipole for the quadrupole is the dodecapole (n=5).

4.2 Quadrupoles

Quadrupoles are used as the main focusing element in most accelerator systems. For the TAMU100, the choice of quadrupole is limited to superconducting quardrupoles, given the limited dipole aperture and required gradients in the strong focusing cyclotron. Superconducting quadrupoles can be classified into two types: iron-dominated, where the iron pole tips shape the fields, and coil-dominated, where the current distribution dominates the field shaping. Since the beam transport chan-

nel, containing the quadrupole, will be housed in the main dipole aperture, any iron used for the quadrupole would alter or short the main dipole field. This limits the choice to a coil-dominated quadrupole.

4.2.1 Coil-dominated Quadrupoles

A number of coil-dominated quadrupole designs have been built or proposed, with the most common being the cos(2θ), first discussed by Beth at Brookhaven [47] and shown in Figure 4.1. The current distribution is described by $I_\theta = I_0 cos(2\theta)$, which is where it derives its name. Another winding scheme is the Panofsky [48] quadrupole, which is a winding on a rectangular aperture. The currents lie along the aperture, as shown in Figure 4.2, with the top and bottom current sheets flowing in the same direction and opposite the side currents. Although we have not completely ruled out using a cos(2θ) design, there are a number of issues which make the Panofsky-style quadrupole more attractive. One of these issues is supporting and aligning the BTC within the sector magnets. The surface of the sector dipole, on which the BTC will sit, will be flat and and would provide a reasonable mating surface for the flat edges of the Panofsky quadrupole.

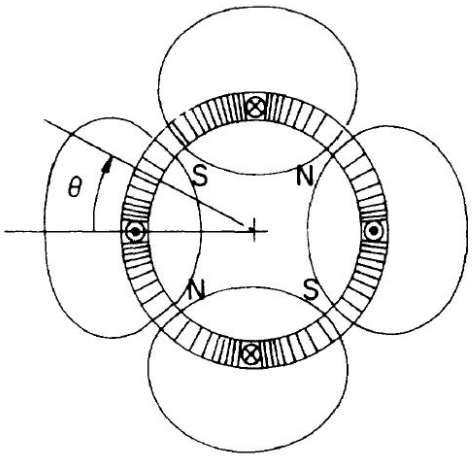

Figure 4.1: Current distribution for a Cos(2θ) magnet [49]

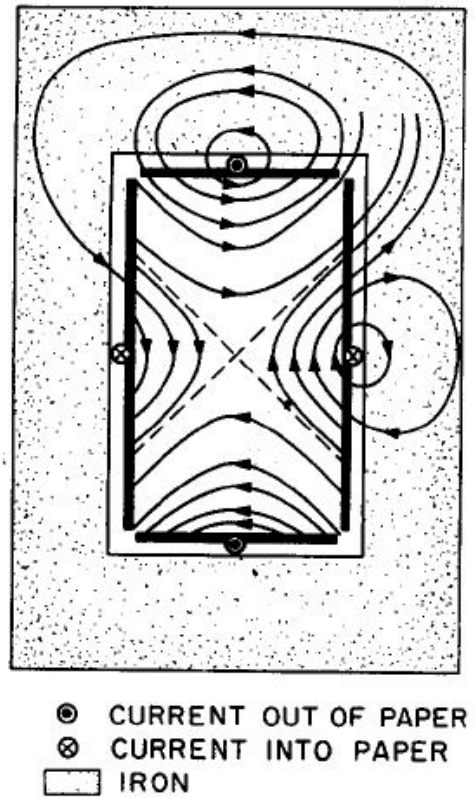

Figure 4.2: Current arrangement in a Panofsky [48] quadrupole

4.3 Trim Dipoles

The other component of the BTC is the outer window-frame dipole winding. Similar to the quadrupole, a dipole winding can be made around a circular aperture with a current distribution according to $I_\theta = I_0 cos(\theta)$. The decision to go with a Panofsky style quadrupole though forces the dipole to also have a rectangular form. The role of this dipole is to provide a correction knob for the main sector dipoles. The quadrupole and trim dipole in the BTC will be powered separately, so the dipole can be add to or reduce the main field.

4.4 Magnetic Modeling

4.4.1 2D

The initial modeling consisted of a 2D cross-section of the beam transport channel with rectangles of iron above and below. Dimensions for the model were set by the main cyclotron parameters and initial beam optics calculations. Magnetic modeling is performed using COMSOL [50], a finite element method (FEM) code. COMSOL has been benchmarked against ROXIE, CERN's widely used software for magnet calculations, and was found to give good agreement and, in some cases, to be faster [50]. The B-H curve used for the iron was taken from Vector Fields OPERA [51] and manually inserted into COMSOL (Figure 4.3).

In a traditional Panofsky quadrupole, the current distribution required for an ideal quadrupole is uniform across the square or rectangular aperture. In our case, the quadrupole is not surrounded by iron, but sits between two iron pole pieces, above and below, which causes an asymmetry in the image currents. This asymmetry in turn produces unwanted higher-order multipoles. The placement of the wires were optimized to reduce the normalized multipoles to the order of 10^{-4}. The higher-order multipoles were calculated at 70% of the beam tube using the Taylor series expansion

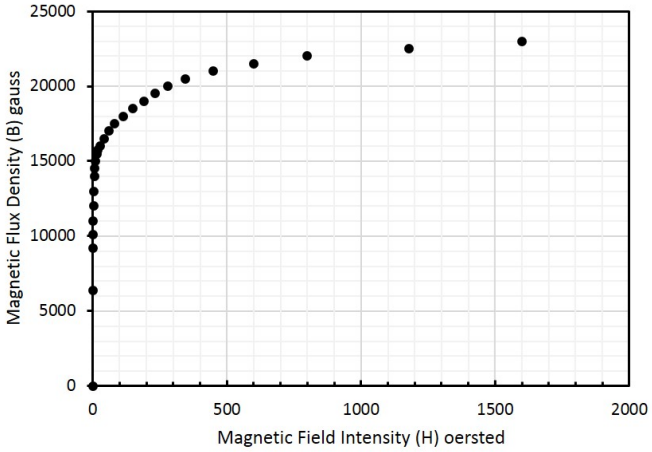

Figure 4.3: B-H curve for Iron according to Vector Fields.

of the B field due to a current carrying wire. The model included a 1T external field which serves two purposes; it ensures a proper magnetic response from the iron and it provides an estimate of the maximum magnetic field the superconducting wire will experience. The 2D model setup and example wire placement can be seen in Figure 4.4. The strengths of the higher order multipoles after optimization are in table 4.1. In COMSOL, the calculation is performed by doing a line integral at the reference radius. The equations for multipole components are given by:

$$\oint \frac{B_y}{2\pi R_{ref}} \ (Dipole) \tag{4.8}$$

$$\oint \frac{B_y cos(tan(y,x))}{\pi R_{ref}^2} \ (Quadrupole) \tag{4.9}$$

$$\oint \frac{B_y cos(ntan(y,x))}{\pi R_{ref}^{n+1}} \ (n-pole), \tag{4.10}$$

where the integral is around the circle at the reference radius.

The construction of the BTC with the stainless steel fins and square spacer rods

Table 4.1: Multipole coefficients for the optimized wire placement in the 2D BTC model

n	b_2	b_3	b_4	b_5	b_6	b_7
normalized coefficient	-6.36x10^{-7}	2.01x10^{-4}	-7.32x10^{-7}	6.95x10^{-4}	1.25x10^{-7}	-1.37x10^{-7}

added a small gap to the center of the wire winding space, this can be seen in Figure 4.4. This gap is unfortunately located as this is where we would like the largest current to be located. This gap was able to be compensated with proper wire spacing and the addition of two gaps in the horizontal plane and another gap in vertical plane. In order to achieve a 6 T/m quadrupole strength across the beam pipe, a maximum field strength of less than 1.5 T will be experienced by the wire. This is within the acceptable field limits for MgB_2 at the desired operating temperature and current (more on this in the following chapter).

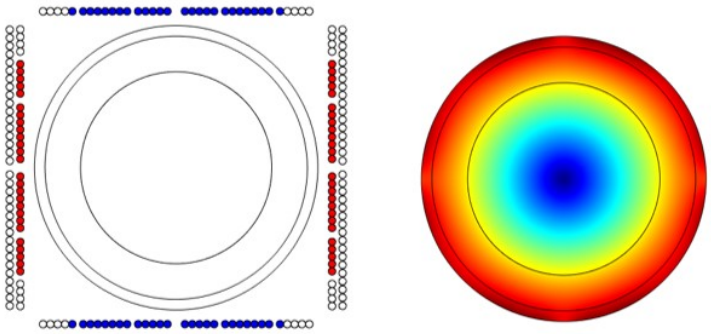

Figure 4.4: (Left) Cross section of beam transport channel with current coming out in blue and going into the page in red. The outermost circles in the image represent the beam pipe, and the inner circle is the reference radius. (Right) Magnetic field in the beam tube with the external dipole subtracted out.

4.4.1.1 Previous BTC Models

Simple 2D models were also made to compare the previous TRITRON and Lord and Hudson designs (Figure 4.5). The achievable gradient in the Lord and Hudson design was to small for our requirements. The issues with TRITRON were discussed previously, and have already been incorporated into our design, namely a larger beam aperture.

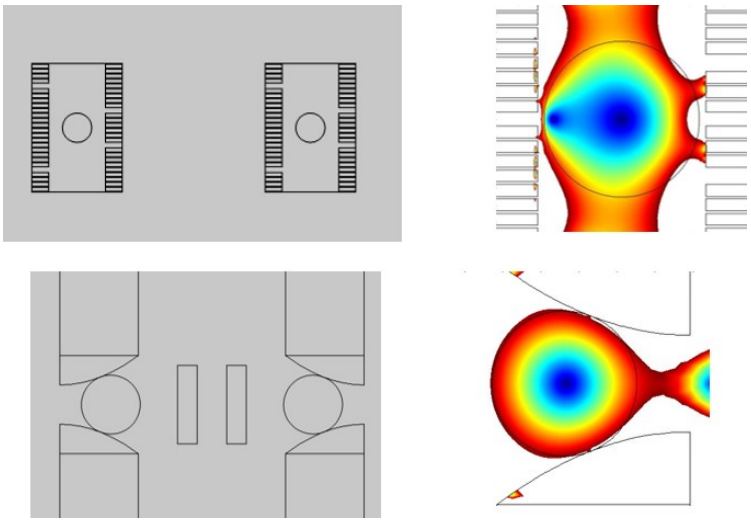

Figure 4.5: COMSOL model of TRITRON (Top) and the Lord and Hudson (Bottom) focusing channels. The non-uniform field in the beam tubes are show to the right of each model

4.4.2 3D

The main body of the BTC is assumed to be uniform, but the regions of the endcap where the wires overlap and turn around introduce higher order multipoles. The modeling of this endcap region must be done as a 3D model. A Solidworks [52]

model of the wires was created and inserted as a sheet current around the endcap (Figure 4.6). This was done to get an initial value for the integrated multipoles through the endcap before a more computationally intensive model of the individual wires was created. The strength of the multipoles are plotted in Figure 4.7 starting from the main body at zero and moving out of the endcap. The integrated multipole components are shown in Figure 4.8 and show the largest multipole to be the dodecapole. Further optimization of individual wire placement would need to be completed to reduce the multipoles in the endcap.

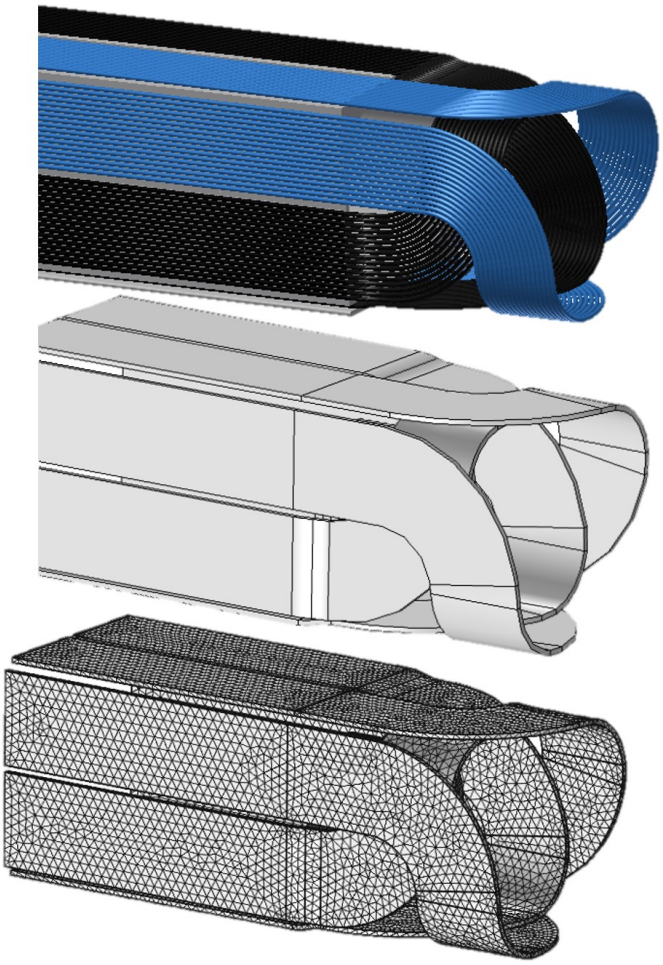

Figure 4.6: (Top) Model showing the quadrupole wires wrapping around the endcap. (Middle) A sheet current approximation to the wires. (Bottom) The meshed Comsol model.

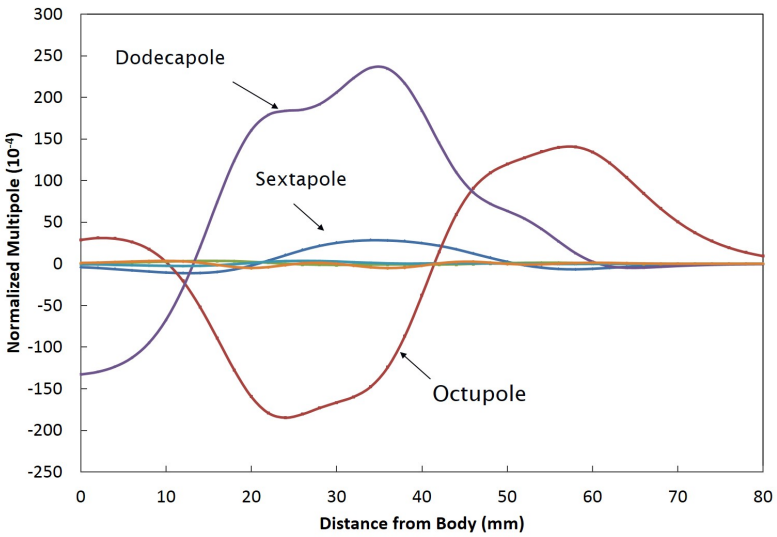

Figure 4.7: Multipoles in the BTC endcap as a function of distance from the body out through the endcap. The multipoles are normalized to the body quadrupole and expressed in "units".

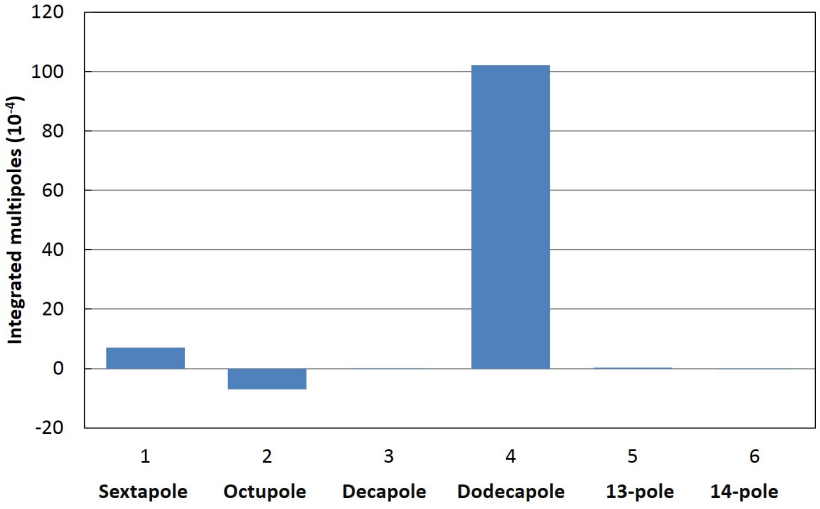

Figure 4.8: Integrated multipoles in the BTC endcap normalized to the main body quadrupole expressed in "units".

4.5 Winding Mandrel

In many magnets a pancake style winding can be used, where the wire is wound on a flat surface around a central mandrel. Panofsky-style magnets can also be wound this way, but the ends of the coil must then be bent up and around to avoid blocking the aperture (Figure 4.9). This out of plane bending would require more space than is available between iron pole pieces in the main cyclotron. The curve of the beam transport channel adds another complication. In large circular machines, SSC or LHC scale, the magnets can be wound as though straight and bent to match the radius of the machine. Unfortunately, this technique cannot be used for small bend radii and an alternative method must be developed. A properly designed winding mandrel must maximize the aperture in the beam transport channel, fit in the opening between pole pieces and neighboring beams, and obey the minimum bend radius set by the superconductor. A corresponding winding technique must also be developed.

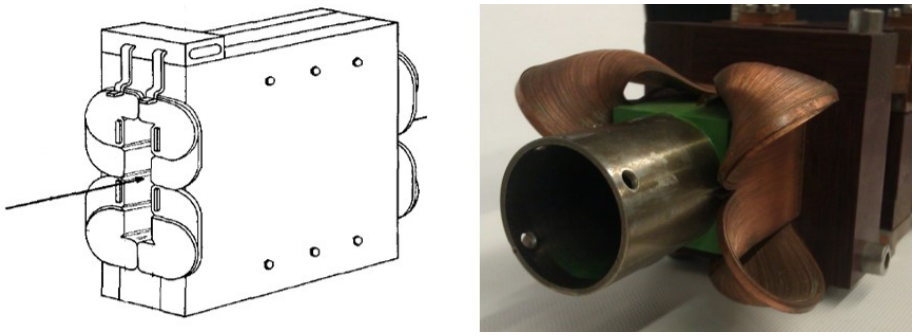

Figure 4.9: (Left) Sketch of rectangular quadrupole from original Panofsky paper [48]. (Right) Brookhaven Superconducting Panofsky quadrupole [53]

4.5.1 Design

4.5.1.1 Initial BTC

The difficulty in winding small round wire, as opposed to Rutherford style cable, on a curved winding mandrel were not completely understood until it was attempted. A previous winding mandrel had been designed and fabricated (Figure 4.10), but no winding attempts had been made. A first round of winding revealed insufficient wire support to hold the wire in place on the endcaps or the main body, where the wire pulled away from the curved portion of the body (Figure 4.11). The wire must be wound on the mandrel and then go through a heat treatment (more about the wire in the following chapter), so no glue or epoxy can be used to secure the wire. Another issue was from interference of the end-cap in the winding process. In order to overcome these issues a number of models, some as exotic as the Brookhaven superconducting quadrupole [53](Figure 4.9), were considered. The wires pulling away from the concave body was expected, and the original idea had been to push the wires in place with a sheet of stainless steel before the heat treatment, but with all the additional problems, a complete redesign was needed.

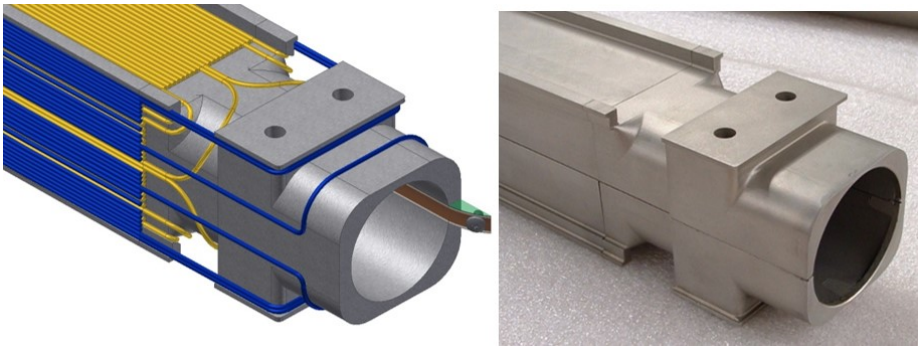

Figure 4.10: Initial beam transport channel model and winding mandrel

Figure 4.11: Initial curved mandrel and beam pipe

4.5.1.2 Second BTC

The redesign of the BTC focused on securing the wires to the curved portion of the body. A square grove was machined down the middle of each side of the BTC. A square rod was then laser welded into this grove to create a raised surface above the main body. Stainless steel fins with holes drilled equally spaced down the middle, were then laser welded to the square rods. The raised fins allowed the wires to slip between the fin and the main body. On the side of the BTC where the winding for the trim dipole is located, two layers of fins were added. Figure 4.12 shows the square rod, fins, and holes in the fins used for laser welding. Another improvement was a series of nesting end-cap pieces to avoid interference while winding. The first layer of the endcap would be welded to the main body. This endcap would allow the winding of two of the four windings (the blue windings in Figure 4.13) required for the quadrupole. After these windings were in place, then next endcap layer would slide on and the remaining two windings (black wires in Figure 4.13) for the quadrupole could be added. The next endcap layer is then added to allow for the first dipole winding, then the remaining endcap piece is slid on to finalize the dipole. The exploded view of the endcap and a cross section of the BTC with quadrupole

and dipole windings are shown in Figure 4.13.

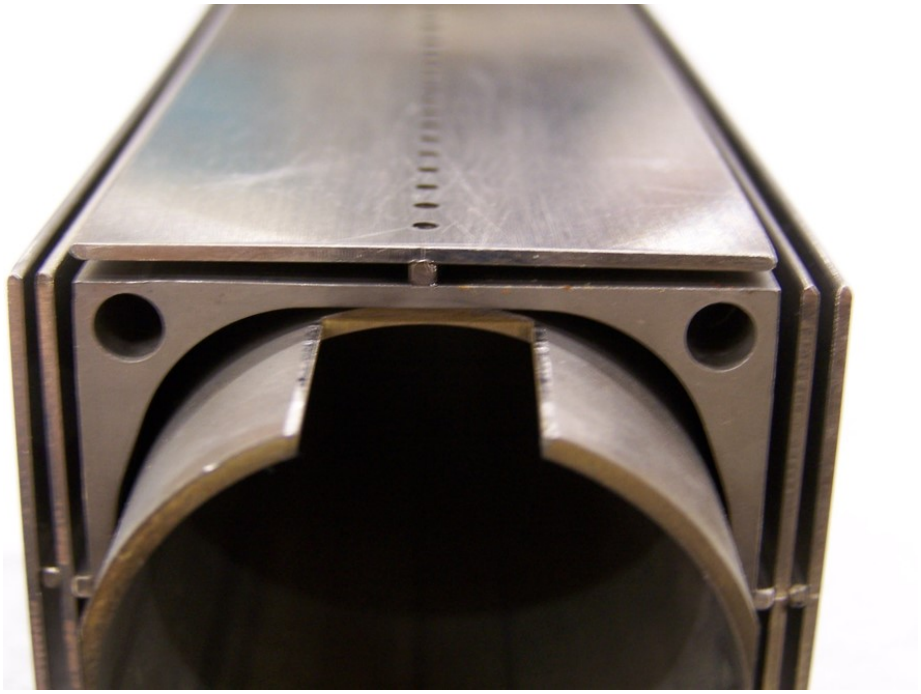

Figure 4.12: Stainless steel fins added to secure the wires to the winding mandrel

The first attempt winding the new mandrel brought out the next issue, the problem of wire climbing from round wires under tension, an example of this can be seen in Figure 4.14. To overcome this issue, a series of tapped holes were added to the endcaps, and a set of winding guides and "cookies" were designed. The guides are temporary aluminum fixtures which act, in a similar manner as the fins, to provide a small channel for the wires to slide into and prevent wire climbing. One of the aluminum winding guides can be seen in Figure 4.15. Once the layer has been wound, the guides are carefully removed and the cookies, which are thinner stainless steel

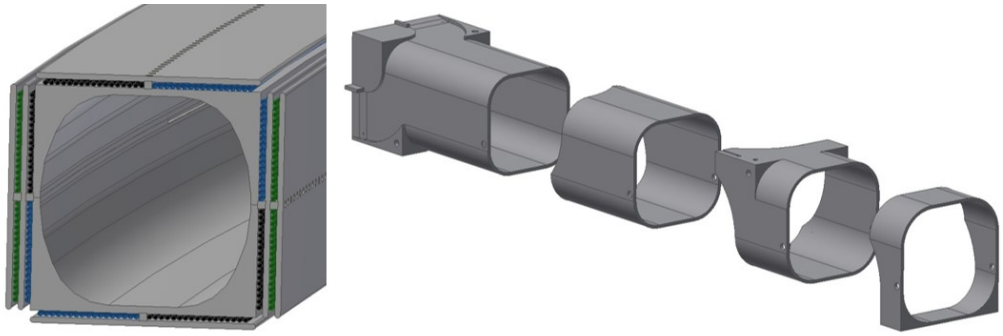

Figure 4.13: (Left) Cross section of the wire windings. The two black and blue inner windings make up the quadrupole, while the two outer green windings are for the trim dipole. (Exploded view of the endcap layers designed to avoid interference while winding.)

pieces, are used to secure the wires for the remainder of the winding process and will remain on the BTC through the heat treatment. An example of a cookie can be seen in Figure 4.16. Although the stainless steel fins hold the wires to the curved side of the body, the curved top wires still want to flex out of place. Two pusher bars were cut on the EDM to match the inner and outer curves of the BTC and hold the wires in after each turn. The pusher bars must be removed, the next wire wound in, and the pusher bars repositioned and clamped after each turn. The pusher bar for the inner curve is pictured in Figure 4.17.

Other winding methods were considered including the direct-wind method at Brookhaven National Lab. In this method the winding mandrel is wrapped with a B-stage epoxy and the wire is also coated with a thin layer of epoxy. Using a large 3-axis machine, they are able to wind the wire on the mandrel in a very precise computer controlled way and using ultrasonics they can locally heat the epoxy on the wire as they push it on the mandrel [54]. The method weakly bonds the wire to the mandrel and must be more securely attached with an outer wrap. All of the

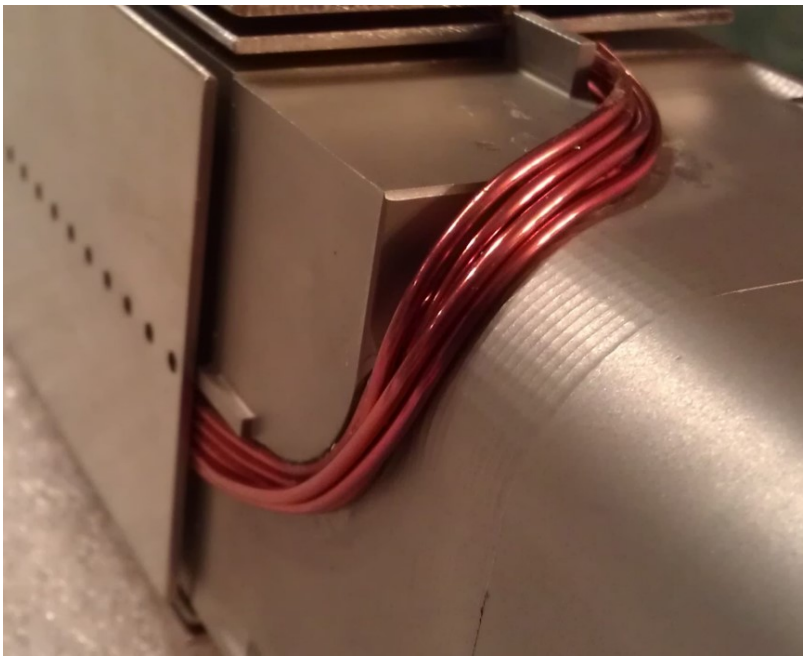

Figure 4.14: Round wires under tension exhibit wire climbing

magnets which have been created this way use reacted wire which does not require any further heat treatment. In order to use this method for MgB_2, unreacted wire must be used, as the minimum bend radius for reacted MgB_2 is on the order of 0.5m. MgB_2 must go through a heat treatment of 650-700 °C for about 30 min and no known B-stage epoxy can survive these temperatures. Another complication for using the direct-wind method for our beam transport channel is the rectangular mandrel. Brett Parker at Brookhaven had already considered winding on non-circular shapes, Figure 4.18, and is confident our geometry could be accomplished with his machine, but until another epoxy or attachment method can be found, this method will not work.

Figure 4.15: Top view of the updated winding mandrel and one of the temporary aluminum winding guides on the endcap.

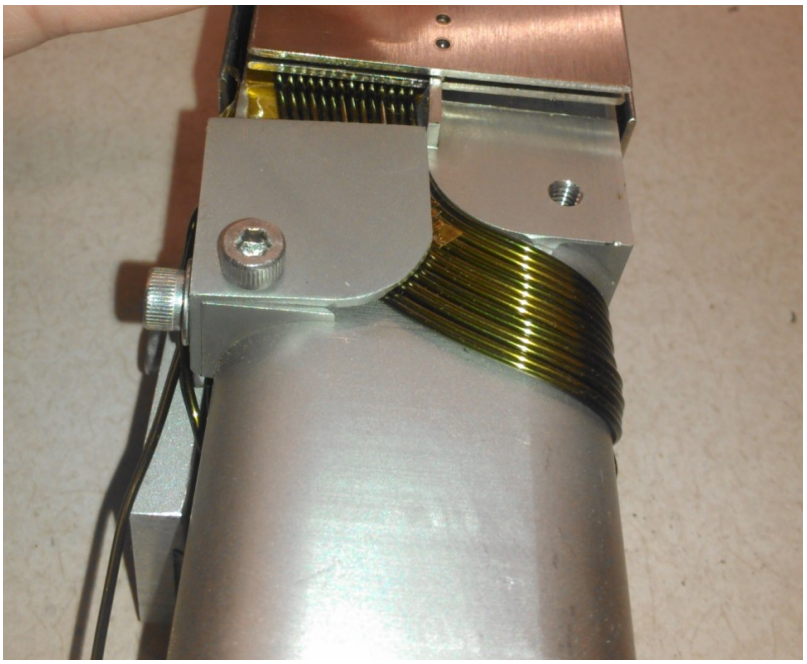

Figure 4.16: Wires held in place by a winding cookie which is screwed into the endcap and holds down the wires

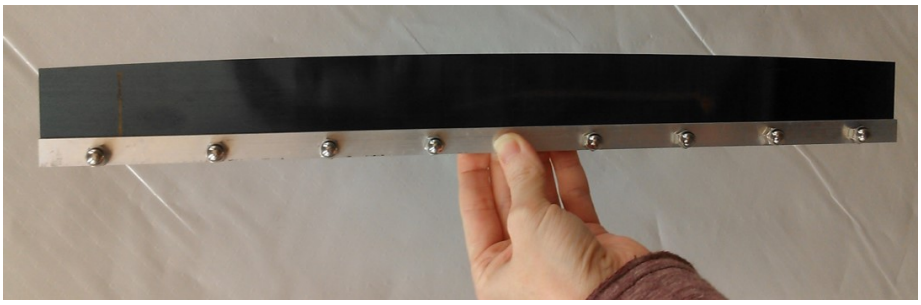

Figure 4.17: A pusher bar for holding the wires in the curve along the top and bottom of the BTC during winding.

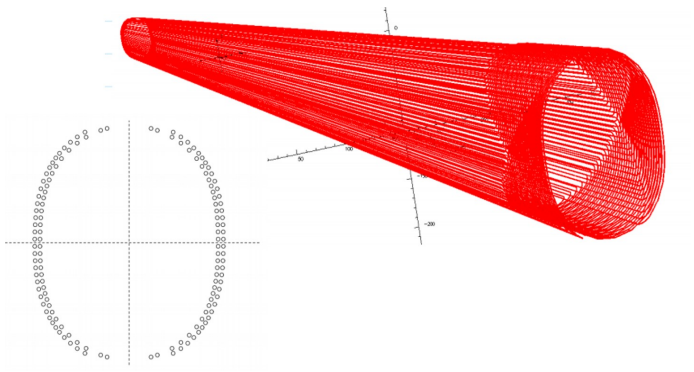

Figure 4.18: Non-circular geometry for direct-wind at BNL. (image courtesy of Brett Parker)

4.6 Winding Table

Having a curved mandrel adds an additional complication to the winding table. The path of the wires over the endcap require the mandrel to be rotated 90 degrees about an axis running through the beam tube. Then, holding this rotated position, the winding table and mandrel must rotate about an axis through the center of the BTC perpendicular to the first rotation. The required range of motion was achieved by mounting a plate on the shaft of the winding table. Two locking pillow block bearings were attached to this table to hold the shaft the mandrel would be mounted on to provide the 90 degree tilt. Winding fixtures were created to hold the BTC up away from the surface of the table to allow room to swing the 90 degrees. Figure 4.19 shows a sketch of the winding table and special endcap winding fixtures.

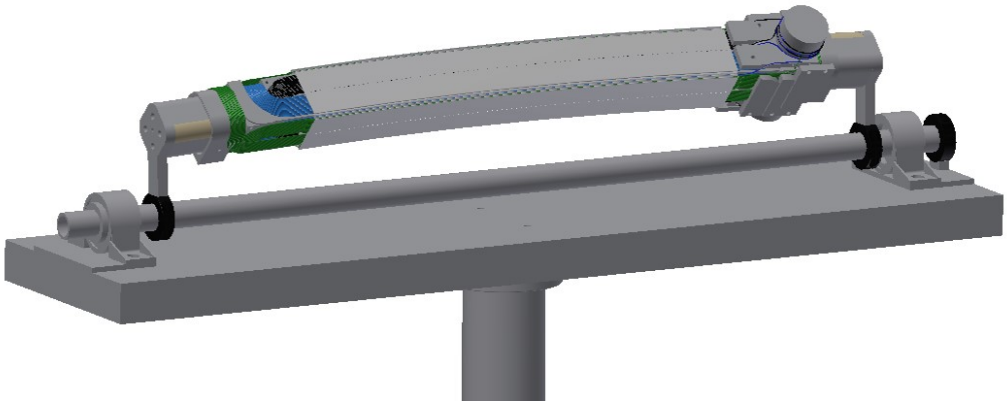

Figure 4.19: CAD drawing of the BTC mounted on the winding table.

5. MAGNESIUM DIBORIDE

5.1 History

The superconducting properties of MgB_2 were only recently discovered in 2001 [55]. The low material cost and relative ease of fabrication make this an attractive superconductor for low field applications. MgB_2 has already been used to wind MRI magnets [56], as potential Fault Current Limiters [57], as superconducting induction heaters [58], and in multiple research magnets. MgB_2 has a higher critical temperature than the the commonly used Nb3Sn and NbTi [59] of 39K which reduces the overall cryogenic costs. The raw materials costs are also about half that for NbTi [60]. Although relatively new to the superconducting scene, MgB_2 wire can be purchased off the shelf from multiple vendors [61, 62].

5.2 Properties

Superconductors used for magnet applications are characterized by three main parameters, the critical temperature (T_c), the critical field (B_c), and the critical current density (J_c). These three parameters are dependent on each other and can be plotted to show the critical surface, above which a superconductor becomes resistive. The critical surface for MgB_2 is shown in Figure 5.1.

The choice of superconductor is narrowed by the required current density, external field, and desired operating temperature. The list of operating parameters for the beam transport channel, Table 5.1, led us to chose MgB_2 for our superconducting wire. The approximately 1 T main dipole field, in which the superconducting beam transport channel will sit, is well below the critical field for MgB_2 at 15 K.

Strain

One major drawback in using MgB_2 wire is the sensitivity to strain for both

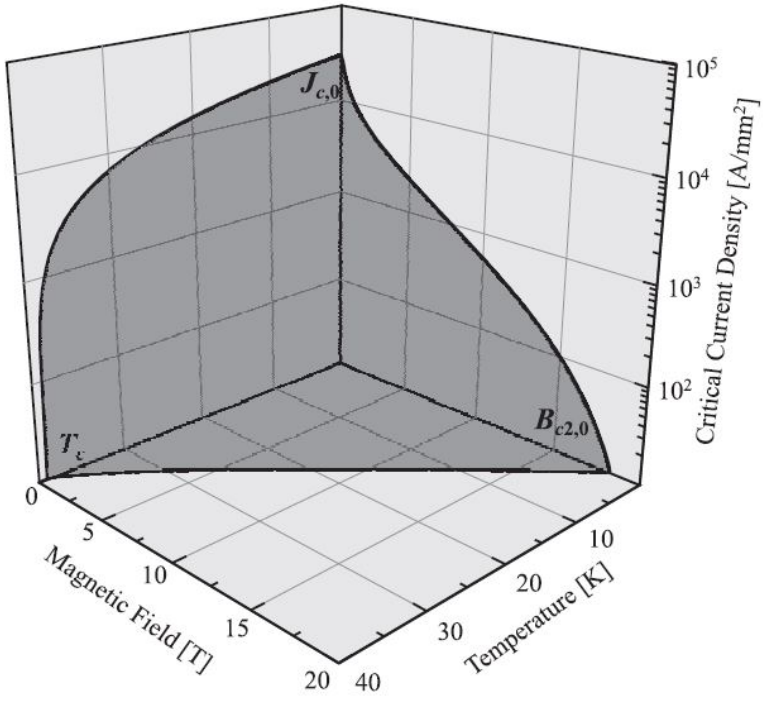

Figure 5.1: Critical surface of MgB_2 [63].

reacted and unreacted wire. The irreversible strain limit for reacted MgB_2 is just under 0.4% [63](Figure 5.2).

$$strain = \frac{wirediameter}{benddiameter}. \tag{5.1}$$

Using a 1 mm wire, this strain would limit the bend radius to a 25 cm bend diameter, which is much larger than the full width of the endcap. For this reason, a wind and react method will need to be used. Few strain degradation studies have been performed for small diameter bend radii on unreacted MgB_2 wire. A 0.689 mm diameter wire wound on a 38.1 mm diameter bend, which according to equation 5.1 corresponds to a 1.8% strain, was found to have no noticeable current degradation

Table 5.1: Operating parameters for the BTC

Parameter	**Desired Value**
Engineering Current Density	320 $\frac{A}{mm^2}$
Operating Temperature	15 K
Max External Field	1.5 T

compared to the short sample [64]. The study also tried a 0.834 mm diameter wire on a 63.5 mm bend, a 1.3% strain, with no degradation. For the beam transport channel, the minimum bend radius which can be achieved is 1.25 cm, or a 2.5 cm diameter, and with a 1 mm diameter wire this corresponds to a 4% strain. Our group has tested MgB_2, which was provided by HyperTech, at radii above and below 1.25 cm with initial promising results [65]. The wire specifications for the Hypertech wire are listed in table 5.2 and a cross section of the wire is shown in Figure 5.3.

Table 5.2: Properties of the MgB_2 wire provided by HyperTech.

Parameter	**Value**
Number of filaments	30 mono
Barrier Material	Niobium
Sheath Material	Monel
Twist Pitch	350 mm
Powder	18%
Bare Wire Diameter	0.99 mm
Insulated Wire Diameter	1.24 mm

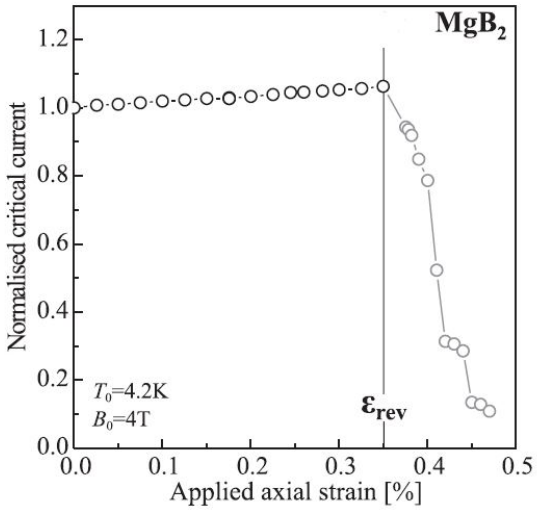

Figure 5.2: Irreversible strain limit in MgB_2 [63].

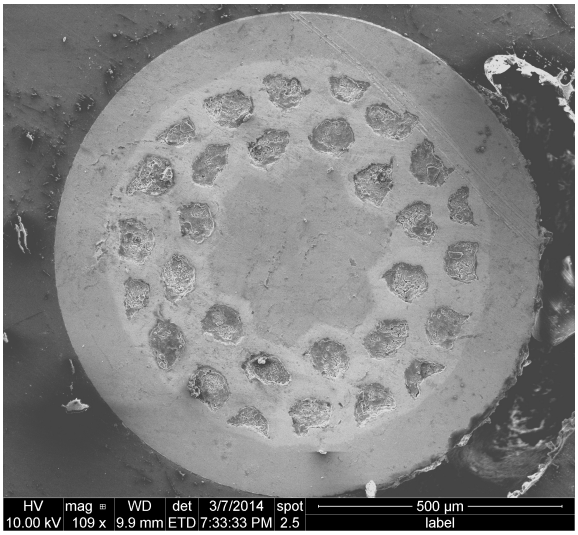

Figure 5.3: Cross section of MgB_2 wire provided by HyperTech.

6. CONCLUSION

6.1 Summary

The Accelerator Research Laboratory has developed a design for a high-power strong-focusing cyclotron. The cyclotron uses two main technologies: a superconducting RF cavity to fully separate the turns and a series of beam transport channels which contains alternating focusing and defocusing quadrupoles to provide the strong focusing. Two major efforts were undertaken in order to validate this design, the linear beam dynamics through the entire TAMU100 and the model and winding of the beam transport channel.

As an initial step in the linear beam dynamics studies, an equilibrium orbit for an ideal particle through the machine was determined. No available optics codes were suitable to complete this task, so a method and Mathematica script was developed. The script started with the overall geometric layout of the sectors and the spacing required for the RF cavities, as well as the RF energy gain profile. An optimization was performed to determine the isochronous spiral orbit given the injection radius, injection energy, and minimum orbit separation. Assuming a hard edge model, the magnetic field, energy in each sector, cavity phase, and trajectory information was determined. The results of this code were used to create 64 sequence files which were used in MAD-X for linear optics calculations. Using MAD-X, the lattice was optimized by adjusting the strengths of the quadrupoles to maintain beam size and to obtain a desired phase advance per cell, for an overall constant horizontal and vertical betatron tune per turn.

The goal for the strong-focusing cyclotron is to accelerate a large current so space charge effects need to be taken into account through particle tracking. As a step in

the direction of this goal, particle tracking was set up in two codes; MAD-X-PTC and Synergia. Both codes needed modifications to properly model our machine. Synergia was chosen for its particle in cell space charge capabilities. A Matlab script was written to add acceleration to MAD-X-PTC for particle tracking. This modified MAD-X-PTC was used as a benchmark against Synergia. In the process of benchmarking, several differences in the codes emerged. Synergia was assuming an RF cavity of zero length so a module was written to add length and the transit time factor to the code. As a default, Synergia also renormalized the strengths of the beamline elements after an RF cavity and this was dealt with by using the 84 sequence file method as in MAD. The main difference found between the two codes is the handling of the curved combined function magnets. The correct treatment of the combined function in MAD-X-PTC and Synergia is still being investigated.

The design and feasibility of the beam transport channel was also investigated. Non-linear magnetic modeling was performed for a 2D cross section of the beam transport channel to determine the required current density for the quadrupole gradient strengths. The placement of the wires were optimized to reduce higher order multipoles induced by the iron in the dipoles above and below the beam transport channels. 3D modeling was also performed on the endcap regions of the beam transport channels to find the integrated multipoles through the endcap.MgB_2 was chosen for the superconductor as it met all design requirements and can operate at a higher critical temperature reducing cryogenic costs. One drawback of MgB2 is the bend radius limitation. A winding mandrel was designed and built to minimize the bending radius of the MgB_2 wire and to withstand the 600-700°C heat treatment. A series of modifications were made to the mandrel to secure the wires during the winding process. A winding table was designed with a mount to provide the full rotation needed in winding the complex beam transport channel magnet. A copper wire winding was

performed to test the winding procedure.

6.2 Future Work

The next main step for the validating the design of the TAMU100 is to include the effects due to space charge. The ability to turn on space charge was one of the main reasons for using, and benchmarking, against Synergia. The framework for this next step has been provided with the sequence files, main scripts, and modifications made to Synergia. Before the space charge can be added, the disagreement on the treatment of the curved combined function magnets must be resolved. Other nonlinear and collective effect for high-current beam transport will also need to be investigated.

The current design for the winding mandrel of the beam transport channel should also be updated. In addition to a simplified endcap winding method, a body design which would eliminate the need for the pusher bar should be used. This new endcap design should include a wire placement scheme to minimize the integrated multipoles through the endcap. Magnetic modeling at the individual wire level should be performed in the endcap region.

Although initial strain tests have been performed on MgB_2, the results were not conclusive. Further testing should be performed to determine the minimum bend radius. A full MgB_2 winding should also be completed.

REFERENCES

[1] Ring cyclotron at the Paul Scherrer Institut. `https://www.psi.ch/`.

[2] W. Wegner. PSI status 2008-developments at the 590 mev proton accelerator facility. *Nucl. Instr. and Methods*, A600(1):5–7, 2009.

[3] E. O. Lawrence and N. E. Edlefsen. The production of high speed protons without the use of high voltages. *Science*, 72:376–377, 1930.

[4] M.S Livingston and J. P. Blewett. *Particle Accelerators*. McGraw-Hill Book Company, Inc., 1962.

[5] H. A. Bethe and M. E. Rose. The maximum energy obtainable from the cyclotron. *Physical Review*, 52(12):1254–1255, 1937.

[6] L. H. Thomas. The paths of ions in the cyclotron. *Physical Review*, 54(8):580–588, 1938.

[7] M. K. Craddock. *AG Focusing in the Thomas Cyclotron of 1938*. Proceedings of Particle Accelerator Conference, Vancouver, Canada, 1-3, 2009.

[8] K. R. Symon, D. W. Kerst, L. W. Jones, L. J. Laslett, and K. M. Terwilliger. Fixed-field alternating-gradient particle accelerators. *Physical Review*, 103(6):1837–1859, 1956.

[9] Y. Jongen, M. Abs, W. Beeckman, W. Kleeven, D. Vanderplassche, S. Zaremba, A. Glazov, S. Gurskiy, G. Karamysheva, and N. Morozov. *Radio Frequency System of the Cyclotron C400 for Hadron Therapy*. Cyclotrons and Their Applications, Giardini Naxos, Italy, 482-484, 2007.

[10] F. M. Russell. A fixed-frequency, fixed-field, high-energy accelerator. *Nuclear Instruments and Methods*, 23:229–230, 1963.

[11] P. Heikkinen. *Cyclotrons*. IAEA Collections, Accelerator Laboratory, Finland.

[12] E. D. Courant, M. S. Livingston, and H. S. Snyder. The strong-focusing synchrotron-a new high energy accelerator. *Physical Review*, 88(5):1190–1196, 1952.

[13] N. Christofilios. *Focusing System for Ions and Electrons*. US Patent 2736799.

[14] R.S. Lord and E.D. Hudson. Magnet for an 800-MeV separated orbit cyclotron. *IEEE Transactions on Nuclear Science*, 12(3):373–376, 1965.

[15] J. A. Martin. *The Separated-Orbit Cyclotron*. International Conference on Isochronous Cyclotrons, Gatlinburg, Tennessee, 288-299, 1966.

[16] U. Trinks, W. Assmann, and G. Hinderer. The TRITRON: A superconducting separated-orbit cyclotron. *Nuclear Instruments and Methods in Physics Research*, A244:273–282, 1986.

[17] A. Cazan, P. Schutz, and U. Trinks. *Commissioning of the First Separated Orbit Cyclotron TRITRON*. International Conference on Cyclotrons and their Applications, Caen, France, 323-326, 1998.

[18] U. Trinks. Superconducting cyclotrons. *Nuclear Instruments and Methods in Physics Research*, A287:224–234, 1990.

[19] J. Comeaux, S. Assadi, K. Badgley, C. Collins, R. Garrison, P. McIntyre, and A. Sattarov. *Injection Sequence for High-Power Isochronous Cyclotrons For ADS Fission*. International Particle Accelerator Conference, New Orleans, Louisiana, 1509-1511, 2012.

[20] M. Bres, A. Chabert, F. Foret, D. T. Tran, and G. Voisin. *The Interdigital H-Type (IH) Structure, An Accelerating Structure for Low Energy Beams*, volume 2. Gordon and Breach, Glasgow, Scotland, 1971.

[21] D. Pogue, N.and Chavez, J. Kellams, P. McIntyre, and A. Sattarov. Strong focusing cyclotrons and its applications. *IEEE Transactions on Applied Superconductivity*, 25(3):436–438, 2014.

[22] Accelerator Research Laboratory, Texas A&M University. http://arl.physics.tamu.edu/.

[23] Wolfram Mathematica 9.0. http://www.wolfram.com/mathematica/.

[24] H. Wiedemann. *Particle Accelerator Physics*, volume 3. Springer, New York, 2007.

[25] A. Chao, K. H. Mess, M. Tigner, and F. Zimmermann. *Handbook of Accelerator Physics and Engineering*, volume 2. World Scientific, 2013.

[26] E. D. Courant and H. S. Snyder. Theory of the alternating-gradient synchrotron. *Annals of Physics*, 3(1):1–48, 1958.

[27] W. Walkinshaw. A spiral ridged bevatron. *A.E.R.E*, 1956. Harwell, England.

[28] Methodical Accelerator Design(MAD). `http://mad.web.cern.ch/mad/`.

[29] Matlab 2014a. `http://www.mathworks.com/products/matlab/`.

[30] K. L. Brown, F. Rothacker, D. C. Carey, and Ch. Iselin. Transport: A computer program for designing charged particle beam transport systems. *SLAC Report*, 91, 1983.

[31] Marylie 3.0. `http://www.physics.umd.edu/dsat/dsatmarylie.html`.

[32] Cosy INFINITY. http://www.bt.pa.msu.edu/index_cosy.htm.

[33] Dan Tyler Abell. *Analytic Properties And Cremona Approximation of Transfer Maps For Hamiltonian Systems*. PhD thesis, University of Maryland, College Park, 1995.

[34] E. Forest. Geometric integration for particle accelerators. *Journal of Physics A: Mathematical and General*, 39:5321–5377, 2006.

[35] S.G. Peggs and R.M. Talman. Nonlinear problems in accelerator physics. *Ann. Rev. Nucl. Part. Sci.*, 36:287–325, 1986.

[36] R.D. Ruth. A canonical integration technique. *IEEE Trans. Nucl. Sci.*, 30:2669–2671, 1983.

[37] E. Forest and R. D. Ruth. Fourth-order symplectic integration. *Physica D*, 43:105–117, 1990.

[38] H. Yoshida. Construction of higher order symplectic integrators. *Physics Letters Al*, 150:262–268, 1990.

[39] E. Forest, F. Scmidt, and E. McIntosh. Introduction to the Polymorphic Tracking Code. http://madx.web.cern.ch/madx/doc/ptc_intro.pdf.

[40] R. Talman and L. Schachinger. Teapot: A thin-element accelerator program for optics and tracking. In *Particle Accelerators*, pages 35–56. Gordon and Breach Science Publishers, Inc., 1987.

[41] G. Ripken and F. Willeke. Methods of beam optics. *DESY*, pages 88–114, 1988.

[42] K. L. Brown. A first and second order matrix theory for the design of beam transport systems and charged particle spectrometers. *SLAC Report*, 75, 1982.

[43] Synergia. https://web.fnal.gov/sites/Synergia/SitePages/Synergia%20Home.aspx.

[44] L. Michelotti. Exact map through ideal bends (again?). *Fermilab*, Conf-95/171, 1995.

[45] L. Michelotti. Private communication, 2015.

[46] Mario Conte and William W. MacKay. *An Introduction to the Physics of Particle Accelerators*. World Scientific Publishing Co. Pte. Ltd., 2008.

[47] R.A. Beth. Elliptical and circular current sheets to produce a prescribed internal field. *IEEE Transactions on Nuclear Science*, 14(3):386–388, 1967.

[48] L. N. Hand and W. K. H. Panofsky. Magnetic quadrupole with rectangular aperture. *Review of Scientific Instruments*, 30(10):927–930, 1959.

[49] R.B. Britton, W.B. Sampson, G.H Morgan, P.F. Dahl, and J.P. Blewett. Superconducting synchrotron magnets. *IEEE Transactions on Nuclear Science*, pages 720–722, 1969.

[50] COMSOL. http://www.comsol.coml.

[51] Vector Fields Opera. http://operafea.com/.

[52] Solidworks. http://www.solidworks.com/.

[53] P.G. Kruger, W.B. Sampson, and R.B. Britton. *Accelerator Dept. Report AADD-104-R*. Brookhaven National Lab, Upton, New York, 1966.

[54] B. Parker. Private communication, 2013.

[55] J. Nagamatsu et al. Superconductivity at 39K in Magnesium Diboride. *Nature*, 410(6824):63–64, 2001.

[56] M. Razeti, S. Angius, L. Bertora, D. Damiani, R. Marabotto, M. Modica, D. Nardelli, M. Perrella, and M. Tassisto. Construction and operation of cryogen free MgB_2 magnets for open MRI systems. *IEEE Transactions on Applied Superconductivity*, 18:882–886, 2008.

[57] X. Pei, A.C. Smith, M. Husband, and M. Rindfleisch. Experimental test on a superconducting fault current limiter using three-strand MgB_2 wire. *IEEE Transactions on Applied Superconductivity*, 22:1–4, 2012.

[58] A. Stenvall, N. Magnusson, Z. Jelinek, G. Grasso, I. Hiltunen, A. Korpela, J. Lehtonen, R. Mikkonen, and M. Runde. Electromagnetic viewpoints on a 200 kW MgB_2 induction heater. *Pysica C: Superconductivity*, 468:487–491, 2008.

[59] S.L. Bud'ko et al. Boron isotope effect in superconducting MgB_2. *Physical Review Letters*, 86(9):1877–1880, 2001.

[60] M. D. Sumption et al. Irreversibility field and flux pinning in MgB_2 with and without SiC additions. *Superconductor Science and Technology*, 17(10):1180–1184, 2004.

[61] Hypertech Research. `www.Hypertechresearch.com`.

[62] ColumbusSuperconductor. `http://www.columbussuperconductors.com`.

[63] H. van Weeren. *Magnesium Diboride Superconductors For Magnet Applications.* PhD thesis, University of Twente, Enschede, 2007.

[64] M.D. Sumption, S. Bohnenstiehl, F. Buta, M. Majoros, S. Kawabata, M. Tomsic, M. Rindfleish, J. Phillips, J. Yue, and E.W. Collings. Wind and react and react and

wind MgB_2 solenoid racetrack and pancake coils. *IEEE Transactions on Applied Superconductivity*, 17(2):2286–2290, 2007.

[65] K. Melconian, K. Damborksy, N. Glasser, E. Holik, J. Kellams, P. McIntyre, N. Pogue, and A. Sattarov. Design and development of a MgB_2-based sector dipole and beam transport channel for a strong-focusing cyclotron. *AIP Conference Proceedings*, 1573:739–741, 2014.

APPENDIX A. SEQUENCE FILES FOR MAD-X-PTC AND SYNERGIA

MAD-X-PTC Sequence File

```
sF11: SBEND,L=0.2279007900,ANGLE=0.4472556077,K1:=kqf1a,THICK=TRUE,APERTYPE=CIRCLE,APERTURE=0.03;
s11: SBEND,L=0.0700000000,ANGLE=0.1373750944,THICK=TRUE,APERTYPE=CIRCLE,APERTURE=0.03;
sD11: SBEND,L=0.2279007900,ANGLE=0.4472556077,K1:=kqd1a,THICK=TRUE,APERTYPE=CIRCLE,APERTURE=0.03;
sF21: SBEND,L=0.2393637800,ANGLE=0.4656413252,K1:=kqf1b,THICK=TRUE,APERTYPE=CIRCLE,APERTURE=0.03;
s21: SBEND,L=0.0700000000,ANGLE=0.1361730366,THICK=TRUE,APERTYPE=CIRCLE,APERTURE=0.03;
sD21: SBEND,L=0.2393637800,ANGLE=0.4656413252,K1:=kqd1b,THICK=TRUE,APERTYPE=CIRCLE,APERTURE=0.03;
sF31: SBEND,L=0.2404674250,ANGLE=0.4528404554,K1:=kqf1c,THICK=TRUE,APERTYPE=CIRCLE,APERTURE=0.03;
s31: SBEND,L=0.0700000000,ANGLE=0.1324295258,THICK=TRUE,APERTYPE=CIRCLE,APERTURE=0.03;
sD31: SBEND,L=0.2404674250,ANGLE=0.4549283866,K1:=kqd1c,THICK=TRUE,APERTYPE=CIRCLE,APERTURE=0.03;
sF41: SBEND,L=0.2433484100,ANGLE=0.4589988987,K1:=kqf1d,THICK=TRUE,APERTYPE=CIRCLE,APERTURE=0.03;
s41: SBEND,L=0.0700000000,ANGLE=0.1320325985,THICK=TRUE,APERTYPE=CIRCLE,APERTURE=0.03;
sD41: SBEND,L=0.2433484100,ANGLE=0.4589988987,K1:=kqd1d,THICK=TRUE,APERTYPE=CIRCLE,APERTURE=0.03;
sF51: SBEND,L=0.2461707650,ANGLE=0.4470921312,K1:=kqf1e,THICK=TRUE,APERTYPE=CIRCLE,APERTURE=0.03;
s51: SBEND,L=0.0700000000,ANGLE=0.1271330866,THICK=TRUE,APERTYPE=CIRCLE,APERTURE=0.03;
sD51: SBEND,L=0.2461707650,ANGLE=0.4470921312,K1:=kqd1e,THICK=TRUE,APERTYPE=CIRCLE,APERTURE=0.03;
sF61: SBEND,L=0.2639128900,ANGLE=0.4740745785,K1:=kqf1f,THICK=TRUE,APERTYPE=CIRCLE,APERTURE=0.03;
s61: SBEND,L=0.0700000000,ANGLE=0.1257430832,THICK=TRUE,APERTYPE=CIRCLE,APERTURE=0.03;
sD61: SBEND,L=0.2639128900,ANGLE=0.4740745785,K1:=kqd1f,THICK=TRUE,APERTYPE=CIRCLE,APERTURE=0.03;
d11: DRIFT, L=0.4019962300;
d2a1: DRIFT, L=0.3968689400;
c11: DRIFT, L=0.0374087700;
d2c1: DRIFT, L=0.3344657900;
d3a1: DRIFT, L=0.3665938500;
c21: DRIFT, L=0.0374081950;
d3c1: DRIFT, L=0.3664306900;
d41: DRIFT, L=0.4041549250;
d5a1: DRIFT, L=0.3711367300;
c31: DRIFT, L=0.0366568500;
d5c1: DRIFT, L=0.3645031300;
d6a1: DRIFT, L=0.4164455700;
c41: DRIFT, L=0.0369916000;
d6c1: DRIFT, L=0.3219282100;
d61: DRIFT, L=0.4076247000;
m11: marker;
```

```
m21: marker;
m31: marker;
m41: marker;
m51: marker;
m61: marker;
sF12: SBEND,L=0.2685317600,ANGLE=0.4559444620,K1:=kqf2a,THICK=TRUE,APERTYPE=CIRCLE,APERTURE=0.03;
s12: SBEND,L=0.0700000000,ANGLE=0.1188541435,THICK=TRUE,APERTYPE=CIRCLE,APERTURE=0.03;
sD12: SBEND,L=0.2685317600,ANGLE=0.4559444620,K1:=kqd2a,THICK=TRUE,APERTYPE=CIRCLE,APERTURE=0.03;
sF22: SBEND,L=0.2806405100,ANGLE=0.4745450918,K1:=kqf2b,THICK=TRUE,APERTYPE=CIRCLE,APERTURE=0.03;
s22: SBEND,L=0.0700000000,ANGLE=0.1183655076,THICK=TRUE,APERTYPE=CIRCLE,APERTURE=0.03;
sD22: SBEND,L=0.2806405100,ANGLE=0.4745450918,K1:=kqd2b,THICK=TRUE,APERTYPE=CIRCLE,APERTURE=0.03;
sF32: SBEND,L=0.2893448750,ANGLE=0.3966910088,K1:=kqf2c,THICK=TRUE,APERTYPE=CIRCLE,APERTURE=0.03;
s32: SBEND,L=0.0700000000,ANGLE=0.0989464087,THICK=TRUE,APERTYPE=CIRCLE,APERTURE=0.03;
sD32: SBEND,L=0.2893448750,ANGLE=0.4089948039,K1:=kqd2c,THICK=TRUE,APERTYPE=CIRCLE,APERTURE=0.03;
sF42: SBEND,L=0.3722747100,ANGLE=0.5371859440,K1:=kqf2d,THICK=TRUE,APERTYPE=CIRCLE,APERTURE=0.03;
s42: SBEND,L=0.0700000000,ANGLE=0.1010087848,THICK=TRUE,APERTYPE=CIRCLE,APERTURE=0.03;
sD42: SBEND,L=0.3722747100,ANGLE=0.5371859440,K1:=kqd2d,THICK=TRUE,APERTYPE=CIRCLE,APERTURE=0.03;
sF52: SBEND,L=0.3828398550,ANGLE=0.4675002117,K1:=kqf2e,THICK=TRUE,APERTYPE=CIRCLE,APERTURE=0.03;
s52: SBEND,L=0.0700000000,ANGLE=0.0854796448,THICK=TRUE,APERTYPE=CIRCLE,APERTURE=0.03;
sD52: SBEND,L=0.3828398550,ANGLE=0.4675002117,K1:=kqd2e,THICK=TRUE,APERTYPE=CIRCLE,APERTURE=0.03;
sF62: SBEND,L=0.4038510550,ANGLE=0.4957461446,K1:=kqf2f,THICK=TRUE,APERTYPE=CIRCLE,APERTURE=0.03;
s62: SBEND,L=0.0700000000,ANGLE=0.0859282889,THICK=TRUE,APERTYPE=CIRCLE,APERTURE=0.03;
sD62: SBEND,L=0.4038510550,ANGLE=0.4957461446,K1:=kqd2f,THICK=TRUE,APERTYPE=CIRCLE,APERTURE=0.03;
d12: DRIFT, L=0.4076247000;
d2a2: DRIFT, L=0.3975249400;
c12: DRIFT, L=0.0407436300;
d2c2: DRIFT, L=0.3387204100;
d3a2: DRIFT, L=0.3690705900;
c22: DRIFT, L=0.0407819100;
d3c2: DRIFT, L=0.3689169400;
d42: DRIFT, L=0.4198962050;
d5a2: DRIFT, L=0.3786526900;
c32: DRIFT, L=0.0477271200;
d5c2: DRIFT, L=0.3732725400;
d6a2: DRIFT, L=0.4156055500;
c42: DRIFT, L=0.0482606200;
d6c2: DRIFT, L=0.3393825000;
d62: DRIFT, L=0.4273608900;
m12: marker;
```

```
m22: marker;
m32: marker;
m42: marker;
m52: marker;
m62: marker;
sF13: SBEND,L=0.4075657250,ANGLE=0.4729890940,K1:=kqf3a,THICK=TRUE,APERTYPE=CIRCLE,APERTURE=0.03;
s13: SBEND,L=0.0700000000,ANGLE=0.0812365578,THICK=TRUE,APERTYPE=CIRCLE,APERTURE=0.03;
sD13: SBEND,L=0.4075657250,ANGLE=0.4729890940,K1:=kqd3a,THICK=TRUE,APERTYPE=CIRCLE,APERTURE=0.03;
sF23: SBEND,L=0.4218007200,ANGLE=0.4928336985,K1:=kqf3b,THICK=TRUE,APERTYPE=CIRCLE,APERTURE=0.03;
s23: SBEND,L=0.0700000000,ANGLE=0.0817882883,THICK=TRUE,APERTYPE=CIRCLE,APERTURE=0.03;
sD23: SBEND,L=0.4218007200,ANGLE=0.4928336985,K1:=kqd3b,THICK=TRUE,APERTYPE=CIRCLE,APERTURE=0.03;
sF33: SBEND,L=0.4241715800,ANGLE=0.4753403473,K1:=kqf3c,THICK=TRUE,APERTYPE=CIRCLE,APERTURE=0.03;
s33: SBEND,L=0.0700000000,ANGLE=0.0788851767,THICK=TRUE,APERTYPE=CIRCLE,APERTURE=0.03;
sD33: SBEND,L=0.4241715800,ANGLE=0.4780121431,K1:=kqd3c,THICK=TRUE,APERTYPE=CIRCLE,APERTURE=0.03;
sF43: SBEND,L=0.4331058150,ANGLE=0.4891727565,K1:=kqf3d,THICK=TRUE,APERTYPE=CIRCLE,APERTURE=0.03;
s43: SBEND,L=0.0700000000,ANGLE=0.0790617253,THICK=TRUE,APERTYPE=CIRCLE,APERTURE=0.03;
sD43: SBEND,L=0.4331058150,ANGLE=0.4891727565,K1:=kqd3d,THICK=TRUE,APERTYPE=CIRCLE,APERTURE=0.03;
sF53: SBEND,L=0.4378921100,ANGLE=0.4723798648,K1:=kqf3e,THICK=TRUE,APERTYPE=CIRCLE,APERTURE=0.03;
s53: SBEND,L=0.0700000000,ANGLE=0.0755130996,THICK=TRUE,APERTYPE=CIRCLE,APERTURE=0.03;
sD53: SBEND,L=0.4378921100,ANGLE=0.4723798648,K1:=kqd3e,THICK=TRUE,APERTYPE=CIRCLE,APERTURE=0.03;
sF63: SBEND,L=0.4602635950,ANGLE=0.5007925508,K1:=kqf3f,THICK=TRUE,APERTYPE=CIRCLE,APERTURE=0.03;
s63: SBEND,L=0.0700000000,ANGLE=0.0761639177,THICK=TRUE,APERTYPE=CIRCLE,APERTURE=0.03;
sD63: SBEND,L=0.4602635950,ANGLE=0.5007925508,K1:=kqd3f,THICK=TRUE,APERTYPE=CIRCLE,APERTURE=0.03;
d13: DRIFT, L=0.4273608900;
d2a3: DRIFT, L=0.3997683700;
c13: DRIFT, L=0.0521483400;
d2c3: DRIFT, L=0.3532705600;
d3a3: DRIFT, L=0.3775406500;
c23: DRIFT, L=0.0523195100;
d3c3: DRIFT, L=0.3774195400;
d43: DRIFT, L=0.4305798200;
d5a3: DRIFT, L=0.3816802200;
c33: DRIFT, L=0.0521863800;
d5c3: DRIFT, L=0.3768049800;
d6a3: DRIFT, L=0.4152671700;
c43: DRIFT, L=0.0527999450;
d6c3: DRIFT, L=0.3464133300;
d63: DRIFT, L=0.4353591150;
m13: marker;
```

```
m23: marker;
m33: marker;
m43: marker;
m53: marker;
m63: marker;
sF14: SBEND,L=0.4641985950,ANGLE=0.4774444363,K1:=kqf4a,THICK=TRUE,APERTYPE=CIRCLE,APERTURE=0.03;
s14: SBEND,L=0.0700000000,ANGLE=0.0719974401,THICK=TRUE,APERTYPE=CIRCLE,APERTURE=0.03;
sD14: SBEND,L=0.4641985950,ANGLE=0.4774444363,K1:=kqd4a,THICK=TRUE,APERTYPE=CIRCLE,APERTURE=0.03;
sF24: SBEND,L=0.4793417250,ANGLE=0.4974086518,K1:=kqf4b,THICK=TRUE,APERTYPE=CIRCLE,APERTURE=0.03;
s24: SBEND,L=0.0700000000,ANGLE=0.0726383784,THICK=TRUE,APERTYPE=CIRCLE,APERTURE=0.03;
sD24: SBEND,L=0.4793417250,ANGLE=0.4974086518,K1:=kqd4b,THICK=TRUE,APERTYPE=CIRCLE,APERTURE=0.03;
sF34: SBEND,L=0.4889286350,ANGLE=0.4391922054,K1:=kqf4c,THICK=TRUE,APERTYPE=CIRCLE,APERTURE=0.03;
s34: SBEND,L=0.0700000000,ANGLE=0.0641368209,THICK=TRUE,APERTYPE=CIRCLE,APERTURE=0.03;
sD34: SBEND,L=0.4889286350,ANGLE=0.4479761186,K1:=kqd4c,THICK=TRUE,APERTYPE=CIRCLE,APERTURE=0.03;
sF44: SBEND,L=0.5578391500,ANGLE=0.5326916304,K1:=kqf4d,THICK=TRUE,APERTYPE=CIRCLE,APERTURE=0.03;
s44: SBEND,L=0.0700000000,ANGLE=0.0668443836,THICK=TRUE,APERTYPE=CIRCLE,APERTURE=0.03;
sD44: SBEND,L=0.5578391500,ANGLE=0.5326916304,K1:=kqd4d,THICK=TRUE,APERTYPE=CIRCLE,APERTURE=0.03;
sF54: SBEND,L=0.5698917400,ANGLE=0.4804630108,K1:=kqf4e,THICK=TRUE,APERTYPE=CIRCLE,APERTURE=0.03;
s54: SBEND,L=0.0700000000,ANGLE=0.0590154382,THICK=TRUE,APERTYPE=CIRCLE,APERTURE=0.03;
sD54: SBEND,L=0.5698917400,ANGLE=0.4804630108,K1:=kqd4e,THICK=TRUE,APERTYPE=CIRCLE,APERTURE=0.03;
sF64: SBEND,L=0.5955816600,ANGLE=0.5089646466,K1:=kqf4f,THICK=TRUE,APERTYPE=CIRCLE,APERTURE=0.03;
s64: SBEND,L=0.0700000000,ANGLE=0.0598197152,THICK=TRUE,APERTYPE=CIRCLE,APERTURE=0.03;
sD64: SBEND,L=0.5955816600,ANGLE=0.5089646466,K1:=kqd4f,THICK=TRUE,APERTYPE=CIRCLE,APERTURE=0.03;
d14: DRIFT, L=0.4353591150;
d2a4: DRIFT, L=0.4006828600;
c14: DRIFT, L=0.0567972300;
d2c4: DRIFT, L=0.3592016200;
d3a4: DRIFT, L=0.3809932900;
c24: DRIFT, L=0.0570225700;
d3c4: DRIFT, L=0.3808854500;
d44: DRIFT, L=0.4454073050;
d5a4: DRIFT, L=0.3889393900;
c34: DRIFT, L=0.0628784150;
d5c4: DRIFT, L=0.3852747600;
d6a4: DRIFT, L=0.4144558500;
c44: DRIFT, L=0.0636839500;
d6c4: DRIFT, L=0.3632712700;
d64: DRIFT, L=0.4545829400;
m14: marker;
```

```
m24: marker;
m34: marker;
m44: marker;
m54: marker;
m64: marker;
sF15: SBEND,L=0.6005918050,ANGLE=0.4851694927,K1:=kqf5a,THICK=TRUE,APERTYPE=CIRCLE,APERTURE=0.03;
s15: SBEND,L=0.0700000000,ANGLE=0.0565473325,THICK=TRUE,APERTYPE=CIRCLE,APERTURE=0.03;
sD15: SBEND,L=0.6005918050,ANGLE=0.4851694927,K1:=kqd5a,THICK=TRUE,APERTYPE=CIRCLE,APERTURE=0.03;
sF25: SBEND,L=0.6179765200,ANGLE=0.5051196558,K1:=kqf5b,THICK=TRUE,APERTYPE=CIRCLE,APERTURE=0.03;
s25: SBEND,L=0.0700000000,ANGLE=0.0572163743,THICK=TRUE,APERTYPE=CIRCLE,APERTURE=0.03;
sD25: SBEND,L=0.6179765200,ANGLE=0.5051196558,K1:=kqd5b,THICK=TRUE,APERTYPE=CIRCLE,APERTURE=0.03;
sF35: SBEND,L=0.6219284700,ANGLE=0.4842746520,K1:=kqf5c,THICK=TRUE,APERTYPE=CIRCLE,APERTURE=0.03;
s35: SBEND,L=0.0700000000,ANGLE=0.0548552001,THICK=TRUE,APERTYPE=CIRCLE,APERTURE=0.03;
sD35: SBEND,L=0.6219284700,ANGLE=0.4873715806,K1:=kqd5c,THICK=TRUE,APERTYPE=CIRCLE,APERTURE=0.03;
sF45: SBEND,L=0.6375578000,ANGLE=0.5037071659,K1:=kqf5d,THICK=TRUE,APERTYPE=CIRCLE,APERTURE=0.03;
s45: SBEND,L=0.0700000000,ANGLE=0.0553040079,THICK=TRUE,APERTYPE=CIRCLE,APERTURE=0.03;
sD45: SBEND,L=0.6375578000,ANGLE=0.5037071659,K1:=kqd5d,THICK=TRUE,APERTYPE=CIRCLE,APERTURE=0.03;
sF55: SBEND,L=0.6446622600,ANGLE=0.4836456748,K1:=kqf5e,THICK=TRUE,APERTYPE=CIRCLE,APERTURE=0.03;
s55: SBEND,L=0.0700000000,ANGLE=0.0525161768,THICK=TRUE,APERTYPE=CIRCLE,APERTURE=0.03;
sD55: SBEND,L=0.6446622600,ANGLE=0.4836456748,K1:=kqd5e,THICK=TRUE,APERTYPE=CIRCLE,APERTURE=0.03;
sF65: SBEND,L=0.6722318950,ANGLE=0.5122062825,K1:=kqf5f,THICK=TRUE,APERTYPE=CIRCLE,APERTURE=0.03;
s65: SBEND,L=0.0700000000,ANGLE=0.0533364157,THICK=TRUE,APERTYPE=CIRCLE,APERTURE=0.03;
sD65: SBEND,L=0.6722318950,ANGLE=0.5122062825,K1:=kqd5f,THICK=TRUE,APERTYPE=CIRCLE,APERTURE=0.03;
d15: DRIFT, L=0.4545829400;
d2a5: DRIFT, L=0.4028861600;
c15: DRIFT, L=0.0679979050;
d2c5: DRIFT, L=0.3734914600;
d3a5: DRIFT, L=0.3893118200;
c25: DRIFT, L=0.0683537600;
d3c5: DRIFT, L=0.3892359500;
d45: DRIFT, L=0.4590446750;
d5a5: DRIFT, L=0.3930513000;
c35: DRIFT, L=0.0689348700;
d5c5: DRIFT, L=0.3900724300;
d6a5: DRIFT, L=0.4139962800;
c45: DRIFT, L=0.0698491400;
d6c5: DRIFT, L=0.3728203700;
d65: DRIFT, L=0.4654721800;
m15: marker;
```

```
m25: marker;
m35: marker;
m45: marker;
m55: marker;
m65: marker;
sF16: SBEND,L=0.6778510750,ANGLE=0.4882338248,K1:=kqf6a,THICK=TRUE,APERTYPE=CIRCLE,APERTURE=0.03;
s16: SBEND,L=0.0700000000,ANGLE=0.0504186967,THICK=TRUE,APERTYPE=CIRCLE,APERTURE=0.03;
sD16: SBEND,L=0.6778510750,ANGLE=0.4882338248,K1:=kqd6a,THICK=TRUE,APERTYPE=CIRCLE,APERTURE=0.03;
sF26: SBEND,L=0.6965055300,ANGLE=0.5081908181,K1:=kqf6b,THICK=TRUE,APERTYPE=CIRCLE,APERTURE=0.03;
s26: SBEND,L=0.0700000000,ANGLE=0.0510740486,THICK=TRUE,APERTYPE=CIRCLE,APERTURE=0.03;
sD26: SBEND,L=0.6965055300,ANGLE=0.5081908181,K1:=kqd6b,THICK=TRUE,APERTYPE=CIRCLE,APERTURE=0.03;
sF36: SBEND,L=0.7065994350,ANGLE=0.4627409094,K1:=kqf6c,THICK=TRUE,APERTYPE=CIRCLE,APERTURE=0.03;
s36: SBEND,L=0.0700000000,ANGLE=0.0465062548,THICK=TRUE,APERTYPE=CIRCLE,APERTURE=0.03;
sD36: SBEND,L=0.7065994350,ANGLE=0.4694470482,K1:=kqd6c,THICK=TRUE,APERTYPE=CIRCLE,APERTURE=0.03;
sF46: SBEND,L=0.7661604900,ANGLE=0.5292794539,K1:=kqf6d,THICK=TRUE,APERTYPE=CIRCLE,APERTURE=0.03;
s46: SBEND,L=0.0700000000,ANGLE=0.0483574424,THICK=TRUE,APERTYPE=CIRCLE,APERTURE=0.03;
sD46: SBEND,L=0.7661604900,ANGLE=0.5292794539,K1:=kqd6d,THICK=TRUE,APERTYPE=CIRCLE,APERTURE=0.03;
sF56: SBEND,L=0.7795555800,ANGLE=0.4879103833,K1:=kqf6e,THICK=TRUE,APERTYPE=CIRCLE,APERTURE=0.03;
s56: SBEND,L=0.0700000000,ANGLE=0.0438117919,THICK=TRUE,APERTYPE=CIRCLE,APERTURE=0.03;
sD56: SBEND,L=0.7795555800,ANGLE=0.4879103833,K1:=kqd6e,THICK=TRUE,APERTYPE=CIRCLE,APERTURE=0.03;
sF66: SBEND,L=0.8105163900,ANGLE=0.5165678901,K1:=kqf6f,THICK=TRUE,APERTYPE=CIRCLE,APERTURE=0.03;
s66: SBEND,L=0.0700000000,ANGLE=0.0446132278,THICK=TRUE,APERTYPE=CIRCLE,APERTURE=0.03;
sD66: SBEND,L=0.8105163900,ANGLE=0.5165678901,K1:=kqd6f,THICK=TRUE,APERTYPE=CIRCLE,APERTURE=0.03;
d16: DRIFT, L=0.4654721800;
d2a6: DRIFT, L=0.4041342100;
c16: DRIFT, L=0.0743424750;
d2c6: DRIFT, L=0.3815858800;
d3a6: DRIFT, L=0.3940238000;
c26: DRIFT, L=0.0747722550;
d3c6: DRIFT, L=0.3939660400;
d46: DRIFT, L=0.4748200200;
d5a6: DRIFT, L=0.4004696000;
c36: DRIFT, L=0.0798612950;
d5c6: DRIFT, L=0.3987278900;
d6a6: DRIFT, L=0.4131671700;
c46: DRIFT, L=0.0809717450;
d6c6: DRIFT, L=0.3900478700;
d66: DRIFT, L=0.4851174250;
m16: marker;
```

```
m26: marker;
m36: marker;
m46: marker;
m56: marker;
m66: marker;
sF17: SBEND,L=0.8172342500,ANGLE=0.4923568063,K1:=kqf7a,THICK=TRUE,APERTYPE=CIRCLE,APERTURE=0.03;
s17: SBEND,L=0.0700000000,ANGLE=0.0421727019,THICK=TRUE,APERTYPE=CIRCLE,APERTURE=0.03;
sD17: SBEND,L=0.8172342500,ANGLE=0.4923568063,K1:=kqd7a,THICK=TRUE,APERTYPE=CIRCLE,APERTURE=0.03;
sF27: SBEND,L=0.8381794250,ANGLE=0.5123342173,K1:=kqf7b,THICK=TRUE,APERTYPE=CIRCLE,APERTURE=0.03;
s27: SBEND,L=0.0700000000,ANGLE=0.0427872531,THICK=TRUE,APERTYPE=CIRCLE,APERTURE=0.03;
sD27: SBEND,L=0.8381794250,ANGLE=0.5123342173,K1:=kqd7b,THICK=TRUE,APERTYPE=CIRCLE,APERTURE=0.03;
sF37: SBEND,L=0.8434605650,ANGLE=0.4911850253,K1:=kqf7c,THICK=TRUE,APERTYPE=CIRCLE,APERTURE=0.03;
s37: SBEND,L=0.0700000000,ANGLE=0.0410209923,THICK=TRUE,APERTYPE=CIRCLE,APERTURE=0.03;
sD37: SBEND,L=0.8434605650,ANGLE=0.4942798482,K1:=kqd7c,THICK=TRUE,APERTYPE=CIRCLE,APERTURE=0.03;
sF47: SBEND,L=0.8623471500,ANGLE=0.5106426064,K1:=kqf7d,THICK=TRUE,APERTYPE=CIRCLE,APERTURE=0.03;
s47: SBEND,L=0.0700000000,ANGLE=0.0414508037,THICK=TRUE,APERTYPE=CIRCLE,APERTURE=0.03;
sD47: SBEND,L=0.8623471500,ANGLE=0.5106426064,K1:=kqd7d,THICK=TRUE,APERTYPE=CIRCLE,APERTURE=0.03;
sF57: SBEND,L=0.8715857700,ANGLE=0.4900902565,K1:=kqf7e,THICK=TRUE,APERTYPE=CIRCLE,APERTURE=0.03;
s57: SBEND,L=0.0700000000,ANGLE=0.0393608055,THICK=TRUE,APERTYPE=CIRCLE,APERTURE=0.03;
sD57: SBEND,L=0.8715857700,ANGLE=0.4900902565,K1:=kqd7e,THICK=TRUE,APERTYPE=CIRCLE,APERTURE=0.03;
sF67: SBEND,L=0.9048602000,ANGLE=0.5188070257,K1:=kqf7f,THICK=TRUE,APERTYPE=CIRCLE,APERTURE=0.03;
s67: SBEND,L=0.0700000000,ANGLE=0.0401349201,THICK=TRUE,APERTYPE=CIRCLE,APERTURE=0.03;
sD67: SBEND,L=0.9048602000,ANGLE=0.5188070257,K1:=kqd7f,THICK=TRUE,APERTYPE=CIRCLE,APERTURE=0.03;
d17: DRIFT, L=0.4851174250;
d2a7: DRIFT, L=0.4063858100;
c17: DRIFT, L=0.0857886850;
d2c7: DRIFT, L=0.3961889700;
d3a7: DRIFT, L=0.4025246900;
c27: DRIFT, L=0.0863518400;
d3c7: DRIFT, L=0.4024995900;
d47: DRIFT, L=0.4905982800;
d5a7: DRIFT, L=0.4055307000;
c37: DRIFT, L=0.0873157900;
d5c7: DRIFT, L=0.4046330300;
d6a7: DRIFT, L=0.4126015100;
c47: DRIFT, L=0.0885600750;
d6c7: DRIFT, L=0.4018012300;
d67: DRIFT, L=0.4985202850;
m17: marker;
```

```
m27: marker;
m37: marker;
m47: marker;
m57: marker;
m67: marker;
sF18: SBEND,L=0.9123276900,ANGLE=0.4944734875,K1:=kqf8a,THICK=TRUE,APERTYPE=CIRCLE,APERTURE=0.03;
s18: SBEND,L=0.0700000000,ANGLE=0.0379393769,THICK=TRUE,APERTYPE=CIRCLE,APERTURE=0.03;
sD18: SBEND,L=0.9123276900,ANGLE=0.4944734875,K1:=kqd8a,THICK=TRUE,APERTYPE=CIRCLE,APERTURE=0.03;
sF28: SBEND,L=0.9348357050,ANGLE=0.5144663592,K1:=kqf8b,THICK=TRUE,APERTYPE=CIRCLE,APERTURE=0.03;
s28: SBEND,L=0.0700000000,ANGLE=0.0385229671,THICK=TRUE,APERTYPE=CIRCLE,APERTURE=0.03;
sD28: SBEND,L=0.9348357050,ANGLE=0.5144663592,K1:=kqd8b,THICK=TRUE,APERTYPE=CIRCLE,APERTURE=0.03;
sF38: SBEND,L=0.9446379700,ANGLE=0.4799062686,K1:=kqf8c,THICK=TRUE,APERTYPE=CIRCLE,APERTURE=0.03;
s38: SBEND,L=0.0700000000,ANGLE=0.0359351259,THICK=TRUE,APERTYPE=CIRCLE,APERTURE=0.03;
sD38: SBEND,L=0.9446379700,ANGLE=0.4849383490,K1:=kqd8c,THICK=TRUE,APERTYPE=CIRCLE,APERTURE=0.03;
sF48: SBEND,L=0.9924152950,ANGLE=0.5247459647,K1:=kqf8d,THICK=TRUE,APERTYPE=CIRCLE,APERTURE=0.03;
s48: SBEND,L=0.0700000000,ANGLE=0.0370129498,THICK=TRUE,APERTYPE=CIRCLE,APERTURE=0.03;
sD48: SBEND,L=0.9924152950,ANGLE=0.5247459647,K1:=kqd8d,THICK=TRUE,APERTYPE=CIRCLE,APERTURE=0.03;
sF58: SBEND,L=1.0064791000,ANGLE=0.4925896292,K1:=kqf8e,THICK=TRUE,APERTYPE=CIRCLE,APERTURE=0.03;
s58: SBEND,L=0.0700000000,ANGLE=0.0342593046,THICK=TRUE,APERTYPE=CIRCLE,APERTURE=0.03;
sD58: SBEND,L=1.0064791000,ANGLE=0.4925896292,K1:=kqd8e,THICK=TRUE,APERTYPE=CIRCLE,APERTURE=0.03;
sF68: SBEND,L=1.0431447050,ANGLE=0.5213809275,K1:=kqf8f,THICK=TRUE,APERTYPE=CIRCLE,APERTURE=0.03;
s68: SBEND,L=0.0700000000,ANGLE=0.0349871545,THICK=TRUE,APERTYPE=CIRCLE,APERTURE=0.03;
sD68: SBEND,L=1.0431447050,ANGLE=0.5213809275,K1:=kqd8f,THICK=TRUE,APERTYPE=CIRCLE,APERTURE=0.03;
d18: DRIFT, L=0.4985202850;
d2a8: DRIFT, L=0.4079219500;
c18: DRIFT, L=0.0935978050;
d2c8: DRIFT, L=0.4061518600;
d3a8: DRIFT, L=0.4083243700;
c28: DRIFT, L=0.0942519500;
d3c8: DRIFT, L=0.4083215600;
d48: DRIFT, L=0.5072350550;
d5a8: DRIFT, L=0.4131454300;
c38: DRIFT, L=0.0982422200;
d5c8: DRIFT, L=0.4130920600;
d6a8: DRIFT, L=0.4169626700;
c48: DRIFT, L=0.0996826800;
d6c8: DRIFT, L=0.4138384700;
d68: DRIFT, L=0.5181655300;
m18: marker;
```

```
m28: marker;
m38: marker;
m48: marker;
m58: marker;
m68: marker;
sF19: SBEND,L=1.0517108600,ANGLE=0.4969065489,K1:=kqf9a,THICK=TRUE,APERTYPE=CIRCLE,APERTURE=0.03;
s19: SBEND,L=0.0700000000,ANGLE=0.0330732141,THICK=TRUE,APERTYPE=CIRCLE,APERTURE=0.03;
sD19: SBEND,L=1.0517108600,ANGLE=0.4969065489,K1:=kqd9a,THICK=TRUE,APERTYPE=CIRCLE,APERTURE=0.03;
sF29: SBEND,L=1.0765095950,ANGLE=0.5169214443,K1:=kqf9b,THICK=TRUE,APERTYPE=CIRCLE,APERTURE=0.03;
s29: SBEND,L=0.0700000000,ANGLE=0.0336127994,THICK=TRUE,APERTYPE=CIRCLE,APERTURE=0.03;
sD29: SBEND,L=1.0765095950,ANGLE=0.5169214443,K1:=kqd9b,THICK=TRUE,APERTYPE=CIRCLE,APERTURE=0.03;
sF39: SBEND,L=1.0819769500,ANGLE=0.4994406268,K1:=kqf9c,THICK=TRUE,APERTYPE=CIRCLE,APERTURE=0.03;
s39: SBEND,L=0.0700000000,ANGLE=0.0324761099,THICK=TRUE,APERTYPE=CIRCLE,APERTURE=0.03;
sD39: SBEND,L=1.0819769500,ANGLE=0.5019771757,K1:=kqd9c,THICK=TRUE,APERTYPE=CIRCLE,APERTURE=0.03;
sF49: SBEND,L=1.0957912550,ANGLE=0.5116023448,K1:=kqf9d,THICK=TRUE,APERTYPE=CIRCLE,APERTURE=0.03;
s49: SBEND,L=0.0700000000,ANGLE=0.0326815568,THICK=TRUE,APERTYPE=CIRCLE,APERTURE=0.03;
sD49: SBEND,L=1.0957912550,ANGLE=0.5116023448,K1:=kqd9d,THICK=TRUE,APERTYPE=CIRCLE,APERTURE=0.03;
sF59: SBEND,L=1.1060604900,ANGLE=0.4940549457,K1:=kqf9e,THICK=TRUE,APERTYPE=CIRCLE,APERTURE=0.03;
s59: SBEND,L=0.0700000000,ANGLE=0.0312675903,THICK=TRUE,APERTYPE=CIRCLE,APERTURE=0.03;
sD59: SBEND,L=1.1060604900,ANGLE=0.4940549457,K1:=kqd9e,THICK=TRUE,APERTYPE=CIRCLE,APERTURE=0.03;
sF69: SBEND,L=1.1452295450,ANGLE=0.5228940481,K1:=kqf9f,THICK=TRUE,APERTYPE=CIRCLE,APERTURE=0.03;
s69: SBEND,L=0.0700000000,ANGLE=0.0319609143,THICK=TRUE,APERTYPE=CIRCLE,APERTURE=0.03;
sD69: SBEND,L=1.1452295450,ANGLE=0.5228940481,K1:=kqd9f,THICK=TRUE,APERTYPE=CIRCLE,APERTURE=0.03;
d19: DRIFT, L=0.5181655300;
d2a9: DRIFT, L=0.4193671700;
c19: DRIFT, L=0.1050440150;
d2c9: DRIFT, L=0.4115613300;
d3a9: DRIFT, L=0.4168514600;
c29: DRIFT, L=0.1058315350;
d3c9: DRIFT, L=0.4168288900;
d49: DRIFT, L=0.5239237900;
d5a9: DRIFT, L=0.4195311800;
c39: DRIFT, L=0.1063083650;
d5c9: DRIFT, L=0.4185723400;
d6a9: DRIFT, L=0.4296232000;
c49: DRIFT, L=0.1078936450;
d6c9: DRIFT, L=0.4132836100;
d69: DRIFT, L=0.5326681050;
m19: marker;
```

```
m29: marker;
m39: marker;
m49: marker;
m59: marker;
m69: marker;
sF110: SBEND,L=1.1546067900,ANGLE=0.4983368935,K1:=kqf10a,THICK=TRUE,APERTYPE=CIRCLE,APERTURE=0.03;
s110: SBEND,L=0.0700000000,ANGLE=0.0302125216,THICK=TRUE,APERTYPE=CIRCLE,APERTURE=0.03;
sD110: SBEND,L=1.1546067900,ANGLE=0.4983368935,K1:=kqd10a,THICK=TRUE,APERTYPE=CIRCLE,APERTURE=0.03;
sF210: SBEND,L=1.1810965950,ANGLE=0.5183668308,K1:=kqf10b,THICK=TRUE,APERTYPE=CIRCLE,APERTURE=0.03;
s210: SBEND,L=0.0700000000,ANGLE=0.0307220242,THICK=TRUE,APERTYPE=CIRCLE,APERTURE=0.03;
sD210: SBEND,L=1.1810965950,ANGLE=0.5183668308,K1:=kqd10b,THICK=TRUE,APERTYPE=CIRCLE,APERTURE=0.03;
sF310: SBEND,L=1.1895958150,ANGLE=0.4937695889,K1:=kqf10c,THICK=TRUE,APERTYPE=CIRCLE,APERTURE=0.03;
s310: SBEND,L=0.0700000000,ANGLE=0.0292642205,THICK=TRUE,APERTYPE=CIRCLE,APERTURE=0.03;
sD310: SBEND,L=1.1895958150,ANGLE=0.4973227753,K1:=kqd10c,THICK=TRUE,APERTYPE=CIRCLE,APERTURE=0.03;
sF410: SBEND,L=1.2211713350,ANGLE=0.5193192530,K1:=kqf10d,THICK=TRUE,APERTYPE=CIRCLE,APERTURE=0.03;
s410: SBEND,L=0.0700000000,ANGLE=0.0297684253,THICK=TRUE,APERTYPE=CIRCLE,APERTURE=0.03;
sD410: SBEND,L=1.2211713350,ANGLE=0.5193192530,K1:=kqd10d,THICK=TRUE,APERTYPE=CIRCLE,APERTURE=0.03;
sF510: SBEND,L=1.2348857200,ANGLE=0.4956097813,K1:=kqf10e,THICK=TRUE,APERTYPE=CIRCLE,APERTURE=0.03;
s510: SBEND,L=0.0700000000,ANGLE=0.0280938423,THICK=TRUE,APERTYPE=CIRCLE,APERTURE=0.03;
sD510: SBEND,L=1.2348857200,ANGLE=0.4956097813,K1:=kqd10e,THICK=TRUE,APERTYPE=CIRCLE,APERTURE=0.03;
sF610: SBEND,L=1.2773483700,ANGLE=0.5243789950,K1:=kqf10f,THICK=TRUE,APERTYPE=CIRCLE,APERTURE=0.03;
s610: SBEND,L=0.0700000000,ANGLE=0.0287365064,THICK=TRUE,APERTYPE=CIRCLE,APERTURE=0.03;
sD610: SBEND,L=1.2773483700,ANGLE=0.5243789950,K1:=kqd10f,THICK=TRUE,APERTYPE=CIRCLE,APERTURE=0.03;
d110: DRIFT, L=0.5326681050;
d2a10: DRIFT, L=0.4301084000;
c110: DRIFT, L=0.1134938800;
d2c10: DRIFT, L=0.4132626300;
d3a10: DRIFT, L=0.4231510200;
c210: DRIFT, L=0.1143798550;
d3c10: DRIFT, L=0.4231045500;
d410: DRIFT, L=0.5404859550;
d5a10: DRIFT, L=0.4277922200;
c310: DRIFT, L=0.1167432750;
d5c10: DRIFT, L=0.4256620000;
d6a10: DRIFT, L=0.4460017200;
c410: DRIFT, L=0.1185159050;
d6c10: DRIFT, L=0.4125658100;
d610: DRIFT, L=0.5514622550;
m110: marker;
```

```
m210: marker;
m310: marker;
m410: marker;
m510: marker;
m610: marker;
sF111: SBEND,L=1.2881311950,ANGLE=0.4999852446,K1:=kqf11a,THICK=TRUE,APERTYPE=CIRCLE,APERTURE=0.03;
s111: SBEND,L=0.0700000000,ANGLE=0.0271703436,THICK=TRUE,APERTYPE=CIRCLE,APERTURE=0.03;
sD111: SBEND,L=1.2881311950,ANGLE=0.4999852446,K1:=kqd11a,THICK=TRUE,APERTYPE=CIRCLE,APERTURE=0.03;
sF211: SBEND,L=1.3168678300,ANGLE=0.5199095725,K1:=kqf11b,THICK=TRUE,APERTYPE=CIRCLE,APERTURE=0.03;
s211: SBEND,L=0.0700000000,ANGLE=0.0276365397,THICK=TRUE,APERTYPE=CIRCLE,APERTURE=0.03;
sD211: SBEND,L=1.3168678300,ANGLE=0.5199095725,K1:=kqd11b,THICK=TRUE,APERTYPE=CIRCLE,APERTURE=0.03;
sF311: SBEND,L=1.3211667800,ANGLE=0.5084517329,K1:=kqf11c,THICK=TRUE,APERTYPE=CIRCLE,APERTURE=0.03;
s311: SBEND,L=0.0700000000,ANGLE=0.0270274818,THICK=TRUE,APERTYPE=CIRCLE,APERTURE=0.03;
sD311: SBEND,L=1.3211667800,ANGLE=0.5101115871,K1:=kqd11c,THICK=TRUE,APERTYPE=CIRCLE,APERTURE=0.03;
sF411: SBEND,L=1.3216350650,ANGLE=0.5090521288,K1:=kqf11d,THICK=TRUE,APERTYPE=CIRCLE,APERTURE=0.03;
s411: SBEND,L=0.0700000000,ANGLE=0.0269617915,THICK=TRUE,APERTYPE=CIRCLE,APERTURE=0.03;
sD411: SBEND,L=1.3216350650,ANGLE=0.5090521288,K1:=kqd11d,THICK=TRUE,APERTYPE=CIRCLE,APERTURE=0.03;
sF511: SBEND,L=1.3315178300,ANGLE=0.4965834065,K1:=kqf11e,THICK=TRUE,APERTYPE=CIRCLE,APERTURE=0.03;
s511: SBEND,L=0.0700000000,ANGLE=0.0261061757,THICK=TRUE,APERTYPE=CIRCLE,APERTURE=0.03;
sD511: SBEND,L=1.3315178300,ANGLE=0.4965834065,K1:=kqd11e,THICK=TRUE,APERTYPE=CIRCLE,APERTURE=0.03;
sF611: SBEND,L=1.3763548250,ANGLE=0.5255110283,K1:=kqf11f,THICK=TRUE,APERTYPE=CIRCLE,APERTURE=0.03;
s611: SBEND,L=0.0700000000,ANGLE=0.0267269539,THICK=TRUE,APERTYPE=CIRCLE,APERTURE=0.03;
sD611: SBEND,L=1.3763548250,ANGLE=0.5255110283,K1:=kqd11f,THICK=TRUE,APERTYPE=CIRCLE,APERTURE=0.03;
d111: DRIFT, L=0.5514622550;
d2a11: DRIFT, L=0.4440523000;
c111: DRIFT, L=0.1244632000;
d2c11: DRIFT, L=0.4154712000;
d3a11: DRIFT, L=0.4313289000;
c211: DRIFT, L=0.1254769900;
d3c11: DRIFT, L=0.4312513900;
d411: DRIFT, L=0.5567740950;
d5a11: DRIFT, L=0.4339888400;
c311: DRIFT, L=0.1245705250;
d5c11: DRIFT, L=0.4309799700;
d6a11: DRIFT, L=0.4582872800;
c411: DRIFT, L=0.1264836850;
d6c11: DRIFT, L=0.4120273900;
d611: DRIFT, L=0.5655026850;
m111: marker;
```

```
m211: marker;
m311: marker;
m411: marker;
m511: marker;
m611: marker;
sF112: SBEND,L=1.3875684200,ANGLE=0.5008107139,K1:=kqf12a,THICK=TRUE,APERTYPE=CIRCLE,APERTURE=0.03;
s112: SBEND,L=0.0700000000,ANGLE=0.0252648803,THICK=TRUE,APERTYPE=CIRCLE,APERTURE=0.03;
sD112: SBEND,L=1.3875684200,ANGLE=0.5008107139,K1:=kqd12a,THICK=TRUE,APERTYPE=CIRCLE,APERTURE=0.03;
sF212: SBEND,L=1.4178868850,ANGLE=0.5208703539,K1:=kqf12b,THICK=TRUE,APERTYPE=CIRCLE,APERTURE=0.03;
s212: SBEND,L=0.0700000000,ANGLE=0.0257149743,THICK=TRUE,APERTYPE=CIRCLE,APERTURE=0.03;
sD212: SBEND,L=1.4178868850,ANGLE=0.5208703539,K1:=kqd12b,THICK=TRUE,APERTYPE=CIRCLE,APERTURE=0.03;
sF312: SBEND,L=1.4231883500,ANGLE=0.5077145485,K1:=kqf12c,THICK=TRUE,APERTYPE=CIRCLE,APERTURE=0.03;
s312: SBEND,L=0.0700000000,ANGLE=0.0250654821,THICK=TRUE,APERTYPE=CIRCLE,APERTURE=0.03;
sD312: SBEND,L=1.4231883500,ANGLE=0.5096128881,K1:=kqd12c,THICK=TRUE,APERTYPE=CIRCLE,APERTURE=0.03;
sF412: SBEND,L=1.4281646650,ANGLE=0.5114779447,K1:=kqf12d,THICK=TRUE,APERTYPE=CIRCLE,APERTURE=0.03;
s412: SBEND,L=0.0700000000,ANGLE=0.0250695575,THICK=TRUE,APERTYPE=CIRCLE,APERTURE=0.03;
sD412: SBEND,L=1.4281646650,ANGLE=0.5114779447,K1:=kqd12d,THICK=TRUE,APERTYPE=CIRCLE,APERTURE=0.03;
sF512: SBEND,L=1.4394490650,ANGLE=0.4975200246,K1:=kqf12e,THICK=TRUE,APERTYPE=CIRCLE,APERTURE=0.03;
s512: SBEND,L=0.0700000000,ANGLE=0.0241942578,THICK=TRUE,APERTYPE=CIRCLE,APERTURE=0.03;
sD512: SBEND,L=1.4394490650,ANGLE=0.4975200246,K1:=kqd12e,THICK=TRUE,APERTYPE=CIRCLE,APERTURE=0.03;
sF612: SBEND,L=1.4870503750,ANGLE=0.5263835265,K1:=kqf12f,THICK=TRUE,APERTYPE=CIRCLE,APERTURE=0.03;
s612: SBEND,L=0.0700000000,ANGLE=0.0247784792,THICK=TRUE,APERTYPE=CIRCLE,APERTURE=0.03;
sD612: SBEND,L=1.4870503750,ANGLE=0.5263835265,K1:=kqd12f,THICK=TRUE,APERTYPE=CIRCLE,APERTURE=0.03;
d112: DRIFT, L=0.5655026850;
d2a12: DRIFT, L=0.4544271000;
c112: DRIFT, L=0.1326248000;
d2c12: DRIFT, L=0.4171144600;
d3a12: DRIFT, L=0.4374135500;
c212: DRIFT, L=0.1337336900;
d3c12: DRIFT, L=0.4373129500;
d412: DRIFT, L=0.5715187750;
d5a12: DRIFT, L=0.4409100200;
c312: DRIFT, L=0.1333130100;
d5c12: DRIFT, L=0.4369197700;
d6a12: DRIFT, L=0.4720093900;
c412: DRIFT, L=0.1353831350;
d6c12: DRIFT, L=0.4114260100;
d612: DRIFT, L=0.5812507700;
m112: marker;
```

```
m212: marker;
m312: marker;
m412: marker;
m512: marker;
m612: marker;
sF113: SBEND,L=1.4994623800,ANGLE=0.5018313001,K1:=kqf13a,THICK=TRUE,APERTYPE=CIRCLE,APERTURE=0.03;
s113: SBEND,L=0.0700000000,ANGLE=0.0234271906,THICK=TRUE,APERTYPE=CIRCLE,APERTURE=0.03;
sD113: SBEND,L=1.4994623800,ANGLE=0.5018313001,K1:=kqd13a,THICK=TRUE,APERTYPE=CIRCLE,APERTURE=0.03;
sF213: SBEND,L=1.5316683800,ANGLE=0.5218041491,K1:=kqf13b,THICK=TRUE,APERTYPE=CIRCLE,APERTURE=0.03;
s213: SBEND,L=0.0700000000,ANGLE=0.0238473882,THICK=TRUE,APERTYPE=CIRCLE,APERTURE=0.03;
sD213: SBEND,L=1.5316683800,ANGLE=0.5218041491,K1:=kqd13b,THICK=TRUE,APERTYPE=CIRCLE,APERTURE=0.03;
sF313: SBEND,L=1.5366475350,ANGLE=0.5103054850,K1:=kqf13c,THICK=TRUE,APERTYPE=CIRCLE,APERTURE=0.03;
s313: SBEND,L=0.0700000000,ANGLE=0.0233218786,THICK=TRUE,APERTYPE=CIRCLE,APERTURE=0.03;
sD313: SBEND,L=1.5366475350,ANGLE=0.5119643886,K1:=kqd13c,THICK=TRUE,APERTYPE=CIRCLE,APERTURE=0.03;
sF413: SBEND,L=1.5371902250,ANGLE=0.5109004267,K1:=kqf13d,THICK=TRUE,APERTYPE=CIRCLE,APERTURE=0.03;
s413: SBEND,L=0.0700000000,ANGLE=0.0232651947,THICK=TRUE,APERTYPE=CIRCLE,APERTURE=0.03;
sD413: SBEND,L=1.5371902250,ANGLE=0.5109004267,K1:=kqd13d,THICK=TRUE,APERTYPE=CIRCLE,APERTURE=0.03;
sF513: SBEND,L=1.5485278450,ANGLE=0.4983368159,K1:=kqf13e,THICK=TRUE,APERTYPE=CIRCLE,APERTURE=0.03;
s513: SBEND,L=0.0700000000,ANGLE=0.0225269292,THICK=TRUE,APERTYPE=CIRCLE,APERTURE=0.03;
sD513: SBEND,L=1.5485278450,ANGLE=0.4983368159,K1:=kqd13e,THICK=TRUE,APERTYPE=CIRCLE,APERTURE=0.03;
sF613: SBEND,L=1.5988204150,ANGLE=0.5273306376,K1:=kqf13f,THICK=TRUE,APERTYPE=CIRCLE,APERTURE=0.03;
s613: SBEND,L=0.0700000000,ANGLE=0.0230877366,THICK=TRUE,APERTYPE=CIRCLE,APERTURE=0.03;
sD613: SBEND,L=1.5988204150,ANGLE=0.5273306376,K1:=kqd13f,THICK=TRUE,APERTYPE=CIRCLE,APERTURE=0.03;
d113: DRIFT, L=0.5812507700;
d2a13: DRIFT, L=0.4661126200;
c113: DRIFT, L=0.1418175100;
d2c13: DRIFT, L=0.4189653200;
d3a13: DRIFT, L=0.4442669300;
c213: DRIFT, L=0.1430335150;
d3c13: DRIFT, L=0.4441403100;
d413: DRIFT, L=0.5872450000;
d5a13: DRIFT, L=0.4479048000;
c313: DRIFT, L=0.1421484500;
d5c13: DRIFT, L=0.4429227200;
d6a13: DRIFT, L=0.4858774000;
c413: DRIFT, L=0.1443772100;
d6c13: DRIFT, L=0.4108182400;
d613: DRIFT, L=0.5971070300;
m113: marker;
```

```
m213: marker;
m313: marker;
m413: marker;
m513: marker;
m613: marker;
sF114: SBEND,L=1.6118015600,ANGLE=0.5025307832,K1:=kqf14a,THICK=TRUE,APERTYPE=CIRCLE,APERTURE=0.03;
s114: SBEND,L=0.0700000000,ANGLE=0.0218247430,THICK=TRUE,APERTYPE=CIRCLE,APERTURE=0.03;
sD114: SBEND,L=1.6118015600,ANGLE=0.5025307832,K1:=kqd14a,THICK=TRUE,APERTYPE=CIRCLE,APERTURE=0.03;
sF214: SBEND,L=1.6458052350,ANGLE=0.5226138382,K1:=kqf14b,THICK=TRUE,APERTYPE=CIRCLE,APERTURE=0.03;
s214: SBEND,L=0.0700000000,ANGLE=0.0222280060,THICK=TRUE,APERTYPE=CIRCLE,APERTURE=0.03;
sD214: SBEND,L=1.6458052350,ANGLE=0.5226138382,K1:=kqd14b,THICK=TRUE,APERTYPE=CIRCLE,APERTURE=0.03;
sF314: SBEND,L=1.6511458300,ANGLE=0.5110977292,K1:=kqf14c,THICK=TRUE,APERTYPE=CIRCLE,APERTURE=0.03;
s314: SBEND,L=0.0700000000,ANGLE=0.0217381986,THICK=TRUE,APERTYPE=CIRCLE,APERTURE=0.03;
sD314: SBEND,L=1.6511458300,ANGLE=0.5127562280,K1:=kqd14c,THICK=TRUE,APERTYPE=CIRCLE,APERTURE=0.03;
sF414: SBEND,L=1.6517280550,ANGLE=0.5116903411,K1:=kqf14d,THICK=TRUE,APERTYPE=CIRCLE,APERTURE=0.03;
s414: SBEND,L=0.0700000000,ANGLE=0.0216853639,THICK=TRUE,APERTYPE=CIRCLE,APERTURE=0.03;
sD414: SBEND,L=1.6517280550,ANGLE=0.5116903411,K1:=kqd14d,THICK=TRUE,APERTYPE=CIRCLE,APERTURE=0.03;
sF514: SBEND,L=1.6638387350,ANGLE=0.4990861803,K1:=kqf14e,THICK=TRUE,APERTYPE=CIRCLE,APERTURE=0.03;
s514: SBEND,L=0.0700000000,ANGLE=0.0209972468,THICK=TRUE,APERTYPE=CIRCLE,APERTURE=0.03;
sD514: SBEND,L=1.6638387350,ANGLE=0.4990861803,K1:=kqd14e,THICK=TRUE,APERTYPE=CIRCLE,APERTURE=0.03;
sF614: SBEND,L=1.7170301850,ANGLE=0.5281095045,K1:=kqf14f,THICK=TRUE,APERTYPE=CIRCLE,APERTURE=0.03;
s614: SBEND,L=0.0700000000,ANGLE=0.0215300032,THICK=TRUE,APERTYPE=CIRCLE,APERTURE=0.03;
sD614: SBEND,L=1.7170301850,ANGLE=0.5281095045,K1:=kqd14f,THICK=TRUE,APERTYPE=CIRCLE,APERTURE=0.03;
d114: DRIFT, L=0.5971070300;
d2a14: DRIFT, L=0.4778346400;
c114: DRIFT, L=0.1510389300;
d2c14: DRIFT, L=0.4208219700;
d3a14: DRIFT, L=0.4511417000;
c214: DRIFT, L=0.1523623850;
d3c14: DRIFT, L=0.4509890000;
d414: DRIFT, L=0.6034360800;
d5a14: DRIFT, L=0.4552992200;
c314: DRIFT, L=0.1514886900;
d5c14: DRIFT, L=0.4492686400;
d6a14: DRIFT, L=0.5005377300;
c414: DRIFT, L=0.1538851450;
d6c14: DRIFT, L=0.4101757400;
d614: DRIFT, L=0.5971070300;
m114: marker;
```

```
m214: marker;
m314: marker;
m414: marker;
m514: marker;
m614: marker;
Beam,particle=proton,sequence=tamusq11,energy=0.94477;
tamusq11: sequence, refer=entry,l = 1.3620755200;
startcell11: marker, at = 0;
m11, at = 0.0000000000;
d11, at = 0.0000000000;
sF11, at = 0.4019962300;
s11, at = 0.6298970200;
sD11, at = 0.6998970200;
d2a1, at = 0.9277978100;
c11, at = 1.3246667500;
endcell11: marker, at = 1.3620755200;
endsequence;
Beam,particle=proton,sequence=tamusq21,energy=0.94539;
tamusq21: sequence, refer=entry,l = 1.3246041650;
startcell21: marker, at = 0;
c11, at = 0.0000000000;
m21, at = 0.0374087700;
d2c1, at = 0.0374087700;
sF21, at = 0.3718745600;
s21, at = 0.6112383400;
sD21, at = 0.6812383400;
d3a1, at = 0.9206021200;
c21, at = 1.2871959700;
endcell21: marker, at = 1.3246041650;
endsequence;
Beam,particle=proton,sequence=tamusq31,energy=0.94602;
tamusq31: sequence, refer=entry,l = 1.3589286600;
startcell31: marker, at = 0;
c21, at = 0.0000000000;
m31, at = 0.0374081950;
d3c1, at = 0.0374081950;
sF31, at = 0.4038388850;
s31, at = 0.6443063100;
sD31, at = 0.7143063100;
```

```
d41, at = 0.9547737350;
endcell31: marker, at = 1.3589286600;
endsequence;
Beam,particle=proton,sequence=tamusq41,energy=0.94602;
tamusq41: sequence, refer=entry,l = 1.3686453250;
startcell41: marker, at = 0;
m41, at = 0.0000000000;
d41, at = 0.0000000000;
sF41, at = 0.4041549250;
s41, at = 0.6475033350;
sD41, at = 0.7175033350;
d5a1, at = 0.9608517450;
c31, at = 1.3319884750;
endcell41: marker, at = 1.3686453250;
endsequence;
Beam,particle=proton,sequence=tamusq51,energy=0.94665;
tamusq51: sequence, refer=entry,l = 1.4169386800;
startcell51: marker, at = 0;
c31, at = 0.0000000000;
m51, at = 0.0366568500;
d5c1, at = 0.0366568500;
sF51, at = 0.4011599800;
s51, at = 0.6473307450;
sD51, at = 0.7173307450;
d6a1, at = 0.9635015100;
c41, at = 1.3799470800;
endcell51: marker, at = 1.4169386800;
endsequence;
Beam,particle=proton,sequence=tamusq61,energy=0.94728;
tamusq61: sequence, refer=entry,l = 1.3643702900;
startcell61: marker, at = 0;
c41, at = 0.0000000000;
m61, at = 0.0369916000;
d6c1, at = 0.0369916000;
sF61, at = 0.3589198100;
s61, at = 0.6228327000;
sD61, at = 0.6928327000;
d61, at = 0.9567455900;
endcell61: marker, at = 1.3643702900;
```

```
endsequence;
Beam,particle=proton,sequence=tamusq12,energy=0.94728;
tamusq12: sequence, refer=entry,l = 1.4529567900;
startcell12: marker, at = 0;
m12, at = 0.0000000000;
d12, at = 0.0000000000;
sF12, at = 0.4076247000;
s12, at = 0.6761564600;
sD12, at = 0.7461564600;
d2a2, at = 1.0146882200;
c12, at = 1.4122131600;
endcell12: marker, at = 1.4529567900;
endsequence;
Beam,particle=proton,sequence=tamusq22,energy=0.94794;
tamusq22: sequence, refer=entry,l = 1.4205975600;
startcell22: marker, at = 0;
c12, at = 0.0000000000;
m22, at = 0.0407436300;
d2c2, at = 0.0407436300;
sF22, at = 0.3794640400;
s22, at = 0.6601045500;
sD22, at = 0.7301045500;
d3a2, at = 1.0107450600;
c22, at = 1.3798156500;
endcell22: marker, at = 1.4205975600;
endsequence;
Beam,particle=proton,sequence=tamusq32,energy=0.94858;
tamusq32: sequence, refer=entry,l = 1.4782848050;
startcell32: marker, at = 0;
c22, at = 0.0000000000;
m32, at = 0.0407819100;
d3c2, at = 0.0407819100;
sF32, at = 0.4096988500;
s32, at = 0.6990437250;
sD32, at = 0.7690437250;
d42, at = 1.0583886000;
endcell32: marker, at = 1.4782848050;
endsequence;
Beam,particle=proton,sequence=tamusq42,energy=0.94858;
```

```
tamusq42: sequence, refer=entry,l = 1.6608254350;
startcell42: marker, at = 0;
m42, at = 0.0000000000;
d42, at = 0.0000000000;
sF42, at = 0.4198962050;
s42, at = 0.7921709150;
sD42, at = 0.8621709150;
d5a2, at = 1.2344456250;
c32, at = 1.6130983150;
endcell42: marker, at = 1.6608254350;
endsequence;
Beam,particle=proton,sequence=tamusq52,energy=0.94930;
tamusq52: sequence, refer=entry,l = 1.7205455400;
startcell52: marker, at = 0;
c32, at = 0.0000000000;
m52, at = 0.0477271200;
d5c2, at = 0.0477271200;
sF52, at = 0.4209996600;
s52, at = 0.8038395150;
sD52, at = 0.8738395150;
d6a2, at = 1.2566793700;
c42, at = 1.6722849200;
endcell52: marker, at = 1.7205455400;
endsequence;
Beam,particle=proton,sequence=tamusq62,energy=0.95006;
tamusq62: sequence, refer=entry,l = 1.6927061200;
startcell62: marker, at = 0;
c42, at = 0.0000000000;
m62, at = 0.0482606200;
d6c2, at = 0.0482606200;
sF62, at = 0.3876431200;
s62, at = 0.7914941750;
sD62, at = 0.8614941750;
d62, at = 1.2653452300;
endcell62: marker, at = 1.6927061200;
endsequence;
Beam,particle=proton,sequence=tamusq13,energy=0.95006;
tamusq13: sequence, refer=entry,l = 1.7644090500;
startcell13: marker, at = 0;
```

```
m13, at = 0.0000000000;
d13, at = 0.0000000000;
sF13, at = 0.4273608900;
s13, at = 0.8349266150;
sD13, at = 0.9049266150;
d2a3, at = 1.3124923400;
c13, at = 1.7122607100;
endcell13: marker, at = 1.7644090500;
endsequence;
Beam,particle=proton,sequence=tamusq23,energy=0.95089;
tamusq23: sequence, refer=entry,l = 1.7488805000;
startcell23: marker, at = 0;
c13, at = 0.0000000000;
m23, at = 0.0521483400;
d2c3, at = 0.0521483400;
sF23, at = 0.4054189000;
s23, at = 0.8272196200;
sD23, at = 0.8972196200;
d3a3, at = 1.3190203400;
c23, at = 1.6965609900;
endcell23: marker, at = 1.7488805000;
endsequence;
Beam,particle=proton,sequence=tamusq33,energy=0.95174;
tamusq33: sequence, refer=entry,l = 1.7786620300;
startcell33: marker, at = 0;
c23, at = 0.0000000000;
m33, at = 0.0523195100;
d3c3, at = 0.0523195100;
sF33, at = 0.4297390500;
s33, at = 0.8539106300;
sD33, at = 0.9239106300;
d43, at = 1.3480822100;
endcell33: marker, at = 1.7786620300;
endsequence;
Beam,particle=proton,sequence=tamusq43,energy=0.95174;
tamusq43: sequence, refer=entry,l = 1.8006580500;
startcell43: marker, at = 0;
m43, at = 0.0000000000;
d43, at = 0.0000000000;
```

```
sF43, at = 0.4305798200;
s43, at = 0.8636856350;
sD43, at = 0.9336856350;
d5a3, at = 1.3667914500;
c33, at = 1.7484716700;
endcell43: marker, at = 1.8006580500;
endsequence;
Beam,particle=proton,sequence=tamusq53,energy=0.95259;
tamusq53: sequence, refer=entry,l = 1.8428426950;
startcell53: marker, at = 0;
c33, at = 0.0000000000;
m53, at = 0.0521863800;
d5c3, at = 0.0521863800;
sF53, at = 0.4289913600;
s53, at = 0.8668834700;
sD53, at = 0.9368834700;
d6a3, at = 1.3747755800;
c43, at = 1.7900427500;
endcell53: marker, at = 1.8428426950;
endsequence;
Beam,particle=proton,sequence=tamusq63,energy=0.95345;
tamusq63: sequence, refer=entry,l = 1.8250995800;
startcell63: marker, at = 0;
c43, at = 0.0000000000;
m63, at = 0.0527999450;
d6c3, at = 0.0527999450;
sF63, at = 0.3992132750;
s63, at = 0.8594768700;
sD63, at = 0.9294768700;
d63, at = 1.3897404650;
endcell63: marker, at = 1.8250995800;
endsequence;
Beam,particle=proton,sequence=tamusq14,energy=0.95345;
tamusq14: sequence, refer=entry,l = 1.8912363950;
startcell14: marker, at = 0;
m14, at = 0.0000000000;
d14, at = 0.0000000000;
sF14, at = 0.4353591150;
s14, at = 0.8995577100;
```

```
sD14, at = 0.9695577100;
d2a4, at = 1.4337563050;
c14, at = 1.8344391650;
endcell14: marker, at = 1.8912363950;
endsequence;
Beam,particle=proton,sequence=tamusq24,energy=0.95438;
tamusq24: sequence, refer=entry,l = 1.8826981600;
startcell24: marker, at = 0;
c14, at = 0.0000000000;
m24, at = 0.0567972300;
d2c4, at = 0.0567972300;
sF24, at = 0.4159988500;
s24, at = 0.8953405750;
sD24, at = 0.9653405750;
d3a4, at = 1.4446823000;
c24, at = 1.8256755900;
endcell24: marker, at = 1.8826981600;
endsequence;
Beam,particle=proton,sequence=tamusq34,energy=0.95530;
tamusq34: sequence, refer=entry,l = 1.9311725950;
startcell34: marker, at = 0;
c24, at = 0.0000000000;
m34, at = 0.0570225700;
d3c4, at = 0.0570225700;
sF34, at = 0.4379080200;
s34, at = 0.9268366550;
sD34, at = 0.9968366550;
d44, at = 1.4857652900;
endcell34: marker, at = 1.9311725950;
endsequence;
Beam,particle=proton,sequence=tamusq44,energy=0.95530;
tamusq44: sequence, refer=entry,l = 2.0829034100;
startcell44: marker, at = 0;
m44, at = 0.0000000000;
d44, at = 0.0000000000;
sF44, at = 0.4454073050;
s44, at = 1.0032464550;
sD44, at = 1.0732464550;
d5a4, at = 1.6310856050;
```

```
c34, at = 2.0200249950;
endcell44: marker, at = 2.0829034100;
endsequence;
Beam,particle=proton,sequence=tamusq54,energy=0.95634;
tamusq54: sequence, refer=entry,l = 2.1360764550;
startcell54: marker, at = 0;
c34, at = 0.0000000000;
m54, at = 0.0628784150;
d5c4, at = 0.0628784150;
sF54, at = 0.4481531750;
s54, at = 1.0180449150;
sD54, at = 1.0880449150;
d6a4, at = 1.6579366550;
c44, at = 2.0723925050;
endcell54: marker, at = 2.1360764550;
endsequence;
Beam,particle=proton,sequence=tamusq64,energy=0.95741;
tamusq64: sequence, refer=entry,l = 2.1427014800;
startcell64: marker, at = 0;
c44, at = 0.0000000000;
m64, at = 0.0636839500;
d6c4, at = 0.0636839500;
sF64, at = 0.4269552200;
s64, at = 1.0225368800;
sD64, at = 1.0925368800;
d64, at = 1.6881185400;
endcell64: marker, at = 2.1427014800;
endsequence;
Beam,particle=proton,sequence=tamusq15,energy=0.95741;
tamusq15: sequence, refer=entry,l = 2.1966506150;
startcell15: marker, at = 0;
m15, at = 0.0000000000;
d15, at = 0.0000000000;
sF15, at = 0.4545829400;
s15, at = 1.0551747450;
sD15, at = 1.1251747450;
d2a5, at = 1.7257665500;
c15, at = 2.1286527100;
endcell15: marker, at = 2.1966506150;
```

```
endsequence;
Beam,particle=proton,sequence=tamusq25,energy=0.95860;
tamusq25: sequence, refer=entry,l = 2.2051079850;
startcell25: marker, at = 0;
c15, at = 0.0000000000;
m25, at = 0.0679979050;
d2c5, at = 0.0679979050;
sF25, at = 0.4414893650;
s25, at = 1.0594658850;
sD25, at = 1.1294658850;
d3a5, at = 1.7474424050;
c25, at = 2.1367542250;
endcell25: marker, at = 2.2051079850;
endsequence;
Beam,particle=proton,sequence=tamusq35,energy=0.95980;
tamusq35: sequence, refer=entry,l = 2.2304913250;
startcell35: marker, at = 0;
c25, at = 0.0000000000;
m35, at = 0.0683537600;
d3c5, at = 0.0683537600;
sF35, at = 0.4575897100;
s35, at = 1.0795181800;
sD35, at = 1.1495181800;
d45, at = 1.7714466500;
endcell35: marker, at = 2.2304913250;
endsequence;
Beam,particle=proton,sequence=tamusq45,energy=0.95980;
tamusq45: sequence, refer=entry,l = 2.2661464450;
startcell45: marker, at = 0;
m45, at = 0.0000000000;
d45, at = 0.0000000000;
sF45, at = 0.4590446750;
s45, at = 1.0966024750;
sD45, at = 1.1666024750;
d5a5, at = 1.8041602750;
c35, at = 2.1972115750;
endcell45: marker, at = 2.2661464450;
endsequence;
Beam,particle=proton,sequence=tamusq55,energy=0.96101;
```

```
tamusq55: sequence, refer=entry,l = 2.3021772400;
startcell55: marker, at = 0;
c35, at = 0.0000000000;
m55, at = 0.0689348700;
d5c5, at = 0.0689348700;
sF55, at = 0.4590073000;
s55, at = 1.1036695600;
sD55, at = 1.1736695600;
d6a5, at = 1.8183318200;
c45, at = 2.2323281000;
endcell55: marker, at = 2.3021772400;
endsequence;
Beam,particle=proton,sequence=tamusq65,energy=0.96226;
tamusq65: sequence, refer=entry,l = 2.3226054800;
startcell65: marker, at = 0;
c45, at = 0.0000000000;
m65, at = 0.0698491400;
d6c5, at = 0.0698491400;
sF65, at = 0.4426695100;
s65, at = 1.1149014050;
sD65, at = 1.1849014050;
d65, at = 1.8571333000;
endcell65: marker, at = 2.3226054800;
endsequence;
Beam,particle=proton,sequence=tamusq16,energy=0.96226;
tamusq16: sequence, refer=entry,l = 2.3696510150;
startcell16: marker, at = 0;
m16, at = 0.0000000000;
d16, at = 0.0000000000;
sF16, at = 0.4654721800;
s16, at = 1.1433232550;
sD16, at = 1.2133232550;
d2a6, at = 1.8911743300;
c16, at = 2.2953085400;
endcell16: marker, at = 2.3696510150;
endsequence;
Beam,particle=proton,sequence=tamusq26,energy=0.96360;
tamusq26: sequence, refer=entry,l = 2.3877354700;
startcell26: marker, at = 0;
```

```
c16, at = 0.0000000000;
m26, at = 0.0743424750;
d2c6, at = 0.0743424750;
sF26, at = 0.4559283550;
s26, at = 1.1524338850;
sD26, at = 1.2224338850;
d3a6, at = 1.9189394150;
c26, at = 2.3129632150;
endcell26: marker, at = 2.3877354700;
endsequence;
Beam,particle=proton,sequence=tamusq36,energy=0.96495;
tamusq36: sequence, refer=entry,l = 2.4267571850;
startcell36: marker, at = 0;
c26, at = 0.0000000000;
m36, at = 0.0747722550;
d3c6, at = 0.0747722550;
sF36, at = 0.4687382950;
s36, at = 1.1753377300;
sD36, at = 1.2453377300;
d46, at = 1.9519371650;
endcell36: marker, at = 2.4267571850;
endsequence;
Beam,particle=proton,sequence=tamusq46,energy=0.96495;
tamusq46: sequence, refer=entry,l = 2.5574718950;
startcell46: marker, at = 0;
m46, at = 0.0000000000;
d46, at = 0.0000000000;
sF46, at = 0.4748200200;
s46, at = 1.2409805100;
sD46, at = 1.3109805100;
d5a6, at = 2.0771410000;
c36, at = 2.4776106000;
endcell46: marker, at = 2.5574718950;
endsequence;
Beam,particle=proton,sequence=tamusq56,energy=0.96642;
tamusq56: sequence, refer=entry,l = 2.6018392600;
startcell56: marker, at = 0;
c36, at = 0.0000000000;
m56, at = 0.0798612950;
```

```
d5c6, at = 0.0798612950;
sF56, at = 0.4785891850;
s56, at = 1.2581447650;
sD56, at = 1.3281447650;
d6a6, at = 2.1077003450;
c46, at = 2.5208675150;
endcell56: marker, at = 2.6018392600;
endsequence;
Beam,particle=proton,sequence=tamusq66,energy=0.96792;
tamusq66: sequence, refer=entry,l = 2.6471698200;
startcell66: marker, at = 0;
c46, at = 0.0000000000;
m66, at = 0.0809717450;
d6c6, at = 0.0809717450;
sF66, at = 0.4710196150;
s66, at = 1.2815360050;
sD66, at = 1.3515360050;
d66, at = 2.1620523950;
endcell66: marker, at = 2.6471698200;
endsequence;
Beam,particle=proton,sequence=tamusq17,energy=0.96792;
tamusq17: sequence, refer=entry,l = 2.6817604200;
startcell17: marker, at = 0;
m17, at = 0.0000000000;
d17, at = 0.0000000000;
sF17, at = 0.4851174250;
s17, at = 1.3023516750;
sD17, at = 1.3723516750;
d2a7, at = 2.1895859250;
c17, at = 2.5959717350;
endcell17: marker, at = 2.6817604200;
endsequence;
Beam,particle=proton,sequence=tamusq27,energy=0.96956;
tamusq27: sequence, refer=entry,l = 2.7172130350;
startcell27: marker, at = 0;
c17, at = 0.0000000000;
m27, at = 0.0857886850;
d2c7, at = 0.0857886850;
sF27, at = 0.4819776550;
```

```
s27, at = 1.3201570800;
sD27, at = 1.3901570800;
d3a7, at = 2.2283365050;
c27, at = 2.6308611950;
endcell27: marker, at = 2.7172130350;
endsequence;
Beam,particle=proton,sequence=tamusq37,energy=0.97122;
tamusq37: sequence, refer=entry,l = 2.7363708400;
startcell37: marker, at = 0;
c27, at = 0.0000000000;
m37, at = 0.0863518400;
d3c7, at = 0.0863518400;
sF37, at = 0.4888514300;
s37, at = 1.3323119950;
sD37, at = 1.4023119950;
d47, at = 2.2457725600;
endcell37: marker, at = 2.7363708400;
endsequence;
Beam,particle=proton,sequence=tamusq47,energy=0.97122;
tamusq47: sequence, refer=entry,l = 2.7781390700;
startcell47: marker, at = 0;
m47, at = 0.0000000000;
d47, at = 0.0000000000;
sF47, at = 0.4905982800;
s47, at = 1.3529454300;
sD47, at = 1.4229454300;
d5a7, at = 2.2852925800;
c37, at = 2.6908232800;
endcell47: marker, at = 2.7781390700;
endsequence;
Beam,particle=proton,sequence=tamusq57,energy=0.97291;
tamusq57: sequence, refer=entry,l = 2.8062819450;
startcell57: marker, at = 0;
c37, at = 0.0000000000;
m57, at = 0.0873157900;
d5c7, at = 0.0873157900;
sF57, at = 0.4919488200;
s57, at = 1.3635345900;
sD57, at = 1.4335345900;
```

```
d6a7, at = 2.3051203600;
c47, at = 2.7177218700;
endcell57: marker, at = 2.8062819450;
endsequence;
Beam,particle=proton,sequence=tamusq67,energy=0.97463;
tamusq67: sequence, refer=entry,l = 2.8686019900;
startcell67: marker, at = 0;
c47, at = 0.0000000000;
m67, at = 0.0885600750;
d6c7, at = 0.0885600750;
sF67, at = 0.4903613050;
s67, at = 1.3952215050;
sD67, at = 1.4652215050;
d67, at = 2.3700817050;
endcell67: marker, at = 2.8686019900;
endsequence;
Beam,particle=proton,sequence=tamusq18,energy=0.97463;
tamusq18: sequence, refer=entry,l = 2.8946954200;
startcell18: marker, at = 0;
m18, at = 0.0000000000;
d18, at = 0.0000000000;
sF18, at = 0.4985202850;
s18, at = 1.4108479750;
sD18, at = 1.4808479750;
d2a8, at = 2.3931756650;
c18, at = 2.8010976150;
endcell18: marker, at = 2.8946954200;
endsequence;
Beam,particle=proton,sequence=tamusq28,energy=0.97647;
tamusq28: sequence, refer=entry,l = 2.9419973950;
startcell28: marker, at = 0;
c18, at = 0.0000000000;
m28, at = 0.0935978050;
d2c8, at = 0.0935978050;
sF28, at = 0.4997496650;
s28, at = 1.4345853700;
sD28, at = 1.5045853700;
d3a8, at = 2.4394210750;
c28, at = 2.8477454450;
```

```
endcell28: marker, at = 2.9419973950;
endsequence;
Beam,particle=proton,sequence=tamusq38,energy=0.97832;
tamusq38: sequence, refer=entry,l = 2.9690845050;
startcell38: marker, at = 0;
c28, at = 0.0000000000;
m38, at = 0.0942519500;
d3c8, at = 0.0942519500;
sF38, at = 0.5025735100;
s38, at = 1.4472114800;
sD38, at = 1.5172114800;
d48, at = 2.4618494500;
endcell38: marker, at = 2.9690845050;
endsequence;
Beam,particle=proton,sequence=tamusq48,energy=0.97832;
tamusq48: sequence, refer=entry,l = 3.0734532950;
startcell48: marker, at = 0;
m48, at = 0.0000000000;
d48, at = 0.0000000000;
sF48, at = 0.5072350550;
s48, at = 1.4996503500;
sD48, at = 1.5696503500;
d5a8, at = 2.5620656450;
c38, at = 2.9752110750;
endcell48: marker, at = 3.0734532950;
endsequence;
Beam,particle=proton,sequence=tamusq58,energy=0.98026;
tamusq58: sequence, refer=entry,l = 3.1109378300;
startcell58: marker, at = 0;
c38, at = 0.0000000000;
m58, at = 0.0982422200;
d5c8, at = 0.0982422200;
sF58, at = 0.5113342800;
s58, at = 1.5178133800;
sD58, at = 1.5878133800;
d6a8, at = 2.5942924800;
c48, at = 3.0112551500;
endcell58: marker, at = 3.1109378300;
endsequence;
```

```
Beam,particle=proton,sequence=tamusq68,energy=0.98223;
tamusq68: sequence, refer=entry,l = 3.1879760900;
startcell68: marker, at = 0;
c48, at = 0.0000000000;
m68, at = 0.0996826800;
d6c8, at = 0.0996826800;
sF68, at = 0.5135211500;
s68, at = 1.5566658550;
sD68, at = 1.6266658550;
d68, at = 2.6698105600;
endcell68: marker, at = 3.1879760900;
endsequence;
Beam,particle=proton,sequence=tamusq19,energy=0.98223;
tamusq19: sequence, refer=entry,l = 3.2159984350;
startcell19: marker, at = 0;
m19, at = 0.0000000000;
d19, at = 0.0000000000;
sF19, at = 0.5181655300;
s19, at = 1.5698763900;
sD19, at = 1.6398763900;
d2a9, at = 2.6915872500;
c19, at = 3.1109544200;
endcell19: marker, at = 3.2159984350;
endsequence;
Beam,particle=proton,sequence=tamusq29,energy=0.98433;
tamusq29: sequence, refer=entry,l = 3.2623075300;
startcell29: marker, at = 0;
c19, at = 0.0000000000;
m29, at = 0.1050440150;
d2c9, at = 0.1050440150;
sF29, at = 0.5166053450;
s29, at = 1.5931149400;
sD29, at = 1.6631149400;
d3a9, at = 2.7396245350;
c29, at = 3.1564759950;
endcell29: marker, at = 3.2623075300;
endsequence;
Beam,particle=proton,sequence=tamusq39,energy=0.98646;
tamusq39: sequence, refer=entry,l = 3.2805381150;
```

```
startcell39: marker, at = 0;
c29, at = 0.0000000000;
m39, at = 0.1058315350;
d3c9, at = 0.1058315350;
sF39, at = 0.5226604250;
s39, at = 1.6046373750;
sD39, at = 1.6746373750;
d49, at = 2.7566143250;
endcell39: marker, at = 3.2805381150;
endsequence;
Beam,particle=proton,sequence=tamusq49,energy=0.98646;
tamusq49: sequence, refer=entry,l = 3.3113458450;
startcell49: marker, at = 0;
m49, at = 0.0000000000;
d49, at = 0.0000000000;
sF49, at = 0.5239237900;
s49, at = 1.6197150450;
sD49, at = 1.6897150450;
d5a9, at = 2.7855063000;
c39, at = 3.2050374800;
endcell49: marker, at = 3.3113458450;
endsequence;
Beam,particle=proton,sequence=tamusq59,energy=0.98860;
tamusq59: sequence, refer=entry,l = 3.3445185300;
startcell59: marker, at = 0;
c39, at = 0.0000000000;
m59, at = 0.1063083650;
d5c9, at = 0.1063083650;
sF59, at = 0.5248807050;
s59, at = 1.6309411950;
sD59, at = 1.7009411950;
d6a9, at = 2.8070016850;
c49, at = 3.2366248850;
endcell59: marker, at = 3.3445185300;
endsequence;
Beam,particle=proton,sequence=tamusq69,energy=0.99077;
tamusq69: sequence, refer=entry,l = 3.4143044500;
startcell69: marker, at = 0;
c49, at = 0.0000000000;
```

```
m69, at = 0.1078936450;
d6c9, at = 0.1078936450;
sF69, at = 0.5211772550;
s69, at = 1.6664068000;
sD69, at = 1.7364068000;
d69, at = 2.8816363450;
endcell69: marker, at = 3.4143044500;
endsequence;
Beam,particle=proton,sequence=tamusq110,energy=0.99077;
tamusq110: sequence, refer=entry,l = 3.4554839650;
startcell110: marker, at = 0;
m110, at = 0.0000000000;
d110, at = 0.0000000000;
sF110, at = 0.5326681050;
s110, at = 1.6872748950;
sD110, at = 1.7572748950;
d2a10, at = 2.9118816850;
c110, at = 3.3419900850;
endcell110: marker, at = 3.4554839650;
endsequence;
Beam,particle=proton,sequence=tamusq210,energy=0.99304;
tamusq210: sequence, refer=entry,l = 3.4964805750;
startcell210: marker, at = 0;
c110, at = 0.0000000000;
m210, at = 0.1134938800;
d2c10, at = 0.1134938800;
sF210, at = 0.5267565100;
s210, at = 1.7078531050;
sD210, at = 1.7778531050;
d3a10, at = 2.9589497000;
c210, at = 3.3821007200;
endcell210: marker, at = 3.4964805750;
endsequence;
Beam,particle=proton,sequence=tamusq310,energy=0.99532;
tamusq310: sequence, refer=entry,l = 3.5271619900;
startcell310: marker, at = 0;
c210, at = 0.0000000000;
m310, at = 0.1143798550;
d3c10, at = 0.1143798550;
```

```
sF310, at = 0.5374844050;
s310, at = 1.7270802200;
sD310, at = 1.7970802200;
d410, at = 2.9866760350;
endcell310: marker, at = 3.5271619900;
endsequence;
Beam,particle=proton,sequence=tamusq410,energy=0.99532;
tamusq410: sequence, refer=entry,l = 3.5973641200;
startcell410: marker, at = 0;
m410, at = 0.0000000000;
d410, at = 0.0000000000;
sF410, at = 0.5404859550;
s410, at = 1.7616572900;
sD410, at = 1.8316572900;
d5a10, at = 3.0528286250;
c310, at = 3.4806208450;
endcell410: marker, at = 3.5973641200;
endsequence;
Beam,particle=proton,sequence=tamusq510,energy=0.99764;
tamusq510: sequence, refer=entry,l = 3.6466943400;
startcell510: marker, at = 0;
c310, at = 0.0000000000;
m510, at = 0.1167432750;
d5c10, at = 0.1167432750;
sF510, at = 0.5424052750;
s510, at = 1.7772909950;
sD510, at = 1.8472909950;
d6a10, at = 3.0821767150;
c410, at = 3.5281784350;
endcell510: marker, at = 3.6466943400;
endsequence;
Beam,particle=proton,sequence=tamusq610,energy=0.99999;
tamusq610: sequence, refer=entry,l = 3.7072407100;
startcell610: marker, at = 0;
c410, at = 0.0000000000;
m610, at = 0.1185159050;
d6c10, at = 0.1185159050;
sF610, at = 0.5310817150;
s610, at = 1.8084300850;
```

```
sD610, at = 1.8784300850;
d610, at = 3.1557784550;
endcell610: marker, at = 3.7072407100;
endsequence;
Beam,particle=proton,sequence=tamusq111,energy=0.99999;
tamusq111: sequence, refer=entry,l = 3.7662401450;
startcell111: marker, at = 0;
m111, at = 0.0000000000;
d111, at = 0.0000000000;
sF111, at = 0.5514622550;
s111, at = 1.8395934500;
sD111, at = 1.9095934500;
d2a11, at = 3.1977246450;
c111, at = 3.6417769450;
endcell111: marker, at = 3.7662401450;
endsequence;
Beam,particle=proton,sequence=tamusq211,energy=1.00241;
tamusq211: sequence, refer=entry,l = 3.8004759500;
startcell211: marker, at = 0;
c111, at = 0.0000000000;
m211, at = 0.1244632000;
d2c11, at = 0.1244632000;
sF211, at = 0.5399344000;
s211, at = 1.8568022300;
sD211, at = 1.9268022300;
d3a11, at = 3.2436700600;
c211, at = 3.6749989600;
endcell211: marker, at = 3.8004759500;
endsequence;
Beam,particle=proton,sequence=tamusq311,energy=1.00484;
tamusq311: sequence, refer=entry,l = 3.8258360350;
startcell311: marker, at = 0;
c211, at = 0.0000000000;
m311, at = 0.1254769900;
d3c11, at = 0.1254769900;
sF311, at = 0.5567283800;
s311, at = 1.8778951600;
sD311, at = 1.9478951600;
d411, at = 3.2690619400;
```

```
endcell311: marker, at = 3.8258360350;
endsequence;
Beam,particle=proton,sequence=tamusq411,energy=1.00484;
tamusq411: sequence, refer=entry,l = 3.8286035900;
startcell411: marker, at = 0;
m411, at = 0.0000000000;
d411, at = 0.0000000000;
sF411, at = 0.5567740950;
s411, at = 1.8784091600;
sD411, at = 1.9484091600;
d5a11, at = 3.2700442250;
c311, at = 3.7040330650;
endcell411: marker, at = 3.8286035900;
endsequence;
Beam,particle=proton,sequence=tamusq511,energy=1.00729;
tamusq511: sequence, refer=entry,l = 3.8733571200;
startcell511: marker, at = 0;
c311, at = 0.0000000000;
m511, at = 0.1245705250;
d5c11, at = 0.1245705250;
sF511, at = 0.5555504950;
s511, at = 1.8870683250;
sD511, at = 1.9570683250;
d6a11, at = 3.2885861550;
c411, at = 3.7468734350;
endcell511: marker, at = 3.8733571200;
endsequence;
Beam,particle=proton,sequence=tamusq611,energy=1.00975;
tamusq611: sequence, refer=entry,l = 3.9267234100;
startcell611: marker, at = 0;
c411, at = 0.0000000000;
m611, at = 0.1264836850;
d6c11, at = 0.1264836850;
sF611, at = 0.5385110750;
s611, at = 1.9148659000;
sD611, at = 1.9848659000;
d611, at = 3.3612207250;
endcell611: marker, at = 3.9267234100;
endsequence;
```

```
Beam,particle=proton,sequence=tamusq112,energy=1.00975;
tamusq112: sequence, refer=entry,l = 3.9976914250;
startcell112: marker, at = 0;
m112, at = 0.0000000000;
d112, at = 0.0000000000;
sF112, at = 0.5655026850;
s112, at = 1.9530711050;
sD112, at = 2.0230711050;
d2a12, at = 3.4106395250;
c112, at = 3.8650666250;
endcell112: marker, at = 3.9976914250;
endsequence;
Beam,particle=proton,sequence=tamusq212,energy=1.01223;
tamusq212: sequence, refer=entry,l = 4.0266602700;
startcell212: marker, at = 0;
c112, at = 0.0000000000;
m212, at = 0.1326248000;
d2c12, at = 0.1326248000;
sF212, at = 0.5497392600;
s212, at = 1.9676261450;
sD212, at = 2.0376261450;
d3a12, at = 3.4555130300;
c212, at = 3.8929265800;
endcell212: marker, at = 4.0266602700;
endsequence;
Beam,particle=proton,sequence=tamusq312,energy=1.01472;
tamusq312: sequence, refer=entry,l = 4.0589421150;
startcell312: marker, at = 0;
c212, at = 0.0000000000;
m312, at = 0.1337336900;
d3c12, at = 0.1337336900;
sF312, at = 0.5710466400;
s312, at = 1.9942349900;
sD312, at = 2.0642349900;
d412, at = 3.4874233400;
endcell312: marker, at = 4.0589421150;
endsequence;
Beam,particle=proton,sequence=tamusq412,energy=1.01472;
tamusq412: sequence, refer=entry,l = 4.0720711350;
```

```
startcell412: marker, at = 0;
m412, at = 0.0000000000;
d412, at = 0.0000000000;
sF412, at = 0.5715187750;
s412, at = 1.9996834400;
sD412, at = 2.0696834400;
d5a12, at = 3.4978481050;
c312, at = 3.9387581250;
endcell412: marker, at = 4.0720711350;
endsequence;
Beam,particle=proton,sequence=tamusq512,energy=1.01722;
tamusq512: sequence, refer=entry,l = 4.1265234350;
startcell512: marker, at = 0;
c312, at = 0.0000000000;
m512, at = 0.1333130100;
d5c12, at = 0.1333130100;
sF512, at = 0.5702327800;
s512, at = 2.0096818450;
sD512, at = 2.0796818450;
d6a12, at = 3.5191309100;
c412, at = 3.9911403000;
endcell512: marker, at = 4.1265234350;
endsequence;
Beam,particle=proton,sequence=tamusq612,energy=1.01973;
tamusq612: sequence, refer=entry,l = 4.1721606650;
startcell612: marker, at = 0;
c412, at = 0.0000000000;
m612, at = 0.1353831350;
d6c12, at = 0.1353831350;
sF612, at = 0.5468091450;
s612, at = 2.0338595200;
sD612, at = 2.1038595200;
d612, at = 3.5909098950;
endcell612: marker, at = 4.1721606650;
endsequence;
Beam,particle=proton,sequence=tamusq113,energy=1.01973;
tamusq113: sequence, refer=entry,l = 4.2581056600;
startcell113: marker, at = 0;
m113, at = 0.0000000000;
```

```
d113, at = 0.0000000000;
sF113, at = 0.5812507700;
s113, at = 2.0807131500;
sD113, at = 2.1507131500;
d2a13, at = 3.6501755300;
c113, at = 4.1162881500;
endcell113: marker, at = 4.2581056600;
endsequence;
Beam,particle=proton,sequence=tamusq213,energy=1.02221;
tamusq213: sequence, refer=entry,l = 4.2814200350;
startcell213: marker, at = 0;
c113, at = 0.0000000000;
m213, at = 0.1418175100;
d2c13, at = 0.1418175100;
sF213, at = 0.5607828300;
s213, at = 2.0924512100;
sD213, at = 2.1624512100;
d3a13, at = 3.6941195900;
c213, at = 4.1383865200;
endcell213: marker, at = 4.2814200350;
endsequence;
Beam,particle=proton,sequence=tamusq313,energy=1.02468;
tamusq313: sequence, refer=entry,l = 4.3177138950;
startcell313: marker, at = 0;
c213, at = 0.0000000000;
m313, at = 0.1430335150;
d3c13, at = 0.1430335150;
sF313, at = 0.5871738250;
s313, at = 2.1238213600;
sD313, at = 2.1938213600;
d413, at = 3.7304688950;
endcell313: marker, at = 4.3177138950;
endsequence;
Beam,particle=proton,sequence=tamusq413,energy=1.02468;
tamusq413: sequence, refer=entry,l = 4.3216787000;
startcell413: marker, at = 0;
m413, at = 0.0000000000;
d413, at = 0.0000000000;
sF413, at = 0.5872450000;
```

```
s413, at = 2.1244352250;
sD413, at = 2.1944352250;
d5a13, at = 3.7316254500;
c313, at = 4.1795302500;
endcell413: marker, at = 4.3216787000;
endsequence;
Beam,particle=proton,sequence=tamusq513,energy=1.02718;
tamusq513: sequence, refer=entry,l = 4.3823814700;
startcell513: marker, at = 0;
c313, at = 0.0000000000;
m513, at = 0.1421484500;
d5c13, at = 0.1421484500;
sF513, at = 0.5850711700;
s513, at = 2.1335990150;
sD513, at = 2.2035990150;
d6a13, at = 3.7521268600;
c413, at = 4.2380042600;
endcell513: marker, at = 4.3823814700;
endsequence;
Beam,particle=proton,sequence=tamusq613,energy=1.02966;
tamusq613: sequence, refer=entry,l = 4.4199433100;
startcell613: marker, at = 0;
c413, at = 0.0000000000;
m613, at = 0.1443772100;
d6c13, at = 0.1443772100;
sF613, at = 0.5551954500;
s613, at = 2.1540158650;
sD613, at = 2.2240158650;
d613, at = 3.8228362800;
endcell613: marker, at = 4.4199433100;
endsequence;
Beam,particle=proton,sequence=tamusq114,energy=1.02966;
tamusq114: sequence, refer=entry,l = 4.5195837200;
startcell114: marker, at = 0;
m114, at = 0.0000000000;
d114, at = 0.0000000000;
sF114, at = 0.5971070300;
s114, at = 2.2089085900;
sD114, at = 2.2789085900;
```

```
d2a14, at = 3.8907101500;
c114, at = 4.3685447900;
endcell114: marker, at = 4.5195837200;
endsequence;
Beam,particle=proton,sequence=tamusq214,energy=1.03206;
tamusq214: sequence, refer=entry,l = 4.5369754550;
startcell214: marker, at = 0;
c114, at = 0.0000000000;
m214, at = 0.1510389300;
d2c14, at = 0.1510389300;
sF214, at = 0.5718609000;
s214, at = 2.2176661350;
sD214, at = 2.2876661350;
d3a14, at = 3.9334713700;
c214, at = 4.3846130700;
endcell214: marker, at = 4.5369754550;
endsequence;
Beam,particle=proton,sequence=tamusq314,energy=1.03443;
tamusq314: sequence, refer=entry,l = 4.5790791250;
startcell314: marker, at = 0;
c214, at = 0.0000000000;
m314, at = 0.1523623850;
d3c14, at = 0.1523623850;
sF314, at = 0.6033513850;
s314, at = 2.2544972150;
sD314, at = 2.3244972150;
d414, at = 3.9756430450;
endcell314: marker, at = 4.5790791250;
endsequence;
Beam,particle=proton,sequence=tamusq414,energy=1.03443;
tamusq414: sequence, refer=entry,l = 4.5836801000;
startcell414: marker, at = 0;
m414, at = 0.0000000000;
d414, at = 0.0000000000;
sF414, at = 0.6034360800;
s414, at = 2.2551641350;
sD414, at = 2.3251641350;
d5a14, at = 3.9768921900;
c314, at = 4.4321914100;
```

```
endcell414: marker, at = 4.5836801000;
endsequence;
Beam,particle=proton,sequence=tamusq514,energy=1.03684;
tamusq514: sequence, refer=entry,l = 4.6528576750;
startcell514: marker, at = 0;
c314, at = 0.0000000000;
m514, at = 0.1514886900;
d5c14, at = 0.1514886900;
sF514, at = 0.6007573300;
s514, at = 2.2645960650;
sD514, at = 2.3345960650;
d6a14, at = 3.9984348000;
c414, at = 4.4989725300;
endcell514: marker, at = 4.6528576750;
endsequence;
Beam,particle=proton,sequence=tamusq614,energy=1.03920;
tamusq614: sequence, refer=entry,l = 4.6652282850;
startcell614: marker, at = 0;
c414, at = 0.0000000000;
m614, at = 0.1538851450;
d6c14, at = 0.1538851450;
sF614, at = 0.5640608850;
s614, at = 2.2810910700;
sD614, at = 2.3510910700;
d614, at = 4.0681212550;
endcell614: marker, at = 4.6652282850;
endsequence;
```

Synergia Sequence File

```
sF11: SBEND,L=0.2279007900,ANGLE=0.4472556077,K1:=kqf1a,THICK=TRUE,APERTYPE=CIRCLE,APERTURE=0.03;
s11: SBEND,L=0.0700000000,ANGLE=0.1373750944,THICK=TRUE,APERTYPE=CIRCLE,APERTURE=0.03;
sD11: SBEND,L=0.2279007900,ANGLE=0.4472556077,K1:=kqd1a,THICK=TRUE,APERTYPE=CIRCLE,APERTURE=0.03;
sF21: SBEND,L=0.2393637800,ANGLE=0.4656413252,K1:=kqf1b,THICK=TRUE,APERTYPE=CIRCLE,APERTURE=0.03;
s21: SBEND,L=0.0700000000,ANGLE=0.1361730366,THICK=TRUE,APERTYPE=CIRCLE,APERTURE=0.03;
sD21: SBEND,L=0.2393637800,ANGLE=0.4656413252,K1:=kqd1b,THICK=TRUE,APERTYPE=CIRCLE,APERTURE=0.03;
sF31: SBEND,L=0.2404674250,ANGLE=0.4528404554,K1:=kqf1c,THICK=TRUE,APERTYPE=CIRCLE,APERTURE=0.03;
s31: SBEND,L=0.0700000000,ANGLE=0.1324295258,THICK=TRUE,APERTYPE=CIRCLE,APERTURE=0.03;
sD31: SBEND,L=0.2404674250,ANGLE=0.4549283866,K1:=kqd1c,THICK=TRUE,APERTYPE=CIRCLE,APERTURE=0.03;
sF41: SBEND,L=0.2433484100,ANGLE=0.4589988987,K1:=kqf1d,THICK=TRUE,APERTYPE=CIRCLE,APERTURE=0.03;
```

```
s41: SBEND,L=0.0700000000,ANGLE=0.1320325985,THICK=TRUE,APERTYPE=CIRCLE,APERTURE=0.03;
sD41: SBEND,L=0.2433484100,ANGLE=0.4589988987,K1:=kqd1d,THICK=TRUE,APERTYPE=CIRCLE,APERTURE=0.03;
sF51: SBEND,L=0.2461707650,ANGLE=0.4470921312,K1:=kqf1e,THICK=TRUE,APERTYPE=CIRCLE,APERTURE=0.03;
s51: SBEND,L=0.0700000000,ANGLE=0.1271330866,THICK=TRUE,APERTYPE=CIRCLE,APERTURE=0.03;
sD51: SBEND,L=0.2461707650,ANGLE=0.4470921312,K1:=kqd1e,THICK=TRUE,APERTYPE=CIRCLE,APERTURE=0.03;
sF61: SBEND,L=0.2639128900,ANGLE=0.4740745785,K1:=kqf1f,THICK=TRUE,APERTYPE=CIRCLE,APERTURE=0.03;
s61: SBEND,L=0.0700000000,ANGLE=0.1257430832,THICK=TRUE,APERTYPE=CIRCLE,APERTURE=0.03;
sD61: SBEND,L=0.2639128900,ANGLE=0.4740745785,K1:=kqd1f,THICK=TRUE,APERTYPE=CIRCLE,APERTURE=0.03;
d11: DRIFT, L=0.4019962300;
d2a1: DRIFT, L=0.3968689400;
c11: RFCAVITY,L=0.0748175400,VOLT=0.71496327,LAG=0.208330,HARMON=1,FREQ=117;
d2c1: DRIFT, L=0.3344657900;
d3a1: DRIFT, L=0.3665938500;
c21: RFCAVITY,L=0.0748163900,VOLT=0.71495631,LAG=0.208330,HARMON=1,FREQ=117;
d3c1: DRIFT, L=0.3664306900;
d41: DRIFT, L=0.4041549250;
d5a1: DRIFT, L=0.3711367300;
c31: RFCAVITY,L=0.0733137000,VOLT=0.70608807,LAG=0.208330,HARMON=1,FREQ=117;
d5c1: DRIFT, L=0.3645031300;
d6a1: DRIFT, L=0.4164455700;
c41: RFCAVITY,L=0.0739832000,VOLT=0.70998016,LAG=0.208330,HARMON=1,FREQ=117;
d6c1: DRIFT, L=0.3219282100;
d61: DRIFT, L=0.4076247000;
sF12: SBEND,L=0.2685317600,ANGLE=0.4559444620,K1:=kqf2a,THICK=TRUE,APERTYPE=CIRCLE,APERTURE=0.03;
s12: SBEND,L=0.0700000000,ANGLE=0.1188541435,THICK=TRUE,APERTYPE=CIRCLE,APERTURE=0.03;
sD12: SBEND,L=0.2685317600,ANGLE=0.4559444620,K1:=kqd2a,THICK=TRUE,APERTYPE=CIRCLE,APERTURE=0.03;
sF22: SBEND,L=0.2806405100,ANGLE=0.4745450918,K1:=kqf2b,THICK=TRUE,APERTYPE=CIRCLE,APERTURE=0.03;
s22: SBEND,L=0.0700000000,ANGLE=0.1183655076,THICK=TRUE,APERTYPE=CIRCLE,APERTURE=0.03;
sD22: SBEND,L=0.2806405100,ANGLE=0.4745450918,K1:=kqd2b,THICK=TRUE,APERTYPE=CIRCLE,APERTURE=0.03;
sF32: SBEND,L=0.2893448750,ANGLE=0.3966910088,K1:=kqf2c,THICK=TRUE,APERTYPE=CIRCLE,APERTURE=0.03;
s32: SBEND,L=0.0700000000,ANGLE=0.0989464087,THICK=TRUE,APERTYPE=CIRCLE,APERTURE=0.03;
sD32: SBEND,L=0.2893448750,ANGLE=0.4089948039,K1:=kqd2c,THICK=TRUE,APERTYPE=CIRCLE,APERTURE=0.03;
sF42: SBEND,L=0.3722747100,ANGLE=0.5371859440,K1:=kqf2d,THICK=TRUE,APERTYPE=CIRCLE,APERTURE=0.03;
s42: SBEND,L=0.0700000000,ANGLE=0.1010087848,THICK=TRUE,APERTYPE=CIRCLE,APERTURE=0.03;
sD42: SBEND,L=0.3722747100,ANGLE=0.5371859440,K1:=kqd2d,THICK=TRUE,APERTYPE=CIRCLE,APERTURE=0.03;
sF52: SBEND,L=0.3828398550,ANGLE=0.4675002117,K1:=kqf2e,THICK=TRUE,APERTYPE=CIRCLE,APERTURE=0.03;
s52: SBEND,L=0.0700000000,ANGLE=0.0854796448,THICK=TRUE,APERTYPE=CIRCLE,APERTURE=0.03;
sD52: SBEND,L=0.3828398550,ANGLE=0.4675002117,K1:=kqd2e,THICK=TRUE,APERTYPE=CIRCLE,APERTURE=0.03;
sF62: SBEND,L=0.4038510550,ANGLE=0.4957461446,K1:=kqf2f,THICK=TRUE,APERTYPE=CIRCLE,APERTURE=0.03;
```

```
s62: SBEND,L=0.0700000000,ANGLE=0.0859282889,THICK=TRUE,APERTYPE=CIRCLE,APERTURE=0.03;
sD62: SBEND,L=0.4038510550,ANGLE=0.4957461446,K1:=kqd2f,THICK=TRUE,APERTYPE=CIRCLE,APERTURE=0.03;
d12: DRIFT, L=0.4076247000;
d2a2: DRIFT, L=0.3975249400;
c12: RFCAVITY,L=0.0814872600,VOLT=0.75992358,LAG=0.208330,HARMON=1,FREQ=117;
d2c2: DRIFT, L=0.3387204100;
d3a2: DRIFT, L=0.3690705900;
c22: RFCAVITY,L=0.0815638200,VOLT=0.76049104,LAG=0.208330,HARMON=1,FREQ=117;
d3c2: DRIFT, L=0.3689169400;
d42: DRIFT, L=0.4198962050;
d5a2: DRIFT, L=0.3786526900;
c32: RFCAVITY,L=0.0954542400,VOLT=0.88109019,LAG=0.208330,HARMON=1,FREQ=117;
d5c2: DRIFT, L=0.3732725400;
d6a2: DRIFT, L=0.4156055500;
c42: RFCAVITY,L=0.0965212400,VOLT=0.89170946,LAG=0.208330,HARMON=1,FREQ=117;
d6c2: DRIFT, L=0.3393825000;
d62: DRIFT, L=0.4273608900;
sF13: SBEND,L=0.4075657250,ANGLE=0.4729890940,K1:=kqf3a,THICK=TRUE,APERTYPE=CIRCLE,APERTURE=0.03;
s13: SBEND,L=0.0700000000,ANGLE=0.0812365578,THICK=TRUE,APERTYPE=CIRCLE,APERTURE=0.03;
sD13: SBEND,L=0.4075657250,ANGLE=0.4729890940,K1:=kqd3a,THICK=TRUE,APERTYPE=CIRCLE,APERTURE=0.03;
sF23: SBEND,L=0.4218007200,ANGLE=0.4928336985,K1:=kqf3b,THICK=TRUE,APERTYPE=CIRCLE,APERTURE=0.03;
s23: SBEND,L=0.0700000000,ANGLE=0.0817882883,THICK=TRUE,APERTYPE=CIRCLE,APERTURE=0.03;
sD23: SBEND,L=0.4218007200,ANGLE=0.4928336985,K1:=kqd3b,THICK=TRUE,APERTYPE=CIRCLE,APERTURE=0.03;
sF33: SBEND,L=0.4241715800,ANGLE=0.4753403473,K1:=kqf3c,THICK=TRUE,APERTYPE=CIRCLE,APERTURE=0.03;
s33: SBEND,L=0.0700000000,ANGLE=0.0788851767,THICK=TRUE,APERTYPE=CIRCLE,APERTURE=0.03;
sD33: SBEND,L=0.4241715800,ANGLE=0.4780121431,K1:=kqd3c,THICK=TRUE,APERTYPE=CIRCLE,APERTURE=0.03;
sF43: SBEND,L=0.4331058150,ANGLE=0.4891727565,K1:=kqf3d,THICK=TRUE,APERTYPE=CIRCLE,APERTURE=0.03;
s43: SBEND,L=0.0700000000,ANGLE=0.0790617253,THICK=TRUE,APERTYPE=CIRCLE,APERTURE=0.03;
sD43: SBEND,L=0.4331058150,ANGLE=0.4891727565,K1:=kqd3d,THICK=TRUE,APERTYPE=CIRCLE,APERTURE=0.03;
sF53: SBEND,L=0.4378921100,ANGLE=0.4723798648,K1:=kqf3e,THICK=TRUE,APERTYPE=CIRCLE,APERTURE=0.03;
s53: SBEND,L=0.0700000000,ANGLE=0.0755130996,THICK=TRUE,APERTYPE=CIRCLE,APERTURE=0.03;
sD53: SBEND,L=0.4378921100,ANGLE=0.4723798648,K1:=kqd3e,THICK=TRUE,APERTYPE=CIRCLE,APERTURE=0.03;
sF63: SBEND,L=0.4602635950,ANGLE=0.5007925508,K1:=kqf3f,THICK=TRUE,APERTYPE=CIRCLE,APERTURE=0.03;
s63: SBEND,L=0.0700000000,ANGLE=0.0761639177,THICK=TRUE,APERTYPE=CIRCLE,APERTURE=0.03;
sD63: SBEND,L=0.4602635950,ANGLE=0.5007925508,K1:=kqd3f,THICK=TRUE,APERTYPE=CIRCLE,APERTURE=0.03;
d13: DRIFT, L=0.4273608900;
d2a3: DRIFT, L=0.3997683700;
c13: RFCAVITY,L=0.1042966800,VOLT=0.97430008,LAG=0.208330,HARMON=1,FREQ=117;
d2c3: DRIFT, L=0.3532705600;
```

```
d3a3: DRIFT, L=0.3775406500;
c23: RFCAVITY,L=0.1046390200,VOLT=0.97813660,LAG=0.208330,HARMON=1,FREQ=117;
d3c3: DRIFT, L=0.3774195400;
d43: DRIFT, L=0.4305798200;
d5a3: DRIFT, L=0.3816802200;
c33: RFCAVITY,L=0.1043727600,VOLT=0.97515129,LAG=0.208330,HARMON=1,FREQ=117;
d5c3: DRIFT, L=0.3768049800;
d6a3: DRIFT, L=0.4152671700;
c43: RFCAVITY,L=0.1055998900,VOLT=0.98899022,LAG=0.208330,HARMON=1,FREQ=117;
d6c3: DRIFT, L=0.3464133300;
d63: DRIFT, L=0.4353591150;
sF14: SBEND,L=0.4641985950,ANGLE=0.4774444363,K1:=kqf4a,THICK=TRUE,APERTYPE=CIRCLE,APERTURE=0.03;
s14: SBEND,L=0.0700000000,ANGLE=0.0719974401,THICK=TRUE,APERTYPE=CIRCLE,APERTURE=0.03;
sD14: SBEND,L=0.4641985950,ANGLE=0.4774444363,K1:=kqd4a,THICK=TRUE,APERTYPE=CIRCLE,APERTURE=0.03;
sF24: SBEND,L=0.4793417250,ANGLE=0.4974086518,K1:=kqf4b,THICK=TRUE,APERTYPE=CIRCLE,APERTURE=0.03;
s24: SBEND,L=0.0700000000,ANGLE=0.0726383784,THICK=TRUE,APERTYPE=CIRCLE,APERTURE=0.03;
sD24: SBEND,L=0.4793417250,ANGLE=0.4974086518,K1:=kqd4b,THICK=TRUE,APERTYPE=CIRCLE,APERTURE=0.03;
sF34: SBEND,L=0.4889286350,ANGLE=0.4391922054,K1:=kqf4c,THICK=TRUE,APERTYPE=CIRCLE,APERTURE=0.03;
s34: SBEND,L=0.0700000000,ANGLE=0.0641368209,THICK=TRUE,APERTYPE=CIRCLE,APERTURE=0.03;
sD34: SBEND,L=0.4889286350,ANGLE=0.4479761186,K1:=kqd4c,THICK=TRUE,APERTYPE=CIRCLE,APERTURE=0.03;
sF44: SBEND,L=0.5578391500,ANGLE=0.5326916304,K1:=kqf4d,THICK=TRUE,APERTYPE=CIRCLE,APERTURE=0.03;
s44: SBEND,L=0.0700000000,ANGLE=0.0668443836,THICK=TRUE,APERTYPE=CIRCLE,APERTURE=0.03;
sD44: SBEND,L=0.5578391500,ANGLE=0.5326916304,K1:=kqd4d,THICK=TRUE,APERTYPE=CIRCLE,APERTURE=0.03;
sF54: SBEND,L=0.5698917400,ANGLE=0.4804630108,K1:=kqf4e,THICK=TRUE,APERTYPE=CIRCLE,APERTURE=0.03;
s54: SBEND,L=0.0700000000,ANGLE=0.0590154382,THICK=TRUE,APERTYPE=CIRCLE,APERTURE=0.03;
sD54: SBEND,L=0.5698917400,ANGLE=0.4804630108,K1:=kqd4e,THICK=TRUE,APERTYPE=CIRCLE,APERTURE=0.03;
sF64: SBEND,L=0.5955816600,ANGLE=0.5089646466,K1:=kqf4f,THICK=TRUE,APERTYPE=CIRCLE,APERTURE=0.03;
s64: SBEND,L=0.0700000000,ANGLE=0.0598197152,THICK=TRUE,APERTYPE=CIRCLE,APERTURE=0.03;
sD64: SBEND,L=0.5955816600,ANGLE=0.5089646466,K1:=kqd4f,THICK=TRUE,APERTYPE=CIRCLE,APERTURE=0.03;
d14: DRIFT, L=0.4353591150;
d2a4: DRIFT, L=0.4006828600;
c14: RFCAVITY,L=0.1135944600,VOLT=1.08391772,LAG=0.208330,HARMON=1,FREQ=117;
d2c4: DRIFT, L=0.3592016200;
d3a4: DRIFT, L=0.3809932900;
c24: RFCAVITY,L=0.1140451400,VOLT=1.08950047,LAG=0.208330,HARMON=1,FREQ=117;
d3c4: DRIFT, L=0.3808854500;
d44: DRIFT, L=0.4454073050;
d5a4: DRIFT, L=0.3889393900;
c34: RFCAVITY,L=0.1257568300,VOLT=1.24207252,LAG=0.208330,HARMON=1,FREQ=117;
```

```
d5c4: DRIFT, L=0.3852747600;
d6a4: DRIFT, L=0.4144558500;
c44: RFCAVITY,L=0.1273679000,VOLT=1.26407040,LAG=0.208330,HARMON=1,FREQ=117;
d6c4: DRIFT, L=0.3632712700;
d64: DRIFT, L=0.4545829400;
sF15: SBEND,L=0.6005918050,ANGLE=0.4851694927,K1:=kqf5a,THICK=TRUE,APERTYPE=CIRCLE,APERTURE=0.03;
s15: SBEND,L=0.0700000000,ANGLE=0.0565473325,THICK=TRUE,APERTYPE=CIRCLE,APERTURE=0.03;
sD15: SBEND,L=0.6005918050,ANGLE=0.4851694927,K1:=kqd5a,THICK=TRUE,APERTYPE=CIRCLE,APERTURE=0.03;
sF25: SBEND,L=0.6179765200,ANGLE=0.5051196558,K1:=kqf5b,THICK=TRUE,APERTYPE=CIRCLE,APERTURE=0.03;
s25: SBEND,L=0.0700000000,ANGLE=0.0572163743,THICK=TRUE,APERTYPE=CIRCLE,APERTURE=0.03;
sD25: SBEND,L=0.6179765200,ANGLE=0.5051196558,K1:=kqd5b,THICK=TRUE,APERTYPE=CIRCLE,APERTURE=0.03;
sF35: SBEND,L=0.6219284700,ANGLE=0.4842746520,K1:=kqf5c,THICK=TRUE,APERTYPE=CIRCLE,APERTURE=0.03;
s35: SBEND,L=0.0700000000,ANGLE=0.0548552001,THICK=TRUE,APERTYPE=CIRCLE,APERTURE=0.03;
sD35: SBEND,L=0.6219284700,ANGLE=0.4873715806,K1:=kqd5c,THICK=TRUE,APERTYPE=CIRCLE,APERTURE=0.03;
sF45: SBEND,L=0.6375578000,ANGLE=0.5037071659,K1:=kqf5d,THICK=TRUE,APERTYPE=CIRCLE,APERTURE=0.03;
s45: SBEND,L=0.0700000000,ANGLE=0.0553040079,THICK=TRUE,APERTYPE=CIRCLE,APERTURE=0.03;
sD45: SBEND,L=0.6375578000,ANGLE=0.5037071659,K1:=kqd5d,THICK=TRUE,APERTYPE=CIRCLE,APERTURE=0.03;
sF55: SBEND,L=0.6446622600,ANGLE=0.4836456748,K1:=kqf5e,THICK=TRUE,APERTYPE=CIRCLE,APERTURE=0.03;
s55: SBEND,L=0.0700000000,ANGLE=0.0525161768,THICK=TRUE,APERTYPE=CIRCLE,APERTURE=0.03;
sD55: SBEND,L=0.6446622600,ANGLE=0.4836456748,K1:=kqd5e,THICK=TRUE,APERTYPE=CIRCLE,APERTURE=0.03;
sF65: SBEND,L=0.6722318950,ANGLE=0.5122062825,K1:=kqf5f,THICK=TRUE,APERTYPE=CIRCLE,APERTURE=0.03;
s65: SBEND,L=0.0700000000,ANGLE=0.0533364157,THICK=TRUE,APERTYPE=CIRCLE,APERTURE=0.03;
sD65: SBEND,L=0.6722318950,ANGLE=0.5122062825,K1:=kqd5f,THICK=TRUE,APERTYPE=CIRCLE,APERTURE=0.03;
d15: DRIFT, L=0.4545829400;
d2a5: DRIFT, L=0.4028861600;
c15: RFCAVITY,L=0.1359958100,VOLT=1.38525067,LAG=0.208330,HARMON=1,FREQ=117;
d2c5: DRIFT, L=0.3734914600;
d3a5: DRIFT, L=0.3893118200;
c25: RFCAVITY,L=0.1367075200,VOLT=1.39547103,LAG=0.208330,HARMON=1,FREQ=117;
d3c5: DRIFT, L=0.3892359500;
d45: DRIFT, L=0.4590446750;
d5a5: DRIFT, L=0.3930513000;
c35: RFCAVITY,L=0.1378697400,VOLT=1.41222519,LAG=0.208330,HARMON=1,FREQ=117;
d5c5: DRIFT, L=0.3900724300;
d6a5: DRIFT, L=0.4139962800;
c45: RFCAVITY,L=0.1396982800,VOLT=1.43873796,LAG=0.208330,HARMON=1,FREQ=117;
d6c5: DRIFT, L=0.3728203700;
d65: DRIFT, L=0.4654721800;
sF16: SBEND,L=0.6778510750,ANGLE=0.4882338248,K1:=kqf6a,THICK=TRUE,APERTYPE=CIRCLE,APERTURE=0.03;
```

```
s16: SBEND,L=0.0700000000,ANGLE=0.0504186967,THICK=TRUE,APERTYPE=CIRCLE,APERTURE=0.03;
sD16: SBEND,L=0.6778510750,ANGLE=0.4882338248,K1:=kqd6a,THICK=TRUE,APERTYPE=CIRCLE,APERTURE=0.03;
sF26: SBEND,L=0.6965055300,ANGLE=0.5081908181,K1:=kqf6b,THICK=TRUE,APERTYPE=CIRCLE,APERTURE=0.03;
s26: SBEND,L=0.0700000000,ANGLE=0.0510740486,THICK=TRUE,APERTYPE=CIRCLE,APERTURE=0.03;
sD26: SBEND,L=0.6965055300,ANGLE=0.5081908181,K1:=kqd6b,THICK=TRUE,APERTYPE=CIRCLE,APERTURE=0.03;
sF36: SBEND,L=0.7065994350,ANGLE=0.4627409094,K1:=kqf6c,THICK=TRUE,APERTYPE=CIRCLE,APERTURE=0.03;
s36: SBEND,L=0.0700000000,ANGLE=0.0465062548,THICK=TRUE,APERTYPE=CIRCLE,APERTURE=0.03;
sD36: SBEND,L=0.7065994350,ANGLE=0.4694470482,K1:=kqd6c,THICK=TRUE,APERTYPE=CIRCLE,APERTURE=0.03;
sF46: SBEND,L=0.7661604900,ANGLE=0.5292794539,K1:=kqf6d,THICK=TRUE,APERTYPE=CIRCLE,APERTURE=0.03;
s46: SBEND,L=0.0700000000,ANGLE=0.0483574424,THICK=TRUE,APERTYPE=CIRCLE,APERTURE=0.03;
sD46: SBEND,L=0.7661604900,ANGLE=0.5292794539,K1:=kqd6d,THICK=TRUE,APERTYPE=CIRCLE,APERTURE=0.03;
sF56: SBEND,L=0.7795555800,ANGLE=0.4879103833,K1:=kqf6e,THICK=TRUE,APERTYPE=CIRCLE,APERTURE=0.03;
s56: SBEND,L=0.0700000000,ANGLE=0.0438117919,THICK=TRUE,APERTYPE=CIRCLE,APERTURE=0.03;
sD56: SBEND,L=0.7795555800,ANGLE=0.4879103833,K1:=kqd6e,THICK=TRUE,APERTYPE=CIRCLE,APERTURE=0.03;
sF66: SBEND,L=0.8105163900,ANGLE=0.5165678901,K1:=kqf6f,THICK=TRUE,APERTYPE=CIRCLE,APERTURE=0.03;
s66: SBEND,L=0.0700000000,ANGLE=0.0446132278,THICK=TRUE,APERTYPE=CIRCLE,APERTURE=0.03;
sD66: SBEND,L=0.8105163900,ANGLE=0.5165678901,K1:=kqd6f,THICK=TRUE,APERTYPE=CIRCLE,APERTURE=0.03;
d16: DRIFT, L=0.4654721800;
d2a6: DRIFT, L=0.4041342100;
c16: RFCAVITY,L=0.1486849500,VOLT=1.57129044,LAG=0.208330,HARMON=1,FREQ=117;
d2c6: DRIFT, L=0.3815858800;
d3a6: DRIFT, L=0.3940238000;
c26: RFCAVITY,L=0.1495445100,VOLT=1.58412495,LAG=0.208330,HARMON=1,FREQ=117;
d3c6: DRIFT, L=0.3939660400;
d46: DRIFT, L=0.4748200200;
d5a6: DRIFT, L=0.4004696000;
c36: RFCAVITY,L=0.1597225900,VOLT=1.73726064,LAG=0.208330,HARMON=1,FREQ=117;
d5c6: DRIFT, L=0.3987278900;
d6a6: DRIFT, L=0.4131671700;
c46: RFCAVITY,L=0.1619434900,VOLT=1.77081250,LAG=0.208330,HARMON=1,FREQ=117;
d6c6: DRIFT, L=0.3900478700;
d66: DRIFT, L=0.4851174250;
sF17: SBEND,L=0.8172342500,ANGLE=0.4923568063,K1:=kqf7a,THICK=TRUE,APERTYPE=CIRCLE,APERTURE=0.03;
s17: SBEND,L=0.0700000000,ANGLE=0.0421727019,THICK=TRUE,APERTYPE=CIRCLE,APERTURE=0.03;
sD17: SBEND,L=0.8172342500,ANGLE=0.4923568063,K1:=kqd7a,THICK=TRUE,APERTYPE=CIRCLE,APERTURE=0.03;
sF27: SBEND,L=0.8381794250,ANGLE=0.5123342173,K1:=kqf7b,THICK=TRUE,APERTYPE=CIRCLE,APERTURE=0.03;
s27: SBEND,L=0.0700000000,ANGLE=0.0427872531,THICK=TRUE,APERTYPE=CIRCLE,APERTURE=0.03;
sD27: SBEND,L=0.8381794250,ANGLE=0.5123342173,K1:=kqd7b,THICK=TRUE,APERTYPE=CIRCLE,APERTURE=0.03;
sF37: SBEND,L=0.8434605650,ANGLE=0.4911850253,K1:=kqf7c,THICK=TRUE,APERTYPE=CIRCLE,APERTURE=0.03;
```

```
s37: SBEND,L=0.0700000000,ANGLE=0.0410209923,THICK=TRUE,APERTYPE=CIRCLE,APERTURE=0.03;
sD37: SBEND,L=0.8434605650,ANGLE=0.4942798482,K1:=kqd7c,THICK=TRUE,APERTYPE=CIRCLE,APERTURE=0.03;
sF47: SBEND,L=0.8623471500,ANGLE=0.5106426064,K1:=kqf7d,THICK=TRUE,APERTYPE=CIRCLE,APERTURE=0.03;
s47: SBEND,L=0.0700000000,ANGLE=0.0414508037,THICK=TRUE,APERTYPE=CIRCLE,APERTURE=0.03;
sD47: SBEND,L=0.8623471500,ANGLE=0.5106426064,K1:=kqd7d,THICK=TRUE,APERTYPE=CIRCLE,APERTURE=0.03;
sF57: SBEND,L=0.8715857700,ANGLE=0.4900902565,K1:=kqf7e,THICK=TRUE,APERTYPE=CIRCLE,APERTURE=0.03;
s57: SBEND,L=0.0700000000,ANGLE=0.0393608055,THICK=TRUE,APERTYPE=CIRCLE,APERTURE=0.03;
sD57: SBEND,L=0.8715857700,ANGLE=0.4900902565,K1:=kqd7e,THICK=TRUE,APERTYPE=CIRCLE,APERTURE=0.03;
sF67: SBEND,L=0.9048602000,ANGLE=0.5188070257,K1:=kqf7f,THICK=TRUE,APERTYPE=CIRCLE,APERTURE=0.03;
s67: SBEND,L=0.0700000000,ANGLE=0.0401349201,THICK=TRUE,APERTYPE=CIRCLE,APERTURE=0.03;
sD67: SBEND,L=0.9048602000,ANGLE=0.5188070257,K1:=kqd7f,THICK=TRUE,APERTYPE=CIRCLE,APERTURE=0.03;
d17: DRIFT, L=0.4851174250;
d2a7: DRIFT, L=0.4063858100;
c17: RFCAVITY,L=0.1715773700,VOLT=1.91590643,LAG=0.208330,HARMON=1,FREQ=117;
d2c7: DRIFT, L=0.3961889700;
d3a7: DRIFT, L=0.4025246900;
c27: RFCAVITY,L=0.1727036800,VOLT=1.93275824,LAG=0.208330,HARMON=1,FREQ=117;
d3c7: DRIFT, L=0.4024995900;
d47: DRIFT, L=0.4905982800;
d5a7: DRIFT, L=0.4055307000;
c37: RFCAVITY,L=0.1746315800,VOLT=1.96151929,LAG=0.208330,HARMON=1,FREQ=117;
d5c7: DRIFT, L=0.4046330300;
d6a7: DRIFT, L=0.4126015100;
c47: RFCAVITY,L=0.1771201500,VOLT=1.99846264,LAG=0.208330,HARMON=1,FREQ=117;
d6c7: DRIFT, L=0.4018012300;
d67: DRIFT, L=0.4985202850;
sF18: SBEND,L=0.9123276900,ANGLE=0.4944734875,K1:=kqf8a,THICK=TRUE,APERTYPE=CIRCLE,APERTURE=0.03;
s18: SBEND,L=0.0700000000,ANGLE=0.0379393769,THICK=TRUE,APERTYPE=CIRCLE,APERTURE=0.03;
sD18: SBEND,L=0.9123276900,ANGLE=0.4944734875,K1:=kqd8a,THICK=TRUE,APERTYPE=CIRCLE,APERTURE=0.03;
sF28: SBEND,L=0.9348357050,ANGLE=0.5144663592,K1:=kqf8b,THICK=TRUE,APERTYPE=CIRCLE,APERTURE=0.03;
s28: SBEND,L=0.0700000000,ANGLE=0.0385229671,THICK=TRUE,APERTYPE=CIRCLE,APERTURE=0.03;
sD28: SBEND,L=0.9348357050,ANGLE=0.5144663592,K1:=kqd8b,THICK=TRUE,APERTYPE=CIRCLE,APERTURE=0.03;
sF38: SBEND,L=0.9446379700,ANGLE=0.4799062686,K1:=kqf8c,THICK=TRUE,APERTYPE=CIRCLE,APERTURE=0.03;
s38: SBEND,L=0.0700000000,ANGLE=0.0359351259,THICK=TRUE,APERTYPE=CIRCLE,APERTURE=0.03;
sD38: SBEND,L=0.9446379700,ANGLE=0.4849383490,K1:=kqd8c,THICK=TRUE,APERTYPE=CIRCLE,APERTURE=0.03;
sF48: SBEND,L=0.9924152950,ANGLE=0.5247459647,K1:=kqf8d,THICK=TRUE,APERTYPE=CIRCLE,APERTURE=0.03;
s48: SBEND,L=0.0700000000,ANGLE=0.0370129498,THICK=TRUE,APERTYPE=CIRCLE,APERTURE=0.03;
sD48: SBEND,L=0.9924152950,ANGLE=0.5247459647,K1:=kqd8d,THICK=TRUE,APERTYPE=CIRCLE,APERTURE=0.03;
sF58: SBEND,L=1.0064791000,ANGLE=0.4925896292,K1:=kqf8e,THICK=TRUE,APERTYPE=CIRCLE,APERTURE=0.03;
```

```
s58: SBEND,L=0.0700000000,ANGLE=0.0342593046,THICK=TRUE,APERTYPE=CIRCLE,APERTURE=0.03;
sD58: SBEND,L=1.0064791000,ANGLE=0.4925896292,K1:=kqd8e,THICK=TRUE,APERTYPE=CIRCLE,APERTURE=0.03;
sF68: SBEND,L=1.0431447050,ANGLE=0.5213809275,K1:=kqf8f,THICK=TRUE,APERTYPE=CIRCLE,APERTURE=0.03;
s68: SBEND,L=0.0700000000,ANGLE=0.0349871545,THICK=TRUE,APERTYPE=CIRCLE,APERTURE=0.03;
sD68: SBEND,L=1.0431447050,ANGLE=0.5213809275,K1:=kqd8f,THICK=TRUE,APERTYPE=CIRCLE,APERTURE=0.03;
d18: DRIFT, L=0.4985202850;
d2a8: DRIFT, L=0.4079219500;
c18: RFCAVITY,L=0.1871956100,VOLT=2.14519769,LAG=0.208330,HARMON=1,FREQ=117;
d2c8: DRIFT, L=0.4061518600;
d3a8: DRIFT, L=0.4083243700;
c28: RFCAVITY,L=0.1885039000,VOLT=2.16383378,LAG=0.208330,HARMON=1,FREQ=117;
d3c8: DRIFT, L=0.4083215600;
d48: DRIFT, L=0.5072350550;
d5a8: DRIFT, L=0.4131454300;
c38: RFCAVITY,L=0.1964844400,VOLT=2.27485552,LAG=0.208330,HARMON=1,FREQ=117;
d5c8: DRIFT, L=0.4130920600;
d6a8: DRIFT, L=0.4169626700;
c48: RFCAVITY,L=0.1993653600,VOLT=2.31365771,LAG=0.208330,HARMON=1,FREQ=117;
d6c8: DRIFT, L=0.4138384700;
d68: DRIFT, L=0.5181655300;
sF19: SBEND,L=1.0517108600,ANGLE=0.4969065489,K1:=kqf9a,THICK=TRUE,APERTYPE=CIRCLE,APERTURE=0.03;
s19: SBEND,L=0.0700000000,ANGLE=0.0330732141,THICK=TRUE,APERTYPE=CIRCLE,APERTURE=0.03;
sD19: SBEND,L=1.0517108600,ANGLE=0.4969065489,K1:=kqd9a,THICK=TRUE,APERTYPE=CIRCLE,APERTURE=0.03;
sF29: SBEND,L=1.0765095950,ANGLE=0.5169214443,K1:=kqf9b,THICK=TRUE,APERTYPE=CIRCLE,APERTURE=0.03;
s29: SBEND,L=0.0700000000,ANGLE=0.0336127994,THICK=TRUE,APERTYPE=CIRCLE,APERTURE=0.03;
sD29: SBEND,L=1.0765095950,ANGLE=0.5169214443,K1:=kqd9b,THICK=TRUE,APERTYPE=CIRCLE,APERTURE=0.03;
sF39: SBEND,L=1.0819769500,ANGLE=0.4994406268,K1:=kqf9c,THICK=TRUE,APERTYPE=CIRCLE,APERTURE=0.03;
s39: SBEND,L=0.0700000000,ANGLE=0.0324761099,THICK=TRUE,APERTYPE=CIRCLE,APERTURE=0.03;
sD39: SBEND,L=1.0819769500,ANGLE=0.5019771757,K1:=kqd9c,THICK=TRUE,APERTYPE=CIRCLE,APERTURE=0.03;
sF49: SBEND,L=1.0957912550,ANGLE=0.5116023448,K1:=kqf9d,THICK=TRUE,APERTYPE=CIRCLE,APERTURE=0.03;
s49: SBEND,L=0.0700000000,ANGLE=0.0326815568,THICK=TRUE,APERTYPE=CIRCLE,APERTURE=0.03;
sD49: SBEND,L=1.0957912550,ANGLE=0.5116023448,K1:=kqd9d,THICK=TRUE,APERTYPE=CIRCLE,APERTURE=0.03;
sF59: SBEND,L=1.1060604900,ANGLE=0.4940549457,K1:=kqf9e,THICK=TRUE,APERTYPE=CIRCLE,APERTURE=0.03;
s59: SBEND,L=0.0700000000,ANGLE=0.0312675903,THICK=TRUE,APERTYPE=CIRCLE,APERTURE=0.03;
sD59: SBEND,L=1.1060604900,ANGLE=0.4940549457,K1:=kqd9e,THICK=TRUE,APERTYPE=CIRCLE,APERTURE=0.03;
sF69: SBEND,L=1.1452295450,ANGLE=0.5228940481,K1:=kqf9f,THICK=TRUE,APERTYPE=CIRCLE,APERTURE=0.03;
s69: SBEND,L=0.0700000000,ANGLE=0.0319609143,THICK=TRUE,APERTYPE=CIRCLE,APERTURE=0.03;
sD69: SBEND,L=1.1452295450,ANGLE=0.5228940481,K1:=kqd9f,THICK=TRUE,APERTYPE=CIRCLE,APERTURE=0.03;
d19: DRIFT, L=0.5181655300;
```

```
d2a9: DRIFT, L=0.4193671700;
c19: RFCAVITY,L=0.2100880300,VOLT=2.45085683,LAG=0.208330,HARMON=1,FREQ=117;
d2c9: DRIFT, L=0.4115613300;
d3a9: DRIFT, L=0.4168514600;
c29: RFCAVITY,L=0.2116630700,VOLT=2.46993202,LAG=0.208330,HARMON=1,FREQ=117;
d3c9: DRIFT, L=0.4168288900;
d49: DRIFT, L=0.5239237900;
d5a9: DRIFT, L=0.4195311800;
c39: RFCAVITY,L=0.2126167300,VOLT=2.48133464,LAG=0.208330,HARMON=1,FREQ=117;
d5c9: DRIFT, L=0.4185723400;
d6a9: DRIFT, L=0.4296232000;
c49: RFCAVITY,L=0.2157872900,VOLT=2.51841629,LAG=0.208330,HARMON=1,FREQ=117;
d6c9: DRIFT, L=0.4132836100;
d69: DRIFT, L=0.5326681050;
sF110: SBEND,L=1.1546067900,ANGLE=0.4983368935,K1:=kqf10a,THICK=TRUE,APERTYPE=CIRCLE,APERTURE=0.03;
s110: SBEND,L=0.0700000000,ANGLE=0.0302125216,THICK=TRUE,APERTYPE=CIRCLE,APERTURE=0.03;
sD110: SBEND,L=1.1546067900,ANGLE=0.4983368935,K1:=kqd10a,THICK=TRUE,APERTYPE=CIRCLE,APERTURE=0.03;
sF210: SBEND,L=1.1810965950,ANGLE=0.5183668308,K1:=kqf10b,THICK=TRUE,APERTYPE=CIRCLE,APERTURE=0.03;
s210: SBEND,L=0.0700000000,ANGLE=0.0307220242,THICK=TRUE,APERTYPE=CIRCLE,APERTURE=0.03;
sD210: SBEND,L=1.1810965950,ANGLE=0.5183668308,K1:=kqd10b,THICK=TRUE,APERTYPE=CIRCLE,APERTURE=0.03;
sF310: SBEND,L=1.1895958150,ANGLE=0.4937695889,K1:=kqf10c,THICK=TRUE,APERTYPE=CIRCLE,APERTURE=0.03;
s310: SBEND,L=0.0700000000,ANGLE=0.0292642205,THICK=TRUE,APERTYPE=CIRCLE,APERTURE=0.03;
sD310: SBEND,L=1.1895958150,ANGLE=0.4973227753,K1:=kqd10c,THICK=TRUE,APERTYPE=CIRCLE,APERTURE=0.03;
sF410: SBEND,L=1.2211713350,ANGLE=0.5193192530,K1:=kqf10d,THICK=TRUE,APERTYPE=CIRCLE,APERTURE=0.03;
s410: SBEND,L=0.0700000000,ANGLE=0.0297684253,THICK=TRUE,APERTYPE=CIRCLE,APERTURE=0.03;
sD410: SBEND,L=1.2211713350,ANGLE=0.5193192530,K1:=kqd10d,THICK=TRUE,APERTYPE=CIRCLE,APERTURE=0.03;
sF510: SBEND,L=1.2348857200,ANGLE=0.4956097813,K1:=kqf10e,THICK=TRUE,APERTYPE=CIRCLE,APERTURE=0.03;
s510: SBEND,L=0.0700000000,ANGLE=0.0280938423,THICK=TRUE,APERTYPE=CIRCLE,APERTURE=0.03;
sD510: SBEND,L=1.2348857200,ANGLE=0.4956097813,K1:=kqd10e,THICK=TRUE,APERTYPE=CIRCLE,APERTURE=0.03;
sF610: SBEND,L=1.2773483700,ANGLE=0.5243789950,K1:=kqf10f,THICK=TRUE,APERTYPE=CIRCLE,APERTURE=0.03;
s610: SBEND,L=0.0700000000,ANGLE=0.0287365064,THICK=TRUE,APERTYPE=CIRCLE,APERTURE=0.03;
sD610: SBEND,L=1.2773483700,ANGLE=0.5243789950,K1:=kqd10f,THICK=TRUE,APERTYPE=CIRCLE,APERTURE=0.03;
d110: DRIFT, L=0.5326681050;
d2a10: DRIFT, L=0.4301084000;
c110: RFCAVITY,L=0.2269877600,VOLT=2.63822502,LAG=0.208330,HARMON=1,FREQ=117;
d2c10: DRIFT, L=0.4132626300;
d3a10: DRIFT, L=0.4231510200;
c210: RFCAVITY,L=0.2287597100,VOLT=2.65543145,LAG=0.208330,HARMON=1,FREQ=117;
d3c10: DRIFT, L=0.4231045500;
```

```
d410: DRIFT, L=0.5404859550;
d5a10: DRIFT, L=0.4277922200;
c310: RFCAVITY,L=0.2334865500,VOLT=2.69877560,LAG=0.208330,HARMON=1,FREQ=117;
d5c10: DRIFT, L=0.4256620000;
d6a10: DRIFT, L=0.4460017200;
c410: RFCAVITY,L=0.2370318100,VOLT=2.72872610,LAG=0.208330,HARMON=1,FREQ=117;
d6c10: DRIFT, L=0.4125658100;
d610: DRIFT, L=0.5514622550;
sF111: SBEND,L=1.2881311950,ANGLE=0.4999852446,K1:=kqf11a,THICK=TRUE,APERTYPE=CIRCLE,APERTURE=0.03;
s111: SBEND,L=0.0700000000,ANGLE=0.0271703436,THICK=TRUE,APERTYPE=CIRCLE,APERTURE=0.03;
sD111: SBEND,L=1.2881311950,ANGLE=0.4999852446,K1:=kqd11a,THICK=TRUE,APERTYPE=CIRCLE,APERTURE=0.03;
sF211: SBEND,L=1.3168678300,ANGLE=0.5199095725,K1:=kqf11b,THICK=TRUE,APERTYPE=CIRCLE,APERTURE=0.03;
s211: SBEND,L=0.0700000000,ANGLE=0.0276365397,THICK=TRUE,APERTYPE=CIRCLE,APERTURE=0.03;
sD211: SBEND,L=1.3168678300,ANGLE=0.5199095725,K1:=kqd11b,THICK=TRUE,APERTYPE=CIRCLE,APERTURE=0.03;
sF311: SBEND,L=1.3211667800,ANGLE=0.5084517329,K1:=kqf11c,THICK=TRUE,APERTYPE=CIRCLE,APERTURE=0.03;
s311: SBEND,L=0.0700000000,ANGLE=0.0270274818,THICK=TRUE,APERTYPE=CIRCLE,APERTURE=0.03;
sD311: SBEND,L=1.3211667800,ANGLE=0.5101115871,K1:=kqd11c,THICK=TRUE,APERTYPE=CIRCLE,APERTURE=0.03;
sF411: SBEND,L=1.3216350650,ANGLE=0.5090521288,K1:=kqf11d,THICK=TRUE,APERTYPE=CIRCLE,APERTURE=0.03;
s411: SBEND,L=0.0700000000,ANGLE=0.0269617915,THICK=TRUE,APERTYPE=CIRCLE,APERTURE=0.03;
sD411: SBEND,L=1.3216350650,ANGLE=0.5090521288,K1:=kqd11d,THICK=TRUE,APERTYPE=CIRCLE,APERTURE=0.03;
sF511: SBEND,L=1.3315178300,ANGLE=0.4965834065,K1:=kqf11e,THICK=TRUE,APERTYPE=CIRCLE,APERTURE=0.03;
s511: SBEND,L=0.0700000000,ANGLE=0.0261061757,THICK=TRUE,APERTYPE=CIRCLE,APERTURE=0.03;
sD511: SBEND,L=1.3315178300,ANGLE=0.4965834065,K1:=kqd11e,THICK=TRUE,APERTYPE=CIRCLE,APERTURE=0.03;
sF611: SBEND,L=1.3763548250,ANGLE=0.5255110283,K1:=kqf11f,THICK=TRUE,APERTYPE=CIRCLE,APERTURE=0.03;
s611: SBEND,L=0.0700000000,ANGLE=0.0267269539,THICK=TRUE,APERTYPE=CIRCLE,APERTURE=0.03;
sD611: SBEND,L=1.3763548250,ANGLE=0.5255110283,K1:=kqd11f,THICK=TRUE,APERTYPE=CIRCLE,APERTURE=0.03;
d111: DRIFT, L=0.5514622550;
d2a11: DRIFT, L=0.4440523000;
c111: RFCAVITY,L=0.2489264000,VOLT=2.81169031,LAG=0.208330,HARMON=1,FREQ=117;
d2c11: DRIFT, L=0.4154712000;
d3a11: DRIFT, L=0.4313289000;
c211: RFCAVITY,L=0.2509539800,VOLT=2.82294000,LAG=0.208330,HARMON=1,FREQ=117;
d3c11: DRIFT, L=0.4312513900;
d411: DRIFT, L=0.5567740950;
d5a11: DRIFT, L=0.4339888400;
c311: RFCAVITY,L=0.2491410500,VOLT=2.81292304,LAG=0.208330,HARMON=1,FREQ=117;
d5c11: DRIFT, L=0.4309799700;
d6a11: DRIFT, L=0.4582872800;
c411: RFCAVITY,L=0.2529673700,VOLT=2.83322480,LAG=0.208330,HARMON=1,FREQ=117;
```

```
d6c11: DRIFT, L=0.4120273900;
d611: DRIFT, L=0.5655026850;
sF112: SBEND,L=1.3875684200,ANGLE=0.5008107139,K1:=kqf12a,THICK=TRUE,APERTYPE=CIRCLE,APERTURE=0.03;
s112: SBEND,L=0.0700000000,ANGLE=0.0252648803,THICK=TRUE,APERTYPE=CIRCLE,APERTURE=0.03;
sD112: SBEND,L=1.3875684200,ANGLE=0.5008107139,K1:=kqd12a,THICK=TRUE,APERTYPE=CIRCLE,APERTURE=0.03;
sF212: SBEND,L=1.4178868850,ANGLE=0.5208703539,K1:=kqf12b,THICK=TRUE,APERTYPE=CIRCLE,APERTURE=0.03;
s212: SBEND,L=0.0700000000,ANGLE=0.0257149743,THICK=TRUE,APERTYPE=CIRCLE,APERTURE=0.03;
sD212: SBEND,L=1.4178868850,ANGLE=0.5208703539,K1:=kqd12b,THICK=TRUE,APERTYPE=CIRCLE,APERTURE=0.03;
sF312: SBEND,L=1.4231883500,ANGLE=0.5077145485,K1:=kqf12c,THICK=TRUE,APERTYPE=CIRCLE,APERTURE=0.03;
s312: SBEND,L=0.0700000000,ANGLE=0.0250654821,THICK=TRUE,APERTYPE=CIRCLE,APERTURE=0.03;
sD312: SBEND,L=1.4231883500,ANGLE=0.5096128881,K1:=kqd12c,THICK=TRUE,APERTYPE=CIRCLE,APERTURE=0.03;
sF412: SBEND,L=1.4281646650,ANGLE=0.5114779447,K1:=kqf12d,THICK=TRUE,APERTYPE=CIRCLE,APERTURE=0.03;
s412: SBEND,L=0.0700000000,ANGLE=0.0250695575,THICK=TRUE,APERTYPE=CIRCLE,APERTURE=0.03;
sD412: SBEND,L=1.4281646650,ANGLE=0.5114779447,K1:=kqd12d,THICK=TRUE,APERTYPE=CIRCLE,APERTURE=0.03;
sF512: SBEND,L=1.4394490650,ANGLE=0.4975200246,K1:=kqf12e,THICK=TRUE,APERTYPE=CIRCLE,APERTURE=0.03;
s512: SBEND,L=0.0700000000,ANGLE=0.0241942578,THICK=TRUE,APERTYPE=CIRCLE,APERTURE=0.03;
sD512: SBEND,L=1.4394490650,ANGLE=0.4975200246,K1:=kqd12e,THICK=TRUE,APERTYPE=CIRCLE,APERTURE=0.03;
sF612: SBEND,L=1.4870503750,ANGLE=0.5263835265,K1:=kqf12f,THICK=TRUE,APERTYPE=CIRCLE,APERTURE=0.03;
s612: SBEND,L=0.0700000000,ANGLE=0.0247784792,THICK=TRUE,APERTYPE=CIRCLE,APERTURE=0.03;
sD612: SBEND,L=1.4870503750,ANGLE=0.5263835265,K1:=kqd12f,THICK=TRUE,APERTYPE=CIRCLE,APERTURE=0.03;
d112: DRIFT, L=0.5655026850;
d2a12: DRIFT, L=0.4544271000;
c112: RFCAVITY,L=0.2652496000,VOLT=2.87568195,LAG=0.208330,HARMON=1,FREQ=117;
d2c12: DRIFT, L=0.4171144600;
d3a12: DRIFT, L=0.4374135500;
c212: RFCAVITY,L=0.2674673800,VOLT=2.87941882,LAG=0.208330,HARMON=1,FREQ=117;
d3c12: DRIFT, L=0.4373129500;
d412: DRIFT, L=0.5715187750;
d5a12: DRIFT, L=0.4409100200;
c312: RFCAVITY,L=0.2666260200,VOLT=2.87814907,LAG=0.208330,HARMON=1,FREQ=117;
d5c12: DRIFT, L=0.4369197700;
d6a12: DRIFT, L=0.4720093900;
c412: RFCAVITY,L=0.2707662700,VOLT=2.88262248,LAG=0.208330,HARMON=1,FREQ=117;
d6c12: DRIFT, L=0.4114260100;
d612: DRIFT, L=0.5812507700;
sF113: SBEND,L=1.4994623800,ANGLE=0.5018313001,K1:=kqf13a,THICK=TRUE,APERTYPE=CIRCLE,APERTURE=0.03;
s113: SBEND,L=0.0700000000,ANGLE=0.0234271906,THICK=TRUE,APERTYPE=CIRCLE,APERTURE=0.03;
sD113: SBEND,L=1.4994623800,ANGLE=0.5018313001,K1:=kqd13a,THICK=TRUE,APERTYPE=CIRCLE,APERTURE=0.03;
sF213: SBEND,L=1.5316683800,ANGLE=0.5218041491,K1:=kqf13b,THICK=TRUE,APERTYPE=CIRCLE,APERTURE=0.03;
```

```
s213: SBEND,L=0.0700000000,ANGLE=0.0238473882,THICK=TRUE,APERTYPE=CIRCLE,APERTURE=0.03;
sD213: SBEND,L=1.5316683800,ANGLE=0.5218041491,K1:=kqd13b,THICK=TRUE,APERTYPE=CIRCLE,APERTURE=0.03;
sF313: SBEND,L=1.5366475350,ANGLE=0.5103054850,K1:=kqf13c,THICK=TRUE,APERTYPE=CIRCLE,APERTURE=0.03;
s313: SBEND,L=0.0700000000,ANGLE=0.0233218786,THICK=TRUE,APERTYPE=CIRCLE,APERTURE=0.03;
sD313: SBEND,L=1.5366475350,ANGLE=0.5119643886,K1:=kqd13c,THICK=TRUE,APERTYPE=CIRCLE,APERTURE=0.03;
sF413: SBEND,L=1.5371902250,ANGLE=0.5109004267,K1:=kqf13d,THICK=TRUE,APERTYPE=CIRCLE,APERTURE=0.03;
s413: SBEND,L=0.0700000000,ANGLE=0.0232651947,THICK=TRUE,APERTYPE=CIRCLE,APERTURE=0.03;
sD413: SBEND,L=1.5371902250,ANGLE=0.5109004267,K1:=kqd13d,THICK=TRUE,APERTYPE=CIRCLE,APERTURE=0.03;
sF513: SBEND,L=1.5485278450,ANGLE=0.4983368159,K1:=kqf13e,THICK=TRUE,APERTYPE=CIRCLE,APERTURE=0.03;
s513: SBEND,L=0.0700000000,ANGLE=0.0225269292,THICK=TRUE,APERTYPE=CIRCLE,APERTURE=0.03;
sD513: SBEND,L=1.5485278450,ANGLE=0.4983368159,K1:=kqd13e,THICK=TRUE,APERTYPE=CIRCLE,APERTURE=0.03;
sF613: SBEND,L=1.5988204150,ANGLE=0.5273306376,K1:=kqf13f,THICK=TRUE,APERTYPE=CIRCLE,APERTURE=0.03;
s613: SBEND,L=0.0700000000,ANGLE=0.0230877366,THICK=TRUE,APERTYPE=CIRCLE,APERTURE=0.03;
sD613: SBEND,L=1.5988204150,ANGLE=0.5273306376,K1:=kqd13f,THICK=TRUE,APERTYPE=CIRCLE,APERTURE=0.03;
d113: DRIFT, L=0.5812507700;
d2a13: DRIFT, L=0.4661126200;
c113: RFCAVITY,L=0.2836350200,VOLT=2.86665146,LAG=0.208330,HARMON=1,FREQ=117;
d2c13: DRIFT, L=0.4189653200;
d3a13: DRIFT, L=0.4442669300;
c213: RFCAVITY,L=0.2860670300,VOLT=2.85826162,LAG=0.208330,HARMON=1,FREQ=117;
d3c13: DRIFT, L=0.4441403100;
d413: DRIFT, L=0.5872450000;
d5a13: DRIFT, L=0.4479048000;
c313: RFCAVITY,L=0.2842969000,VOLT=2.86454367,LAG=0.208330,HARMON=1,FREQ=117;
d5c13: DRIFT, L=0.4429227200;
d6a13: DRIFT, L=0.4858774000;
c413: RFCAVITY,L=0.2887544200,VOLT=2.84690477,LAG=0.208330,HARMON=1,FREQ=117;
d6c13: DRIFT, L=0.4108182400;
d613: DRIFT, L=0.5971070300;
sF114: SBEND,L=1.6118015600,ANGLE=0.5025307832,K1:=kqf14a,THICK=TRUE,APERTYPE=CIRCLE,APERTURE=0.03;
s114: SBEND,L=0.0700000000,ANGLE=0.0218247430,THICK=TRUE,APERTYPE=CIRCLE,APERTURE=0.03;
sD114: SBEND,L=1.6118015600,ANGLE=0.5025307832,K1:=kqd14a,THICK=TRUE,APERTYPE=CIRCLE,APERTURE=0.03;
sF214: SBEND,L=1.6458052350,ANGLE=0.5226138382,K1:=kqf14b,THICK=TRUE,APERTYPE=CIRCLE,APERTURE=0.03;
s214: SBEND,L=0.0700000000,ANGLE=0.0222280060,THICK=TRUE,APERTYPE=CIRCLE,APERTURE=0.03;
sD214: SBEND,L=1.6458052350,ANGLE=0.5226138382,K1:=kqd14b,THICK=TRUE,APERTYPE=CIRCLE,APERTURE=0.03;
sF314: SBEND,L=1.6511458300,ANGLE=0.5110977292,K1:=kqf14c,THICK=TRUE,APERTYPE=CIRCLE,APERTURE=0.03;
s314: SBEND,L=0.0700000000,ANGLE=0.0217381986,THICK=TRUE,APERTYPE=CIRCLE,APERTURE=0.03;
sD314: SBEND,L=1.6511458300,ANGLE=0.5127562280,K1:=kqd14c,THICK=TRUE,APERTYPE=CIRCLE,APERTURE=0.03;
sF414: SBEND,L=1.6517280550,ANGLE=0.5116903411,K1:=kqf14d,THICK=TRUE,APERTYPE=CIRCLE,APERTURE=0.03;
```

```
s414: SBEND,L=0.0700000000,ANGLE=0.0216853639,THICK=TRUE,APERTYPE=CIRCLE,APERTURE=0.03;
sD414: SBEND,L=1.6517280550,ANGLE=0.5116903411,K1:=kqd14d,THICK=TRUE,APERTYPE=CIRCLE,APERTURE=0.03;
sF514: SBEND,L=1.6638387350,ANGLE=0.4990861803,K1:=kqf14e,THICK=TRUE,APERTYPE=CIRCLE,APERTURE=0.03;
s514: SBEND,L=0.0700000000,ANGLE=0.0209972468,THICK=TRUE,APERTYPE=CIRCLE,APERTURE=0.03;
sD514: SBEND,L=1.6638387350,ANGLE=0.4990861803,K1:=kqd14e,THICK=TRUE,APERTYPE=CIRCLE,APERTURE=0.03;
sF614: SBEND,L=1.7170301850,ANGLE=0.5281095045,K1:=kqf14f,THICK=TRUE,APERTYPE=CIRCLE,APERTURE=0.03;
s614: SBEND,L=0.0700000000,ANGLE=0.0215300032,THICK=TRUE,APERTYPE=CIRCLE,APERTURE=0.03;
sD614: SBEND,L=1.7170301850,ANGLE=0.5281095045,K1:=kqd14f,THICK=TRUE,APERTYPE=CIRCLE,APERTURE=0.03;
d114: DRIFT, L=0.5971070300;
d2a14: DRIFT, L=0.4778346400;
c114: RFCAVITY,L=0.3020778600,VOLT=2.75666440,LAG=0.208330,HARMON=1,FREQ=117;
d2c14: DRIFT, L=0.4208219700;
d3a14: DRIFT, L=0.4511417000;
c214: RFCAVITY,L=0.3047247700,VOLT=2.73169298,LAG=0.208330,HARMON=1,FREQ=117;
d3c14: DRIFT, L=0.4509890000;
d414: DRIFT, L=0.6034360800;
d5a14: DRIFT, L=0.4552992200;
c314: RFCAVITY,L=0.3029773800,VOLT=2.74844912,LAG=0.208330,HARMON=1,FREQ=117;
d5c14: DRIFT, L=0.4492686400;
d6a14: DRIFT, L=0.5005377300;
c414: RFCAVITY,L=0.3077702900,VOLT=2.69993888,LAG=0.208330,HARMON=1,FREQ=117;
d6c14: DRIFT, L=0.4101757400;
d614: DRIFT, L=0.5971070300;
Beam,particle=proton,sequence=tamusq11,energy=0.94477;
tamusq11: sequence, refer=entry,l = 1.3994842900;
startcell11: marker, at = 0;
d11, at = 0.0000000000;
sF11, at = 0.4019962300;
s11, at = 0.6298970200;
sD11, at = 0.6998970200;
d2a1, at = 0.9277978100;
c11, at = 1.3246667500;
endcell11: marker, at = 1.3994842900;
endsequence;
Beam,particle=proton,sequence=tamusq21,energy=0.94539;
tamusq21: sequence, refer=entry,l = 1.3246035900;
startcell21: marker, at = 0;
d2c1, at = 0.0000000000;
sF21, at = 0.3344657900;
```

```
s21, at = 0.5738295700;
sD21, at = 0.6438295700;
d3a1, at = 0.8831933500;
c21, at = 1.2497872000;
endcell21: marker, at = 1.3246035900;
endsequence;
Beam,particle=proton,sequence=tamusq31,energy=0.94602;
tamusq31: sequence, refer=entry,l = 1.3215204650;
startcell31: marker, at = 0;
d3c1, at = 0.0000000000;
sF31, at = 0.3664306900;
s31, at = 0.6068981150;
sD31, at = 0.6768981150;
d41, at = 0.9173655400;
endcell31: marker, at = 1.3215204650;
endsequence;
Beam,particle=proton,sequence=tamusq41,energy=0.94602;
tamusq41: sequence, refer=entry,l = 1.4053021750;
startcell41: marker, at = 0;
d41, at = 0.0000000000;
sF41, at = 0.4041549250;
s41, at = 0.6475033350;
sD41, at = 0.7175033350;
d5a1, at = 0.9608517450;
c31, at = 1.3319884750;
endcell41: marker, at = 1.4053021750;
endsequence;
Beam,particle=proton,sequence=tamusq51,energy=0.94665;
tamusq51: sequence, refer=entry,l = 1.4172734300;
startcell51: marker, at = 0;
d5c1, at = 0.0000000000;
sF51, at = 0.3645031300;
s51, at = 0.6106738950;
sD51, at = 0.6806738950;
d6a1, at = 0.9268446600;
c41, at = 1.3432902300;
endcell51: marker, at = 1.4172734300;
endsequence;
Beam,particle=proton,sequence=tamusq61,energy=0.94728;
```

```
tamusq61: sequence, refer=entry,l = 1.3273786900;
startcell61: marker, at = 0;
d6c1, at = 0.0000000000;
sF61, at = 0.3219282100;
s61, at = 0.5858411000;
sD61, at = 0.6558411000;
d61, at = 0.9197539900;
endcell61: marker, at = 1.3273786900;
endsequence;
Beam,particle=proton,sequence=tamusq12,energy=0.94728;
tamusq12: sequence, refer=entry,l = 1.4937004200;
startcell12: marker, at = 0;
d12, at = 0.0000000000;
sF12, at = 0.4076247000;
s12, at = 0.6761564600;
sD12, at = 0.7461564600;
d2a2, at = 1.0146882200;
c12, at = 1.4122131600;
endcell12: marker, at = 1.4937004200;
endsequence;
Beam,particle=proton,sequence=tamusq22,energy=0.94794;
tamusq22: sequence, refer=entry,l = 1.4206358400;
startcell22: marker, at = 0;
d2c2, at = 0.0000000000;
sF22, at = 0.3387204100;
s22, at = 0.6193609200;
sD22, at = 0.6893609200;
d3a2, at = 0.9700014300;
c22, at = 1.3390720200;
endcell22: marker, at = 1.4206358400;
endsequence;
Beam,particle=proton,sequence=tamusq32,energy=0.94858;
tamusq32: sequence, refer=entry,l = 1.4375028950;
startcell32: marker, at = 0;
d3c2, at = 0.0000000000;
sF32, at = 0.3689169400;
s32, at = 0.6582618150;
sD32, at = 0.7282618150;
d42, at = 1.0176066900;
```

```
endcell32: marker, at = 1.4375028950;
endsequence;
Beam,particle=proton,sequence=tamusq42,energy=0.94858;
tamusq42: sequence, refer=entry,l = 1.7085525550;
startcell42: marker, at = 0;
d42, at = 0.0000000000;
sF42, at = 0.4198962050;
s42, at = 0.7921709150;
sD42, at = 0.8621709150;
d5a2, at = 1.2344456250;
c32, at = 1.6130983150;
endcell42: marker, at = 1.7085525550;
endsequence;
Beam,particle=proton,sequence=tamusq52,energy=0.94930;
tamusq52: sequence, refer=entry,l = 1.7210790400;
startcell52: marker, at = 0;
d5c2, at = 0.0000000000;
sF52, at = 0.3732725400;
s52, at = 0.7561123950;
sD52, at = 0.8261123950;
d6a2, at = 1.2089522500;
c42, at = 1.6245578000;
endcell52: marker, at = 1.7210790400;
endsequence;
Beam,particle=proton,sequence=tamusq62,energy=0.95006;
tamusq62: sequence, refer=entry,l = 1.6444455000;
startcell62: marker, at = 0;
d6c2, at = 0.0000000000;
sF62, at = 0.3393825000;
s62, at = 0.7432335550;
sD62, at = 0.8132335550;
d62, at = 1.2170846100;
endcell62: marker, at = 1.6444455000;
endsequence;
Beam,particle=proton,sequence=tamusq13,energy=0.95006;
tamusq13: sequence, refer=entry,l = 1.8165573900;
startcell13: marker, at = 0;
d13, at = 0.0000000000;
sF13, at = 0.4273608900;
```

```
s13, at = 0.8349266150;
sD13, at = 0.9049266150;
d2a3, at = 1.3124923400;
c13, at = 1.7122607100;
endcell13: marker, at = 1.8165573900;
endsequence;
Beam,particle=proton,sequence=tamusq23,energy=0.95089;
tamusq23: sequence, refer=entry,l = 1.7490516700;
startcell23: marker, at = 0;
d2c3, at = 0.0000000000;
sF23, at = 0.3532705600;
s23, at = 0.7750712800;
sD23, at = 0.8450712800;
d3a3, at = 1.2668720000;
c23, at = 1.6444126500;
endcell23: marker, at = 1.7490516700;
endsequence;
Beam,particle=proton,sequence=tamusq33,energy=0.95174;
tamusq33: sequence, refer=entry,l = 1.7263425200;
startcell33: marker, at = 0;
d3c3, at = 0.0000000000;
sF33, at = 0.3774195400;
s33, at = 0.8015911200;
sD33, at = 0.8715911200;
d43, at = 1.2957627000;
endcell33: marker, at = 1.7263425200;
endsequence;
Beam,particle=proton,sequence=tamusq43,energy=0.95174;
tamusq43: sequence, refer=entry,l = 1.8528444300;
startcell43: marker, at = 0;
d43, at = 0.0000000000;
sF43, at = 0.4305798200;
s43, at = 0.8636856350;
sD43, at = 0.9336856350;
d5a3, at = 1.3667914500;
c33, at = 1.7484716700;
endcell43: marker, at = 1.8528444300;
endsequence;
Beam,particle=proton,sequence=tamusq53,energy=0.95259;
```

```
tamusq53: sequence, refer=entry,l = 1.8434562600;
startcell53: marker, at = 0;
d5c3, at = 0.0000000000;
sF53, at = 0.3768049800;
s53, at = 0.8146970900;
sD53, at = 0.8846970900;
d6a3, at = 1.3225892000;
c43, at = 1.7378563700;
endcell53: marker, at = 1.8434562600;
endsequence;
Beam,particle=proton,sequence=tamusq63,energy=0.95345;
tamusq63: sequence, refer=entry,l = 1.7722996350;
startcell63: marker, at = 0;
d6c3, at = 0.0000000000;
sF63, at = 0.3464133300;
s63, at = 0.8066769250;
sD63, at = 0.8766769250;
d63, at = 1.3369405200;
endcell63: marker, at = 1.7722996350;
endsequence;
Beam,particle=proton,sequence=tamusq14,energy=0.95345;
tamusq14: sequence, refer=entry,l = 1.9480336250;
startcell14: marker, at = 0;
d14, at = 0.0000000000;
sF14, at = 0.4353591150;
s14, at = 0.8995577100;
sD14, at = 0.9695577100;
d2a4, at = 1.4337563050;
c14, at = 1.8344391650;
endcell14: marker, at = 1.9480336250;
endsequence;
Beam,particle=proton,sequence=tamusq24,energy=0.95438;
tamusq24: sequence, refer=entry,l = 1.8829235000;
startcell24: marker, at = 0;
d2c4, at = 0.0000000000;
sF24, at = 0.3592016200;
s24, at = 0.8385433450;
sD24, at = 0.9085433450;
d3a4, at = 1.3878850700;
```

```
c24, at = 1.7688783600;
endcell24: marker, at = 1.8829235000;
endsequence;
Beam,particle=proton,sequence=tamusq34,energy=0.95530;
tamusq34: sequence, refer=entry,l = 1.8741500250;
startcell34: marker, at = 0;
d3c4, at = 0.0000000000;
sF34, at = 0.3808854500;
s34, at = 0.8698140850;
sD34, at = 0.9398140850;
d44, at = 1.4287427200;
endcell34: marker, at = 1.8741500250;
endsequence;
Beam,particle=proton,sequence=tamusq44,energy=0.95530;
tamusq44: sequence, refer=entry,l = 2.1457818250;
startcell44: marker, at = 0;
d44, at = 0.0000000000;
sF44, at = 0.4454073050;
s44, at = 1.0032464550;
sD44, at = 1.0732464550;
d5a4, at = 1.6310856050;
c34, at = 2.0200249950;
endcell44: marker, at = 2.1457818250;
endsequence;
Beam,particle=proton,sequence=tamusq54,energy=0.95634;
tamusq54: sequence, refer=entry,l = 2.1368819900;
startcell54: marker, at = 0;
d5c4, at = 0.0000000000;
sF54, at = 0.3852747600;
s54, at = 0.9551665000;
sD54, at = 1.0251665000;
d6a4, at = 1.5950582400;
c44, at = 2.0095140900;
endcell54: marker, at = 2.1368819900;
endsequence;
Beam,particle=proton,sequence=tamusq64,energy=0.95741;
tamusq64: sequence, refer=entry,l = 2.0790175300;
startcell64: marker, at = 0;
d6c4, at = 0.0000000000;
```

```
sF64, at = 0.3632712700;
s64, at = 0.9588529300;
sD64, at = 1.0288529300;
d64, at = 1.6244345900;
endcell64: marker, at = 2.0790175300;
endsequence;
Beam,particle=proton,sequence=tamusq15,energy=0.95741;
tamusq15: sequence, refer=entry,l = 2.2646485200;
startcell15: marker, at = 0;
d15, at = 0.0000000000;
sF15, at = 0.4545829400;
s15, at = 1.0551747450;
sD15, at = 1.1251747450;
d2a5, at = 1.7257665500;
c15, at = 2.1286527100;
endcell15: marker, at = 2.2646485200;
endsequence;
Beam,particle=proton,sequence=tamusq25,energy=0.95860;
tamusq25: sequence, refer=entry,l = 2.2054638400;
startcell25: marker, at = 0;
d2c5, at = 0.0000000000;
sF25, at = 0.3734914600;
s25, at = 0.9914679800;
sD25, at = 1.0614679800;
d3a5, at = 1.6794445000;
c25, at = 2.0687563200;
endcell25: marker, at = 2.2054638400;
endsequence;
Beam,particle=proton,sequence=tamusq35,energy=0.95980;
tamusq35: sequence, refer=entry,l = 2.1621375650;
startcell35: marker, at = 0;
d3c5, at = 0.0000000000;
sF35, at = 0.3892359500;
s35, at = 1.0111644200;
sD35, at = 1.0811644200;
d45, at = 1.7030928900;
endcell35: marker, at = 2.1621375650;
endsequence;
Beam,particle=proton,sequence=tamusq45,energy=0.95980;
```

```
tamusq45: sequence, refer=entry,l = 2.3350813150;
startcell45: marker, at = 0;
d45, at = 0.0000000000;
sF45, at = 0.4590446750;
s45, at = 1.0966024750;
sD45, at = 1.1666024750;
d5a5, at = 1.8041602750;
c35, at = 2.1972115750;
endcell45: marker, at = 2.3350813150;
endsequence;
Beam,particle=proton,sequence=tamusq55,energy=0.96101;
tamusq55: sequence, refer=entry,l = 2.3030915100;
startcell55: marker, at = 0;
d5c5, at = 0.0000000000;
sF55, at = 0.3900724300;
s55, at = 1.0347346900;
sD55, at = 1.1047346900;
d6a5, at = 1.7493969500;
c45, at = 2.1633932300;
endcell55: marker, at = 2.3030915100;
endsequence;
Beam,particle=proton,sequence=tamusq65,energy=0.96226;
tamusq65: sequence, refer=entry,l = 2.2527563400;
startcell65: marker, at = 0;
d6c5, at = 0.0000000000;
sF65, at = 0.3728203700;
s65, at = 1.0450522650;
sD65, at = 1.1150522650;
d65, at = 1.7872841600;
endcell65: marker, at = 2.2527563400;
endsequence;
Beam,particle=proton,sequence=tamusq16,energy=0.96226;
tamusq16: sequence, refer=entry,l = 2.4439934900;
startcell16: marker, at = 0;
d16, at = 0.0000000000;
sF16, at = 0.4654721800;
s16, at = 1.1433232550;
sD16, at = 1.2133232550;
d2a6, at = 1.8911743300;
```

```
c16, at = 2.2953085400;
endcell16: marker, at = 2.4439934900;
endsequence;
Beam,particle=proton,sequence=tamusq26,energy=0.96360;
tamusq26: sequence, refer=entry,l = 2.3881652500;
startcell26: marker, at = 0;
d2c6, at = 0.0000000000;
sF26, at = 0.3815858800;
s26, at = 1.0780914100;
sD26, at = 1.1480914100;
d3a6, at = 1.8445969400;
c26, at = 2.2386207400;
endcell26: marker, at = 2.3881652500;
endsequence;
Beam,particle=proton,sequence=tamusq36,energy=0.96495;
tamusq36: sequence, refer=entry,l = 2.3519849300;
startcell36: marker, at = 0;
d3c6, at = 0.0000000000;
sF36, at = 0.3939660400;
s36, at = 1.1005654750;
sD36, at = 1.1705654750;
d46, at = 1.8771649100;
endcell36: marker, at = 2.3519849300;
endsequence;
Beam,particle=proton,sequence=tamusq46,energy=0.96495;
tamusq46: sequence, refer=entry,l = 2.6373331900;
startcell46: marker, at = 0;
d46, at = 0.0000000000;
sF46, at = 0.4748200200;
s46, at = 1.2409805100;
sD46, at = 1.3109805100;
d5a6, at = 2.0771410000;
c36, at = 2.4776106000;
endcell46: marker, at = 2.6373331900;
endsequence;
Beam,particle=proton,sequence=tamusq56,energy=0.96642;
tamusq56: sequence, refer=entry,l = 2.6029497100;
startcell56: marker, at = 0;
d5c6, at = 0.0000000000;
```

```
sF56, at = 0.3987278900;
s56, at = 1.1782834700;
sD56, at = 1.2482834700;
d6a6, at = 2.0278390500;
c46, at = 2.4410062200;
endcell56: marker, at = 2.6029497100;
endsequence;
Beam,particle=proton,sequence=tamusq66,energy=0.96792;
tamusq66: sequence, refer=entry,l = 2.5661980750;
startcell66: marker, at = 0;
d6c6, at = 0.0000000000;
sF66, at = 0.3900478700;
s66, at = 1.2005642600;
sD66, at = 1.2705642600;
d66, at = 2.0810806500;
endcell66: marker, at = 2.5661980750;
endsequence;
Beam,particle=proton,sequence=tamusq17,energy=0.96792;
tamusq17: sequence, refer=entry,l = 2.7675491050;
startcell17: marker, at = 0;
d17, at = 0.0000000000;
sF17, at = 0.4851174250;
s17, at = 1.3023516750;
sD17, at = 1.3723516750;
d2a7, at = 2.1895859250;
c17, at = 2.5959717350;
endcell17: marker, at = 2.7675491050;
endsequence;
Beam,particle=proton,sequence=tamusq27,energy=0.96956;
tamusq27: sequence, refer=entry,l = 2.7177761900;
startcell27: marker, at = 0;
d2c7, at = 0.0000000000;
sF27, at = 0.3961889700;
s27, at = 1.2343683950;
sD27, at = 1.3043683950;
d3a7, at = 2.1425478200;
c27, at = 2.5450725100;
endcell27: marker, at = 2.7177761900;
endsequence;
```

```
Beam,particle=proton,sequence=tamusq37,energy=0.97122;
tamusq37: sequence, refer=entry,l = 2.6500190000;
startcell37: marker, at = 0;
d3c7, at = 0.0000000000;
sF37, at = 0.4024995900;
s37, at = 1.2459601550;
sD37, at = 1.3159601550;
d47, at = 2.1594207200;
endcell37: marker, at = 2.6500190000;
endsequence;
Beam,particle=proton,sequence=tamusq47,energy=0.97122;
tamusq47: sequence, refer=entry,l = 2.8654548600;
startcell47: marker, at = 0;
d47, at = 0.0000000000;
sF47, at = 0.4905982800;
s47, at = 1.3529454300;
sD47, at = 1.4229454300;
d5a7, at = 2.2852925800;
c37, at = 2.6908232800;
endcell47: marker, at = 2.8654548600;
endsequence;
Beam,particle=proton,sequence=tamusq57,energy=0.97291;
tamusq57: sequence, refer=entry,l = 2.8075262300;
startcell57: marker, at = 0;
d5c7, at = 0.0000000000;
sF57, at = 0.4046330300;
s57, at = 1.2762188000;
sD57, at = 1.3462188000;
d6a7, at = 2.2178045700;
c47, at = 2.6304060800;
endcell57: marker, at = 2.8075262300;
endsequence;
Beam,particle=proton,sequence=tamusq67,energy=0.97463;
tamusq67: sequence, refer=entry,l = 2.7800419150;
startcell67: marker, at = 0;
d6c7, at = 0.0000000000;
sF67, at = 0.4018012300;
s67, at = 1.3066614300;
sD67, at = 1.3766614300;
```

```
d67, at = 2.2815216300;
endcell67: marker, at = 2.7800419150;
endsequence;
Beam,particle=proton,sequence=tamusq18,energy=0.97463;
tamusq18: sequence, refer=entry,l = 2.9882932250;
startcell18: marker, at = 0;
d18, at = 0.0000000000;
sF18, at = 0.4985202850;
s18, at = 1.4108479750;
sD18, at = 1.4808479750;
d2a8, at = 2.3931756650;
c18, at = 2.8010976150;
endcell18: marker, at = 2.9882932250;
endsequence;
Beam,particle=proton,sequence=tamusq28,energy=0.97647;
tamusq28: sequence, refer=entry,l = 2.9426515400;
startcell28: marker, at = 0;
d2c8, at = 0.0000000000;
sF28, at = 0.4061518600;
s28, at = 1.3409875650;
sD28, at = 1.4109875650;
d3a8, at = 2.3458232700;
c28, at = 2.7541476400;
endcell28: marker, at = 2.9426515400;
endsequence;
Beam,particle=proton,sequence=tamusq38,energy=0.97832;
tamusq38: sequence, refer=entry,l = 2.8748325550;
startcell38: marker, at = 0;
d3c8, at = 0.0000000000;
sF38, at = 0.4083215600;
s38, at = 1.3529595300;
sD38, at = 1.4229595300;
d48, at = 2.3675975000;
endcell38: marker, at = 2.8748325550;
endsequence;
Beam,particle=proton,sequence=tamusq48,energy=0.97832;
tamusq48: sequence, refer=entry,l = 3.1716955150;
startcell48: marker, at = 0;
d48, at = 0.0000000000;
```

```
sF48, at = 0.5072350550;
s48, at = 1.4996503500;
sD48, at = 1.5696503500;
d5a8, at = 2.5620656450;
c38, at = 2.9752110750;
endcell48: marker, at = 3.1716955150;
endsequence;
Beam,particle=proton,sequence=tamusq58,energy=0.98026;
tamusq58: sequence, refer=entry,l = 3.1123782900;
startcell58: marker, at = 0;
d5c8, at = 0.0000000000;
sF58, at = 0.4130920600;
s58, at = 1.4195711600;
sD58, at = 1.4895711600;
d6a8, at = 2.4960502600;
c48, at = 2.9130129300;
endcell58: marker, at = 3.1123782900;
endsequence;
Beam,particle=proton,sequence=tamusq68,energy=0.98223;
tamusq68: sequence, refer=entry,l = 3.0882934100;
startcell68: marker, at = 0;
d6c8, at = 0.0000000000;
sF68, at = 0.4138384700;
s68, at = 1.4569831750;
sD68, at = 1.5269831750;
d68, at = 2.5701278800;
endcell68: marker, at = 3.0882934100;
endsequence;
Beam,particle=proton,sequence=tamusq19,energy=0.98223;
tamusq19: sequence, refer=entry,l = 3.3210424500;
startcell19: marker, at = 0;
d19, at = 0.0000000000;
sF19, at = 0.5181655300;
s19, at = 1.5698763900;
sD19, at = 1.6398763900;
d2a9, at = 2.6915872500;
c19, at = 3.1109544200;
endcell19: marker, at = 3.3210424500;
endsequence;
```

```
Beam,particle=proton,sequence=tamusq29,energy=0.98433;
tamusq29: sequence, refer=entry,l = 3.2630950500;
startcell29: marker, at = 0;
d2c9, at = 0.0000000000;
sF29, at = 0.4115613300;
s29, at = 1.4880709250;
sD29, at = 1.5580709250;
d3a9, at = 2.6345805200;
c29, at = 3.0514319800;
endcell29: marker, at = 3.2630950500;
endsequence;
Beam,particle=proton,sequence=tamusq39,energy=0.98646;
tamusq39: sequence, refer=entry,l = 3.1747065800;
startcell39: marker, at = 0;
d3c9, at = 0.0000000000;
sF39, at = 0.4168288900;
s39, at = 1.4988058400;
sD39, at = 1.5688058400;
d49, at = 2.6507827900;
endcell39: marker, at = 3.1747065800;
endsequence;
Beam,particle=proton,sequence=tamusq49,energy=0.98646;
tamusq49: sequence, refer=entry,l = 3.4176542100;
startcell49: marker, at = 0;
d49, at = 0.0000000000;
sF49, at = 0.5239237900;
s49, at = 1.6197150450;
sD49, at = 1.6897150450;
d5a9, at = 2.7855063000;
c39, at = 3.2050374800;
endcell49: marker, at = 3.4176542100;
endsequence;
Beam,particle=proton,sequence=tamusq59,energy=0.98860;
tamusq59: sequence, refer=entry,l = 3.3461038100;
startcell59: marker, at = 0;
d5c9, at = 0.0000000000;
sF59, at = 0.4185723400;
s59, at = 1.5246328300;
sD59, at = 1.5946328300;
```

```
d6a9, at = 2.7006933200;
c49, at = 3.1303165200;
endcell59: marker, at = 3.3461038100;
endsequence;
Beam,particle=proton,sequence=tamusq69,energy=0.99077;
tamusq69: sequence, refer=entry,l = 3.3064108050;
startcell69: marker, at = 0;
d6c9, at = 0.0000000000;
sF69, at = 0.4132836100;
s69, at = 1.5585131550;
sD69, at = 1.6285131550;
d69, at = 2.7737427000;
endcell69: marker, at = 3.3064108050;
endsequence;
Beam,particle=proton,sequence=tamusq110,energy=0.99077;
tamusq110: sequence, refer=entry,l = 3.5689778450;
startcell110: marker, at = 0;
d110, at = 0.0000000000;
sF110, at = 0.5326681050;
s110, at = 1.6872748950;
sD110, at = 1.7572748950;
d2a10, at = 2.9118816850;
c110, at = 3.3419900850;
endcell110: marker, at = 3.5689778450;
endsequence;
Beam,particle=proton,sequence=tamusq210,energy=0.99304;
tamusq210: sequence, refer=entry,l = 3.4973665500;
startcell210: marker, at = 0;
d2c10, at = 0.0000000000;
sF210, at = 0.4132626300;
s210, at = 1.5943592250;
sD210, at = 1.6643592250;
d3a10, at = 2.8454558200;
c210, at = 3.2686068400;
endcell210: marker, at = 3.4973665500;
endsequence;
Beam,particle=proton,sequence=tamusq310,energy=0.99532;
tamusq310: sequence, refer=entry,l = 3.4127821350;
startcell310: marker, at = 0;
```

```
d3c10, at = 0.0000000000;
sF310, at = 0.4231045500;
s310, at = 1.6127003650;
sD310, at = 1.6827003650;
d410, at = 2.8722961800;
endcell310: marker, at = 3.4127821350;
endsequence;
Beam,particle=proton,sequence=tamusq410,energy=0.99532;
tamusq410: sequence, refer=entry,l = 3.7141073950;
startcell410: marker, at = 0;
d410, at = 0.0000000000;
sF410, at = 0.5404859550;
s410, at = 1.7616572900;
sD410, at = 1.8316572900;
d5a10, at = 3.0528286250;
c310, at = 3.4806208450;
endcell410: marker, at = 3.7141073950;
endsequence;
Beam,particle=proton,sequence=tamusq510,energy=0.99764;
tamusq510: sequence, refer=entry,l = 3.6484669700;
startcell510: marker, at = 0;
d5c10, at = 0.0000000000;
sF510, at = 0.4256620000;
s510, at = 1.6605477200;
sD510, at = 1.7305477200;
d6a10, at = 2.9654334400;
c410, at = 3.4114351600;
endcell510: marker, at = 3.6484669700;
endsequence;
Beam,particle=proton,sequence=tamusq610,energy=0.99999;
tamusq610: sequence, refer=entry,l = 3.5887248050;
startcell610: marker, at = 0;
d6c10, at = 0.0000000000;
sF610, at = 0.4125658100;
s610, at = 1.6899141800;
sD610, at = 1.7599141800;
d610, at = 3.0372625500;
endcell610: marker, at = 3.5887248050;
endsequence;
```

```
Beam,particle=proton,sequence=tamusq111,energy=0.99999;
tamusq111: sequence, refer=entry,l = 3.8907033450;
startcell111: marker, at = 0;
d111, at = 0.0000000000;
sF111, at = 0.5514622550;
s111, at = 1.8395934500;
sD111, at = 1.9095934500;
d2a11, at = 3.1977246450;
c111, at = 3.6417769450;
endcell111: marker, at = 3.8907033450;
endsequence;
Beam,particle=proton,sequence=tamusq211,energy=1.00241;
tamusq211: sequence, refer=entry,l = 3.8014897400;
startcell211: marker, at = 0;
d2c11, at = 0.0000000000;
sF211, at = 0.4154712000;
s211, at = 1.7323390300;
sD211, at = 1.8023390300;
d3a11, at = 3.1192068600;
c211, at = 3.5505357600;
endcell211: marker, at = 3.8014897400;
endsequence;
Beam,particle=proton,sequence=tamusq311,energy=1.00484;
tamusq311: sequence, refer=entry,l = 3.7003590450;
startcell311: marker, at = 0;
d3c11, at = 0.0000000000;
sF311, at = 0.4312513900;
s311, at = 1.7524181700;
sD311, at = 1.8224181700;
d411, at = 3.1435849500;
endcell311: marker, at = 3.7003590450;
endsequence;
Beam,particle=proton,sequence=tamusq411,energy=1.00484;
tamusq411: sequence, refer=entry,l = 3.9531741150;
startcell411: marker, at = 0;
d411, at = 0.0000000000;
sF411, at = 0.5567740950;
s411, at = 1.8784091600;
sD411, at = 1.9484091600;
```

```
d5a11, at = 3.2700442250;
c311, at = 3.7040330650;
endcell411: marker, at = 3.9531741150;
endsequence;
Beam,particle=proton,sequence=tamusq511,energy=1.00729;
tamusq511: sequence, refer=entry,l = 3.8752702800;
startcell511: marker, at = 0;
d5c11, at = 0.0000000000;
sF511, at = 0.4309799700;
s511, at = 1.7624978000;
sD511, at = 1.8324978000;
d6a11, at = 3.1640156300;
c411, at = 3.6223029100;
endcell511: marker, at = 3.8752702800;
endsequence;
Beam,particle=proton,sequence=tamusq611,energy=1.00975;
tamusq611: sequence, refer=entry,l = 3.8002397250;
startcell611: marker, at = 0;
d6c11, at = 0.0000000000;
sF611, at = 0.4120273900;
s611, at = 1.7883822150;
sD611, at = 1.8583822150;
d611, at = 3.2347370400;
endcell611: marker, at = 3.8002397250;
endsequence;
Beam,particle=proton,sequence=tamusq112,energy=1.00975;
tamusq112: sequence, refer=entry,l = 4.1303162250;
startcell112: marker, at = 0;
d112, at = 0.0000000000;
sF112, at = 0.5655026850;
s112, at = 1.9530711050;
sD112, at = 2.0230711050;
d2a12, at = 3.4106395250;
c112, at = 3.8650666250;
endcell112: marker, at = 4.1303162250;
endsequence;
Beam,particle=proton,sequence=tamusq212,energy=1.01223;
tamusq212: sequence, refer=entry,l = 4.0277691600;
startcell212: marker, at = 0;
```

```
d2c12, at = 0.0000000000;
sF212, at = 0.4171144600;
s212, at = 1.8350013450;
sD212, at = 1.9050013450;
d3a12, at = 3.3228882300;
c212, at = 3.7603017800;
endcell212: marker, at = 4.0277691600;
endsequence;
Beam,particle=proton,sequence=tamusq312,energy=1.01472;
tamusq312: sequence, refer=entry,l = 3.9252084250;
startcell312: marker, at = 0;
d3c12, at = 0.0000000000;
sF312, at = 0.4373129500;
s312, at = 1.8605013000;
sD312, at = 1.9305013000;
d412, at = 3.3536896500;
endcell312: marker, at = 3.9252084250;
endsequence;
Beam,particle=proton,sequence=tamusq412,energy=1.01472;
tamusq412: sequence, refer=entry,l = 4.2053841450;
startcell412: marker, at = 0;
d412, at = 0.0000000000;
sF412, at = 0.5715187750;
s412, at = 1.9996834400;
sD412, at = 2.0696834400;
d5a12, at = 3.4978481050;
c312, at = 3.9387581250;
endcell412: marker, at = 4.2053841450;
endsequence;
Beam,particle=proton,sequence=tamusq512,energy=1.01722;
tamusq512: sequence, refer=entry,l = 4.1285935600;
startcell512: marker, at = 0;
d5c12, at = 0.0000000000;
sF512, at = 0.4369197700;
s512, at = 1.8763688350;
sD512, at = 1.9463688350;
d6a12, at = 3.3858179000;
c412, at = 3.8578272900;
endcell512: marker, at = 4.1285935600;
```

```
endsequence;
Beam,particle=proton,sequence=tamusq612,energy=1.01973;
tamusq612: sequence, refer=entry,l = 4.0367775300;
startcell612: marker, at = 0;
d6c12, at = 0.0000000000;
sF612, at = 0.4114260100;
s612, at = 1.8984763850;
sD612, at = 1.9684763850;
d612, at = 3.4555267600;
endcell612: marker, at = 4.0367775300;
endsequence;
Beam,particle=proton,sequence=tamusq113,energy=1.01973;
tamusq113: sequence, refer=entry,l = 4.3999231700;
startcell113: marker, at = 0;
d113, at = 0.0000000000;
sF113, at = 0.5812507700;
s113, at = 2.0807131500;
sD113, at = 2.1507131500;
d2a13, at = 3.6501755300;
c113, at = 4.1162881500;
endcell113: marker, at = 4.3999231700;
endsequence;
Beam,particle=proton,sequence=tamusq213,energy=1.02221;
tamusq213: sequence, refer=entry,l = 4.2826360400;
startcell213: marker, at = 0;
d2c13, at = 0.0000000000;
sF213, at = 0.4189653200;
s213, at = 1.9506337000;
sD213, at = 2.0206337000;
d3a13, at = 3.5523020800;
c213, at = 3.9965690100;
endcell213: marker, at = 4.2826360400;
endsequence;
Beam,particle=proton,sequence=tamusq313,energy=1.02468;
tamusq313: sequence, refer=entry,l = 4.1746803800;
startcell313: marker, at = 0;
d3c13, at = 0.0000000000;
sF313, at = 0.4441403100;
s313, at = 1.9807878450;
```

```
sD313, at = 2.0507878450;
d413, at = 3.5874353800;
endcell313: marker, at = 4.1746803800;
endsequence;
Beam,particle=proton,sequence=tamusq413,energy=1.02468;
tamusq413: sequence, refer=entry,l = 4.4638271500;
startcell413: marker, at = 0;
d413, at = 0.0000000000;
sF413, at = 0.5872450000;
s413, at = 2.1244352250;
sD413, at = 2.1944352250;
d5a13, at = 3.7316254500;
c313, at = 4.1795302500;
endcell413: marker, at = 4.4638271500;
endsequence;
Beam,particle=proton,sequence=tamusq513,energy=1.02718;
tamusq513: sequence, refer=entry,l = 4.3846102300;
startcell513: marker, at = 0;
d5c13, at = 0.0000000000;
sF513, at = 0.4429227200;
s513, at = 1.9914505650;
sD513, at = 2.0614505650;
d6a13, at = 3.6099784100;
c413, at = 4.0958558100;
endcell513: marker, at = 4.3846102300;
endsequence;
Beam,particle=proton,sequence=tamusq613,energy=1.02966;
tamusq613: sequence, refer=entry,l = 4.2755661000;
startcell613: marker, at = 0;
d6c13, at = 0.0000000000;
sF613, at = 0.4108182400;
s613, at = 2.0096386550;
sD613, at = 2.0796386550;
d613, at = 3.6784590700;
endcell613: marker, at = 4.2755661000;
endsequence;
Beam,particle=proton,sequence=tamusq114,energy=1.02966;
tamusq114: sequence, refer=entry,l = 4.6706226500;
startcell114: marker, at = 0;
```

```
d114, at = 0.0000000000;
sF114, at = 0.5971070300;
s114, at = 2.2089085900;
sD114, at = 2.2789085900;
d2a14, at = 3.8907101500;
c114, at = 4.3685447900;
endcell114: marker, at = 4.6706226500;
endsequence;
Beam,particle=proton,sequence=tamusq214,energy=1.03206;
tamusq214: sequence, refer=entry,l = 4.5382989100;
startcell214: marker, at = 0;
d2c14, at = 0.0000000000;
sF214, at = 0.4208219700;
s214, at = 2.0666272050;
sD214, at = 2.1366272050;
d3a14, at = 3.7824324400;
c214, at = 4.2335741400;
endcell214: marker, at = 4.5382989100;
endsequence;
Beam,particle=proton,sequence=tamusq314,energy=1.03443;
tamusq314: sequence, refer=entry,l = 4.4267167400;
startcell314: marker, at = 0;
d3c14, at = 0.0000000000;
sF314, at = 0.4509890000;
s314, at = 2.1021348300;
sD314, at = 2.1721348300;
d414, at = 3.8232806600;
endcell314: marker, at = 4.4267167400;
endsequence;
Beam,particle=proton,sequence=tamusq414,energy=1.03443;
tamusq414: sequence, refer=entry,l = 4.7351687900;
startcell414: marker, at = 0;
d414, at = 0.0000000000;
sF414, at = 0.6034360800;
s414, at = 2.2551641350;
sD414, at = 2.3251641350;
d5a14, at = 3.9768921900;
c314, at = 4.4321914100;
endcell414: marker, at = 4.7351687900;
```

```
endsequence;
Beam,particle=proton,sequence=tamusq514,energy=1.03684;
tamusq514: sequence, refer=entry,l = 4.6552541300;
startcell514: marker, at = 0;
d5c14, at = 0.0000000000;
sF514, at = 0.4492686400;
s514, at = 2.1131073750;
sD514, at = 2.1831073750;
d6a14, at = 3.8469461100;
c414, at = 4.3474838400;
endcell514: marker, at = 4.6552541300;
endsequence;
Beam,particle=proton,sequence=tamusq614,energy=1.03920;
tamusq614: sequence, refer=entry,l = 4.5113431400;
startcell614: marker, at = 0;
d6c14, at = 0.0000000000;
sF614, at = 0.4101757400;
s614, at = 2.1272059250;
sD614, at = 2.1972059250;
d614, at = 3.9142361100;
endcell614: marker, at = 4.5113431400;
endsequence;
```